A common European approach to the regulatory testing of nanomaterials

NANoREG

Grant Agreement Number 310584

Deliverable D 5.07

Develop a rapid high throughput screening methodology to evaluate nanomaterial toxicity

Due date of deliverable: *2016/09/31*
Actual submission date: *2016/05/31*

Author(s) and company:	Maria Dusinska (NILU), Mihaela Roxana Cimpan (UiB), David Carlander (NIA), Kevin Hogveen/Valérie Fessard (ANSES), Blanca Suarez (Gaiker), Ricardo Marcos/Laura Vila (UAB), Irina Estrela-Lopis (ULEI), Romain Grall/Sylvie Chevillard (CEA), Jan Topinka/Tana Brzicova (IEM), Diana Boraschi (CNR), Andrew R Collins/Sergey Shaposhnikov (CBT), Maria Joao Silva (INSA)
Work package/task:	WP5 / Task 5.6
Document status:	draft / final
Confidentiality:	confidential / restricted / public
Key words:	High throughput, high content

DOCUMENT HISTORY

Version	*Date*	*Reason of change*
1	2015/09/31	First draft ready
2	2016/03/31	Second draft – Paper published - submitted to the Management board
3	2016/05/31	Deliverable finalised – The title corrected and annexes included
4	2016/11/07	Comments from PO considered and the deliverable updated
5	2016/11/29	Deliverable updated and submitted to PO
6	2017/07/13	Deliverable restructured and submitted to PO
7	2017/03/18	Revised deliverable submitted to PO
8	2017/08/09	Project Office harmonized lay-out

This project has received funding from the European Union
Seventh Framework Programme (FP7/2007-2013)
under grant agreement no 310584

Lead beneficiary for this deliverable: Norwegian Institute for Air Research (NILU; 16)

Owner(s) of this document	
Owner of the content	NILU – partner 16
Co-Owner 1	Gaiker – partner 11
Co-Owner 2	CEA- partner 23
Co-Owner 3	ULEI – partner 45
Co-Owner 4	UAB – partner 27
Co-Owner 5	ANSES – partner 35
Co-Owner 6	NIA – partner 12
Co-Owner 7	TCD – partner 14
Co-Owner 8	CNR – partner 31
Co-Owner 9	UiB – partner 39
Co-Owner 10	KI – partner 15
Co- Owner 11	Comet Biotech AS
Co-Owner 12	Ciber Epidemiologia y Salud Pública, ISCIII, Spain
Co-Owner 13	Institute of Experimental Medicine AS CR, Czech Republic
Co-Owner 14	National Institute of Health Doctor Ricardo Jorge
Co-Owner 15	National Institute of Metrology Quality and Technology, Brazil

Table of Content

1 Description of task

This task aimed to evaluate the suitability of different high throughput and high content analysis technologies to assess in a reliable, robust, time- and cost-efficient manner the toxicity of manufactured nanomaterials (MNMs) employed in the NANoREG project. To keep up with innovation and the rapidly growing number and complexity of MNMs, such methods and testing platforms are urgently needed. High throughput and high content screening are technologies commonly used by pharmaceutical companies to assess their chemicals in a fast way, which provide information regarding relevant endpoints. Methods appropriate for MNM toxicity testing need to be developed, standardised and validated due to specific needs and challenges, such as possible interference of MNMs with the testing techniques and the accompanying physico-chemical evaluation.

The latest methodologies have been reviewed and compared to evaluate their capacity to constitute a testing strategy aimed to support health impact considerations related to MNMs. This task involved in-vitro toxicity testing, matching where appropriate the same endpoints as tested in other WPs in NANoREG.

The following stepwise approach was employed:

Step 1: Perform several high throughput in vitro toxicity tests covering different endpoints, e.g., cytotoxicity (apoptosis, necrosis, oxidative stress, inflammation), genotoxicity (micronucleus, Comet assay, gene mutation), cellular morphology, cell cycle, nucleocytoplasmic translocation, skin and ocular toxicity, effects on the Immunological system, neuronal cells and vascular system.

Step 2: Compare results of different assays for each endpoint.

Step 3: Compare results with those from in vitro (Task 5.5) and if possible in vivo (WP4) studies.

Step 4: Develop a rapid high throughput screening methodology to reliably evaluate MNMs toxicity taking into account advances achived in other FP projects (COMICS, NanoTEST).

Size distributions of MNMs in stock (batch) solution and appropriate assay media and buffers were also analyzed throughout the biological testing. The role played by physico-chemical parameters, e.g., chemical composition, size, shape, z-potential, was evaluated.
The main aim was to evaluate the suitability of the high throughput and high contact analysis techniques employed in task 5.6 to study the toxicity of MNMs, by identifying strengths and limitations of these techniques.

The *in vitro* toxicity screening methodologies, some already established and others developed in this task, could be useful for the development of a decision tree (Task 5.7) and regulatory framework/toolbox (Task 1.4).

This task will make use of the results from Task 6.2 (Safe by design: lessons learned from drug development testing). The results of this task can be used in the development of the risk assessment decision tree (Task 5.7), the regulatory framework/toolbox (Task 1.4) and the safe by design concept (Task 6.2).

2 Description of work & main achievements

2.1 Summary

With the growing numbers and complexity of MNMs there is a huge demand to come up with rapid and reliable ways of testing MNM safety, preferably using in vitro approaches, to avoid the ethical dilemmas associated with animal research. To develop intelligent testing strategies for risk assessment of MNMs, based on grouping and read-across approaches and to satisfy regulatory goals, predictive models should be developed based on a wide pool of reliable data. The adoption of high throughput screening (HTS) and high content analysis (HCA) for MNM toxicity testing allows the testing of large numbers of different materials at different concentrations and time points and on different types of cells, reduces the effect of inter-experimental variation, and also makes substantial savings in time and cost. HTS/HCA approaches facilitate the classification of the key biological indicators of MNM-cell interactions. Validation of *in vitro* HTS tests is required, taking account of relevance to *in vivo* results. HTS/HCA approaches are needed to assess dose- and time-dependent toxicity, allowing prediction of *in vivo* adverse effects.

The data obtained from the following HTS/HCA methods are currently being analysed and the methods are being validated: Label-free cellular screening of MNM uptake, HCA, HTS flow cytometry, Impedance-based monitoring, Multiplex analysis of secreted products, real time RT-PCR, and genotoxicity methods, namely: HTS comet assay, HTS in vitro micronucleus assay, and gene mutation assay. There are technical challenges related to HTS/HCA for MNM testing, as toxicity screening needs to be coupled with characterization of MNMs in exposure medium prior to and at the end of the test; also possible interference of MNMs with HTS/HCA techniques is a concern.

Task 5.6 has investigated the cyto- and geno-toxicity of a total of 23 MNMs on cell lines representative of main organs of exposure and retention: a common cell line, i.e., A549 (alveoli), V79 (lung fibroblast), Calu-3 & BEAS-2B (bronchia), Caki-1 (kidney), Hep3B (liver), Caco-2 (intenstine), SaOS-2 (bone), primary gingival fibroblasts (GF) (oral), TK6 L5178Y & THP-1 & U937 (blood system and immune response).

The following MNMs were used in task 5.6: TiO_2 NM-100, NM-101, NM-103 and NM-104; ZnO NM-110, NM-111; SiO_2 NM-200, and NM-203; CeO_2 NM-212; $BaSO_4$ NM-220; Ag NM-300K and NM-302; carbon nanotubes NM-400, NM-401, NM-411; red and green fluorescent negatively or positively charged SiO_2 (provided by IIT) SiO_2@IIT 50 red(+), SiO_2@IIT 50 red(-), SiO_2@IIT 50 green(+), SiO_2@IIT 50 green(-), SiO_2@IIT 115 red(+), SiO_2@IIT 115 red(-), SiO_2@IIT25 red(+), and SiO_2@IIT25 red(-).

Eleven MNMs were common for the partners in task 5.6: TiO_2 NM-100, NM-101, NM-103; ZnO NM-110, NM-111; SiO_2 NM-200, and NM-203; CeO_2 NM-212; $BaSO_4$ NM-220; Ag NM-300K and NM-302.

The main achievements of task 5.6 are:

1. **Stable dispersions have been obtained using the NANOGENOTOX protocol**
   Analyses of size distribution of MNMs in water-BSA stock solution and in complete cell culture media at the beginning, during and at the end of exposure were performed.

2. **Development of *in vitro* cellular models and exposure protocols and establishment of individual and common protocols for relevant key endpoints**
   - A common cell line, A549, from the same batch has been used in task 5.6 for comparison of results and method validation.
   - A set of common concentrations covering a range relevant for both cyto- and genotoxicity.
   - Expression of doses both as µg/mL and µg/cm^2.

- A common exposure duration of 24 h.
- A set of 11 common MNMs representative for each MNM category.

3. Assessment of potential toxicity of MNMs using both common and different assays and protocols

3.1. *Impedance-based real time assessment of cell viability*, attachment and proliferation (xCELLIgence, ACEA Biosciences Inc.), at concentrations 2, 10, 20, 50, 100 µg/mL corresponding to 1, 5, 10, 25, and 50 µg/cm^2. The following preliminary toxicity rankings were obtained on:
A549, GF, SaOs-2 cells (UiB 39): NM-300k > NM-111 > NM-110 > NM-302 >> NM-101, NM-103 > NM-220 > NM-203, NM-212, NM-100, NM-200 > SiO_2@IIT-25nm-green(-), SiO_2@IIT-115nm-red(+) > SiO_2@IIT-50nm-red(+), SiO_2@IIT-50nm-red(-), SiO_2@IIT-50nm-green(-), SiO_2@IIT-50nm-green(+), SiO_2@IIT-115nm-red(-).
A549 cells (CEA 23): NM-300k, NM-110 > NM-302, NM-200 > NM-100, NM-203 > NM-212, NM-220, NM-103.
Caki-1 cells, (CEA 23): NM-300k, NM-110 > NM-302 > NM-100, NM-203, NM-212, NM-220 > NM-103, NM-200 > NM-101.
HEP3B cells (CEA 23): NM-302, NM-300k, NM-110 > NM-212, NM-203 > NM-200, NM-103 > NM-220, NM-100.
Calu-3 cells (CEA 23): NM-300k > NM-302, NM-100 > NM-200 > NM-103, NM-220 > NM-203, NM-212.

3.2 *Microfluidic-chip impedance-based flow cytometry* (Ampha Z30, Amphasys AG), at concentrations 2, 10, 20, 50, 100 µg/mL corresponding to 1, 5, 10, 25, and 50 µg/cm^2. The following preliminary toxicity ranking was obtained on *U937 cells*:
UiB (39): NM-300k > SiO_2@IIT 115nm red(+) and SiO_2@IIT 50nm red(-) > NM101, NM-302 > NM-100, NM-103, SiO_2@IIT 50nm red(+) > NM-200, NM-203.

3.3. *Real time RT-PCR* (IL-6, IL-6, Bcl-2, Bax, RIPK1, FAS, SOD1, SOD2, NFKb1), at concentrations 2 and 100 µg/mL, the following preliminary toxicity ranking was obtained on *A549 and GF cells*:
UiB (39): The following ranking can be suggested: NM-300k > NM-110 > NM-103 > NM-302 >> NM-101 > NM-203 > NM-212, NM-220 > NM-100, NM-200.

The toxicity rankings obtained above are preliminary, the final ranking will be given after data analyses and method validations will be finalized (they are currently being performed). Although differences could be seen with regard to the sensitivity of each cell type, method (xCELLigence, AmphaZ30, real time RT-PCR) and laboratory performing the tests, the overall toxicity ranking was concordant for all three methods and partners involved, indicating that the methods are robust and can be employed in nanotoxicity testing. The most toxic particles at were NM-300k, NM-302, NM-110, and NM-111.

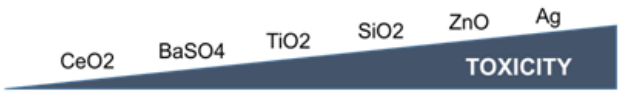

3.4 *Two colorimetric assays: AlamarBlue (NILU, CBT) and MTS (IEM)* have been used to investigate viability of A549 cells after exposure to 23 MNMs (AlamarBlue) or 11 MNMs (MTS assay), respectively at concentration range from 0.1 to 75 µg/cm^2 showing good concordance with impedance based assays. Additional control MNMs without cells need to be added to check for the interference of MNMs with assay but overall these assays give good results that are in concordance with other cytotoxicity tests, such as impedance based assays. Alamar Blue was used by NILU together with the Comet assay. As with

impedance based tests silver and ZnO are the most cytotoxic MNMs. For MTS assay NM110 (ZnO) and NM300k (silver) were also most cytotoxic in A549 cells.

3.5 *Colony Forming Efficiency (CFE)* Assay (NILU, INSA) measuring cell death and ability of cells to grow and form colonies after continuous exposure, usually 10-12 days while colonies are formed. The assay gives information about cytotoxic as well as cytostatic effects. The CFE assay appeared specifically suitable for assessment of MNMs toxicity *in vitro*, as it is label-free. The CFE assay optimised and standardised for MNMs testing by the JRC was further miniaturised by NILU and standardised with testing 20 MNMs. Preliminary data show that the most toxic MNMs are carbon nanotubes, silver and ZnO.

3.6 *Genotoxicity* is crucial when assessing the safety of MNMs and thus all genotoxicity endpoints need to be evaluated for the risk assessment. These include gene mutation, chromosomal damage (clastogenicity) and numerical chromosomal damage (aneuploidy). Based on our data we suggest to include DNA damage (strand breaks and specific DNA lesions such as DNA oxidation). These are transient DNA lesions but can serve as good indicators of genotoxicity. Moreower, high throughput modifications of available genotoxicity assays such as comet assay allow to investigate wast number of MNMs in much shorter time than standard assays.

3.6.1 *The high throughput comet assay* was performed by NILU, CBT, UAB and IEM. The modified version detecting strand breaks as well as oxidised DNA lesions (using formamidopyrimidine glycosylase- FPG) was used to detect also oxidative stress at the level of DNA.
Preliminary *genotoxicity* data from complete set of MNMs based on the comet assay on *A549* cells (NILU) show ranking after
3h exposure: NM-111 > NM-302 > NM-110 > NM-300K > NM-203 > NM-100 > NM-220 > NM-103 > NM-104 > NM-212 > NM-101 > NM-200
24h exposure: NM-110 > NM-302 > NM-111 > NM-300K > NM-100 > NM-200 > NM-203 > NM-101 > NM-220 > NM-103 > NM-104.

Within the comet assay we tested over 20 MNMs (NILU), CBT evaluated 18 MNMs and UAB and IEM 7-11 MNMs. Comparison within 7 laboratories both using standard comet assay (2 gels) or HTS comet assay (12 or 20 mini gels) shows some variation in genotoxic potency among different comet assay protocols but generaly results are in good concordance.

Our data obtained with HTS comet assay show that a 24 h incubation alone is not sufficient to detect damaging effects of certain MNMs on DNA. The use of FPG is important as it allows detection of oxidative damage to DNA which would otherwise be missed. We also found that a small increase in concentration can have profound effects in terms of genotoxicity.

3.6.2 Gene mutation (NILU, INSA) and micronucleus assay (UAB, NILU, IEM). Altogether 11 MNMs have been tested for *gene mutation*: NM-100, 101, 103, 104, 110, 300, 302, 401, 200, 203, 220. Among them carbon nanotubes NM-401 and silver nanorods NM-302 showed strong positive mutation potential. In this case, the effect was most likely due to shape rather than to chemical composition. Preliminary data from the micronucleus assay show slight positive effect in BEAS2B cells for NM-200 and 302.

3.7 *MNM cellular translocation and uptake quantification by means of label-free dosimetric and imaging techniques (ULEI 45)*

3.7.1 *Molecule-based imaging technique: confocal Raman microspectroscopy (CRM)*

Intracellular uptake and distribution pattern of CeO_2 (NM-212), $BaSO_4$ (NM-220), ZnO (NM-110) and TiO_2 (NM-103, NM-104) were monitored in human epithelial lung A549 and Caco-2 cells. Quantification of NP uptake weighted to cellular protein content, internalization as well as their co-localization with different cell components and biomolecules were studied with respect to the toxic effects of these MNMs observed *in vitro* and *in vivo* studies (WP4). The monitoring of MNMs in A549 and Caco-2 cancer cells showed different uptake and intracellular processing for the various MNMs.

ZnO (NM-110) were seen attached to the cell membrane and internalized only peripherally in the cell, remaining in close vicinity to the plasma membrane. The phonon bands, characteristic for the crystalline structure of internalized particles, disappeared completely after very short time. This proves a fast dissolution of ZnO (NM-110) after passing through the cell membrane within a time of 20 min. ZnO (NM-110), which were observed during the whole exposure time, were found to be accumulated at the membrane surface from the outside. The very high rate of Zn^{2+} release explains the high toxicity ranking of ZnO NPs.

Different uptake and translocation were seen for CeO_2 (NM-212) and $BaSO_4$ (NM-220). CeO_2 were found in peripheral cytoplasm close to the cell membrane (early endosomes) and in perinuclear regions (late endosomes/endolysosoms). Instead, $BaSO_4$ were almost entirely accumulated in the endoplasmic reticulum (ER) in the close vicinity to the nucleus membrane. A specific co-localization of $BaSO_4$ (NM-220) with ribosomes associated with ER was observed. Additionally, quantification of CeO_2 (NM-212) and $BaSO_4$ (NM-220) uptake weighted to cellular protein content at the single cell level was performed. The uptake rate was ca. 3.5 times higher for CeO_2 compared to $BaSO_4$ NP in the A549 cells exposed to NPs at up to 100 µg/ml concentration.

3.7.2. *Element based dosimetric/imaging techniques*

The comparison of in vivo and in vitro uptake based on the knowledge of intracellular effective dose in culture cells and tissues was performed. The question of vitro-vivo relevance was addressed.

IBM method supports the CRM results showing a high uptake rate of CeO_2 (NM-212) in spite of their very low toxicity ranking.

The following uptake ranking was obtained in A549 cells exposed for 24h: NM-212 >> NM-110 > NM-103 > NM-104.

The element content and intracellular distribution of CeO_2 NPs were studied and compared to cellular uptake at a single cell level from the 28 day CeO_2 inhalation study on Wistar rats. The average concentration of Ce in cells exposed to 10 µg/ml CeO_2 (NM-212) was ca. 17.000 ppm. The mean cerium concentration in the septum of single alveoli was 10 times lower than in the in vivo experiments. Even the concentration in “hot spots” in alveolar septum was 3 times lower.

3.8 *High Content Analysis* (ANSES 35)

Six MNMs (NM-103, NM-104, NM-203, NM-200, NM-110 and NM-300K) were tested by HCA in Caco-2 and A549 cells. Eight markers of cellular toxicity were analyzed in each cell line and for each MNM the Cytotoxicity (cell count, nuclear size and nuclear intensity), Apoptosis (active Caspase-3), genotoxicity (γH2AX, ATM phospho S1981, p53 phospho S15), and cell cycle (Ki-67) were assessed.

Only NM-300K and NM-110 generated cytotoxic responses in either cell line. In Caco-2 cells, NM-300K was the most cytotoxic, whereas in A549 cells NM-110 was slightly more

cytotoxic. Interestingly, in both cell lines, treatment with NM-300K resulted in a significant increase in nuclear size and nuclear intensity at non-cytotoxic concentrations.
NM-300K appeared to induce considerably greater genotoxic effects in Caco-2 cells compared to A549 cells, as seen by significant increases in γH2AX, ATM phospho S1981 and p53 phospho S15 levels at relatively low concentrations. In A549 cells however, it was NM-110 that induced the markers of genotoxicity, whereas NM-300K induced these markers only at cytotoxic concentrations.

4. **Human in vitro whole blood assay (WBA) to determine MNM contamination with endotoxin** (CNR 31).
   The WBA assay adapted to NANoREG requirements (see SOP in Annex 5) was applied to MNMs after having determined their contamination with endotoxin. The ability of 16 NANoREG core materials**,** of which 11 used in task 5.6, all at 100 μg/ml, to induce an inflammatory response in human blood leukocytes was examined. At this concentration, some of the MNMs were still measurably contaminated with endotoxin, although at low levels.

   The majority of the MNMs had no direct inflammation-inducing effect in the WBA, except for NM-110- (uncoated ZnO particles), as compared to the positive control (LPS 2.5 ng/ml).
   In addition to their possible direct inflammatory effect, the capacity of MNMs to interfere with the inflammation-inducing capacity of LPS was evaluated. The results indicate that several MNMs had little/no effect on the LPS capacity of inducing IL-1β production (NM-100, NM-103, NM-200, NM-212, NM-220, NM-300K, NM-302), while a few had some enhancing effect (NM-101, NM-110, NM203, the latter very pronounced). On the other hand, only one MNM had an appreciable inhibitory effect, *i.e.*, NM-111 (ZnO particles with a triethoxicaprylsilane coating).

5. **Advantages and challenges of HTS/HCA approaches in MNM safety evaluation have been identified**
   A thorough literature review and analysis of HTS/HCA methods used in nanotoxicity testing, including the ones used in NANoREG, have been done by the task 5.6 partners and presented in a review article[191]. Advantages and challenges pertaining to HTS/HCA approaches in MNM safety evaluation have been identified and are also summarised in the paper Collins et al. 2016[191], Annex 1) and are also presented in this deliverable (see Table 1, Annex 2).

Methodological considerations:

5.1 *Challenges related to high-throughput suitability of NANoREG protocols for dispersion and physico-chemical characterisation of MNM.*
A common bottleneck for most partners in task 5.6 was represented by the fact that only one NM could be dispersed at a time and in addition by the hydrodynamic diameter measurements that had to be done in parallel. The reason for not being able to fully explore the HTS/HCA methods for MNM testing is time consuming, low throughput MNM characterisation. One of the requirements in the NANoREG project was to characterise MNMs always before, during and after the treatment of cells and thus in vitro HTS/HCA testing had to be coupled with characterisation. Characterisation methods, however, are not yet developed for HTS. This is the biggest challenge for MNM testing with HTS/HCA approaches.

To at least partially overcome the restrictions imposed by low throughput characterisation, for cytoxicity/genotoxicity HTS one partner (NILU 16) modified the study design to be able to test four MNMs in one run, including characterisation of MNMs before during and after the treatment and using 2 methods for cytotoxicity, several endpoints for genotoxicity, two cell lines and two treatment time points. ANSES (35) opted also for testing several MNMs at a time, still only a maximum of 4 MNMs could be tested in a single test due to the time constraints of the dispersion protocol (approximately 25 minutes per MNM). Using HCA, while only a limited number of MNMs could be tested within a single test, several different

cellular markers were analyzed in a single test. So, although the number of MNMs that could be tested was limited, large amounts of quantitative data were extracted for each MNM.

To make the most of both the dispersion obtained and of the amount of MNM in each vial UiB (39), NILU (16) and other partners tried to circumvent this by exposing several cell lines to more concentrations of the same NM in order. However, the number of cell types that could be handled simultaneously was limited.

One partner (UAB 27) has tested the effect that freezing in liquid nitrogen of several aliquoted dispersions of metal oxides and MWCNT MNMs had and found out that they maintained their physico-chemical characteristics upon thawing[188]. This approach indicates that exposure to frozen pre-dispersed MNMs can be done. The method needs further testing for validation and to find out for which types of particles and dispersion media it is suited for.

General recommendations, though not for high throughput, were made by one partner (UiB 39): use of thicker probe, replaceable tip, beaker with stage (plate that keeps probe more stable and allows its immersion at same depth each time), hold vial by screw lock, and cooling-ice always on top/around vial via buoyancy. For calibration (optimization): mathematics for calibration of small vessels (including heat loss through vessel walls) and automatic temperature logging by (small) temperature probe(s).

5.2 Genotoxicity vs. Cytotoxicity

An important part of genotoxicity testing is that each assay has to be performed within a specific toxicity range. This is crucial especially for the comet assay where nontoxic up to mild toxic concentrations should be used to avoid false positive results that might occur when toxic concentrations are applied. The *clonogenic assay (CFE),* as one of the earliest cytotoxicity test, gives an overview on both cytotoxic as well as cytostatic effect and can be used for calculation of lethal concentration 50% (LC50). This assay is not prone to interference and thus is specifically useful for testing MNMs. The assay is time consuming, however during the NANoREG project the throughput of this assay was increased by using a 6 well format and currently a 24 well format assay is under development. The *AlamarBlue* assay was successfully applied and its robustness increased in combination with the comet assay. NB! AlamarBlue and other spectroscopic methods must be checked for the interference with MNMs. Among other tests, the Impedance test is reliable and a suitable test to establish LC50.

For *in vitro* genotoxicity assessment all major endpoints should be covered: DNA damage, gene mutations, chromosome breakage and/or rearrangements (clastogenicity), and numerical chromosome aberrations (aneuploidy) should be evaluated. Representative assays that are able to measure these endpoints are the comet assay, mammalian gene mutation and micronucleus assays. The standard low throughput genotoxicity assays applied for hazard assessment of chemicals are also applied for MNMs. Within the task 5.6 we adopted, developed, applied and standardized medium/high throughput genotoxicity assays based on standard already accepted tests, namely *mini-gel comet assay* for detection of DNA strand breaks and DNA oxidation lesions (oxidized purines), medium throughput gene mutation assay on 96 well format (Mouse lymphoma tests) and flow cytometry micronucleus assay.

Within the comet assay we tested over 20 MNMs. Comparison within 7 laboratories both using standard comet assay (2 gels) or HTS comet assay (12 or 20 mini gels) shows good concordance.

For *point gene mutation*, the most commonly used assay the Ames test could not be applied especially because of bacteria as biological model, the bacterial wall and limited or no uptake of MNMs. Thus, the mammalian gene mutation test was the only option. Two gene mutation assays have been used, the point mutation in Hprt and Tk locus using V79 or mouse lymphoma L5178Y cells. Both assays are still very laborious but Mouse lymphoma assay in Tk locus has the advantage that a 96 well format can be used. This assay can be further adapted towards increasing of throughput. However, p53 competent cells should be preferably applied.

Impedance-based assays have the advantage of being label-free, non-invasive and less prone to interferences from MNMs. They can be used as a first line of cytotoxicity screening, especially the ones that perform continuous monitoring of the cells and which can give indications regarding relevant time-points and concentrations for more in depth mechanistic investigations.

5.3. *MNM cellular translocation and uptake quantification by means of label-free dosimetric and imaging techniques*

Confocal Raman microspectroscopy as a fast, label-free and non-invasive imaging technique provides unique information about translocation and fate of NPs at subcellular level. The living cells as well as formaldehyde-fixed cells were investigated with the CRM at an excitation wavelength of 532 nm and a spatial resolution of about 260 nm.

Ion beam microscopy as a label-free imaging technique represents an unique possibility to perform the spatial resolved element analysis at single cell level. Two IBM techniques, as micro-resolved proton induced X-ray emission (μPIXE) and Rutherford backscattering (μRBS) analysis, were applied to quantify the intracellular concentration of NPs in alveolar cell under *in vitro* and *in vivo* condition. The comparison of in vivo and in vitro uptake based on the knowledge on intracellular effective dose in culture cells and tissues was performed. The question of vitro-vivo relevance was addressed. IBM method supported the CRM results showing the high uptake rate of CeO_2 NM-212.

The comparison of *in vitro* and *in vivo* intracellular concentrations has a fundamental meaning for addressing the question of the *vitro-vivo* relevance on quantitative basis. There could be two ways for assessing the *in vitro-vivo* relevance question: i) intracellular concentration under in vitro condition can be matched to in vivo concentrations by means of adjusting the applied dose; ii) comparison of toxic effects in vitro and in vivo on the basis of knowledge on intracellular effective dose in culture cells and tissues.

6. Establisment, optimization and evaluation of the suitability of different HTS/HCA methods to assess toxicity of MNMs

Several methods have been improved prior to and during the NANoREG project by the task 5.6 partners and can be applied in hazard assessment of MNMs (uptake, quantification, real-time and endpoint impedance-based methods, colony forming efficiency, comet assay, micronucleus assay, HCA).

The use of a microchip-based bioimpedance flow cytometry method (Ampha Z30) for nanotoxicity testing was successfully established for the first time in the NANoREG project.

A microfluidic prototype for HTS impedance-based cell analysis of MNM-toxicity in biomimetic dynamic conditions was designed and produced.

Within the task 5.6, up to 23 NANoREG MNMs have been tested by different HTS/HCA methods addressing the main toxicity endpoints, especially cytotoxicity and genotoxicity. A considerable amount of data has been generated and all data have been uploaded to the ISA-TAB database and in CIRCABC for further analysis within NanoReg2 project (for overview of data available see the NANoREG Results repository. The data obtained show that the HTS/HCA methods employed

are faster, more economical, are of high quality and show lower variation. Preliminary cytotoxicity and genotoxicity rankings show good concordance between themselves and with standard approaches. These data will be used for further analysis within the NanoReg2 project and for grouping, read across and development of in silico methods.

The testing strategy for in situ characterization, cytotoxicity and genotoxicity was designed with increased throughput that allows to test several MNMs in several cell lines, either continuously or at specific time points in one experiment. Nevertheless, coupling HTS methods with in situ characterization appeared to be biggest challenge as characterization is time consuming and limits the efficiency and robustness of HTS/HCA.

Each of the abovementioned techniques has both advantages and limitations and combinations of techniques are needed to answer the specific questions related to hazard evaluation of MNMs.

2.2 Background of the task

The three aims of task 5.6 'Develop a rapid high throughput screening methodology' were to review and evaluate existing HTS/HCA methods, develop and applied them to assess toxicity of the MNMs in NANoREG and to develop a strategy/strategies for the use of HTS/HCA methodologies.

Manufactured nanomaterials (with at least one dimension <100 nm) and nanoparticles (NPs - with all three dimensions <100 nm) are considered as distinct from normal chemical compounds and bulk materials on account of their size, chemical composition, shape, surface structure, surface charge, aggregation and solubility[1,2]. The extraordinary physicochemical properties of MNMs have accelerated their incorporation into diverse industrial and domestic products. Although their presence in consumer products represents a major concern for public health safety agencies as well as for consumers, the potential impact of these products on human health has been poorly characterised. At present, the very limited, and often conflicting data derived from published literature – and the fact that different MNMs are physico-chemically so heterogeneous – make it difficult to generalise about health risks associated with exposure to MNMs. There is therefore an urgent need to clarify the toxic effects of NPs and MNMs and to elucidate the mechanisms involved in their toxicity. The field of nanotechnology has expanded exponentially, and NPs and MNMs with simple to very complex composition, in a wide range of materials, sizes, shapes and structures are currently produced[8] . In view of the large number of MNMs currently in use, high throughput screening (HTS) techniques aimed at accurately assessing and predicting toxicity are clearly needed; provided that reliable toxicity metrics will be established, the HTS approach will generate large and valuable data sets[3,4].

Up to now, there has been no consensus regarding models and tests that should be used to analyse the *in vitro* toxicity of NPs/NMs and at present no clear regulatory guidelines on testing and evaluation are available[5-7]. The heterogeneity and increasing complexity of MNMs severely limit the feasibility of producing general toxicity protocols to address MNM risk assessment. However, reliable, robust and validated protocols for testing NP/MNM toxicity (Table 1, Annex 2) are essential for human and environmental risk assessment[5,8,9].

Compared with *in vivo* approaches, *in vitro* methods to address MNM-induced toxicity have the advantages of simplicity, economy, and shorter time required for investigation; they can aid in revealing general mechanisms underlying the effects of MNMs on cells, and can provide a basis for evaluating potential risks of exposure. However, obtaining toxicological data from *in vitro* assays alone has potential limitations since the behaviour of cells with MNMs in culture differs from their behaviour in the complex biological systems of the whole organism [9].This is attributed to what is known as 'coordinated tissue response', perhaps the most under-researched area in the field of toxicology[5]. Ideally, when considering screening novel MNMs for toxic effects we should use a combination of *in vitro* methods simulating as closely as possible *in vivo* conditions.

HTS is defined as the use of automated tools to facilitate rapid execution of a large number and variety of biological assays that may include several substances in each assay[4]. HTS was introduced in the pharmaceutical and chemical industries as a rapid way of evaluating effects of many novel compounds. With the rapid growth of MNM production, HTS methods are needed to allow toxicity testing of large numbers of materials in a timely manner and with savings in labour costs. HTS *in vitro* facilitates the hazard ranking of MNMs, through the generation of a database with all reported effects on biological and environmental systems, thus novel MNMs can be prioritised for *in vivo* testing. Recently, an effective HTS model for investigating the toxic effects of several metal-oxide NPs[10], based on a hazard ranking system using HTS, gave results that were mostly comparable to *in vivo* results in zebra fish embryos with the same NPs.

One of the main priorities in nanotoxicology is the development new or adaptation of existing instruments and methods[118] that recreate the biological environment and type of exposure to MNMs to increase the in vivo relevance of HTS/HCA and are not distorted by MNM interference. An important source of confounding or conflicting data in nanotoxicity testing is represented by MNM interference with assay components and/or detection systems[58,181]. Some of the most encountered interferences are with fluorescent markers, which could be adsorbed onto MNMs preventing the markers from being available to bind to cellular structures of interest. In some cases, MNMs fluoresce themselves and/or are able to act as fluorescence quenchers. A general drawback is that a good quantification of fluorescence is difficult to obtain. During handling through multiple steps in traditional toxicity assays cells can become permanently modified and damaged. Such assays are oftentimes time-consuming, labour-intensive, and complex[53]. Another drawback of many traditional methods is that they can only evidence effects at a specific point in time and thus do not give an overview of the biokinetic behaviour and of the real time interactions between biological structures and toxicants over time[53].

The need for label-free detection methods has emerged, especially in nanotoxicity studies, because of the possible interferences of MNNs with labelling-substances and detection systems[58,181]. **Impedance-based assays** that measure the electrical properties of cells are label-free and represent a reliable alternative with the potential to become a method of choice for the initial screening of MNMs' toxic effects. These methods analyse matter either by their active or passive electrical properties[189]. Impedance-based monitoring takes advantage of the passive properties of an object, which occur when the object is composed of dissipative elements, such as ohmic resistors or conservative elements such as capacitances and inductances[86] It measures how much objects, such as cells, impede a flow of electrical current. Proliferation, growth, morphology, and adhesion can be measured by applying an electric source to an electrode covered by cells, and measuring how the cells impede the current[86]. By using alternating current (AC) information about the properties of the cells as a function of signal frequency is obtained. Cell membranes are insulating structures with an abundance of negatively charged molecules on the inside as compared to the outside, which give rise to the resting potential of the membrane[86]. When a time-oscillating electric field is applied, a change in the charge distribution will ensue, with charged molecules trying to follow the electric field. The polarisation effect depends on frequency and gives rise to α-, β- and γ dielectric dispersions[86] (Fig. 1).

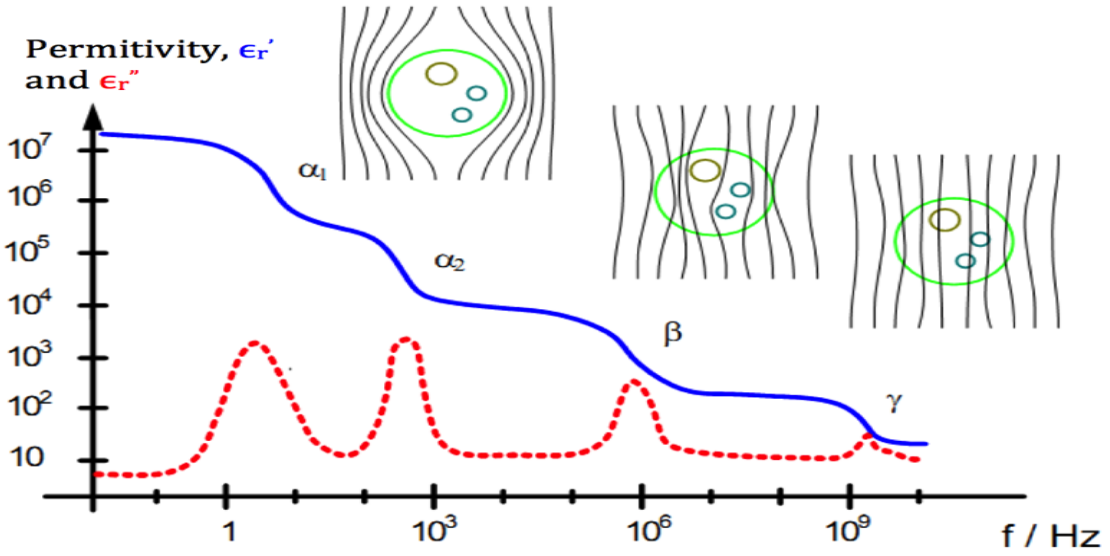

Fig. 1. Dispersion types. *The higher frequencies allow easier passage of current through the cell. The real dielectric number ϵ_r' is shown in blue, while the imaginary part ϵ_r'' is shown in red. α -dispersion has an active cell-membrane effect. In β-dispersion, the passive cell membrane-capacitance is observed. The γ-dispersion is due to polarisation of the medium in the cell (water, salts, proteins). (Figure adapted by Pliquett from Schwan and Kay (1957) and used with permission).*

For a cell placed between two electrodes, there is a relationship between the different dispersions and the polarisation of the cell (Fig. 2). At low frequencies, a lateral movement of ions along insulating membranes takes place, giving rise to α-dispersion. As a result, a high polarisation of the membrane is obtained together with a high permittivity. Impedance measuring at low frequencies gives information about the size of the cell[99]. When frequency is increased, the charged molecules cannot follow the electric field anymore, because of its rapid fluctuation, leading to a decrease in the capacitance of the membrane[190]. Between 100 kHz and 10 MHz the rapid depolarisation known as β-dispersion can be observed and measurements within this range can give information about membrane properties[86, 190]. At very high frequencies (1GHz), γ-dispersion occurs as a result of the polarisation of water, salts and proteins in the cell.

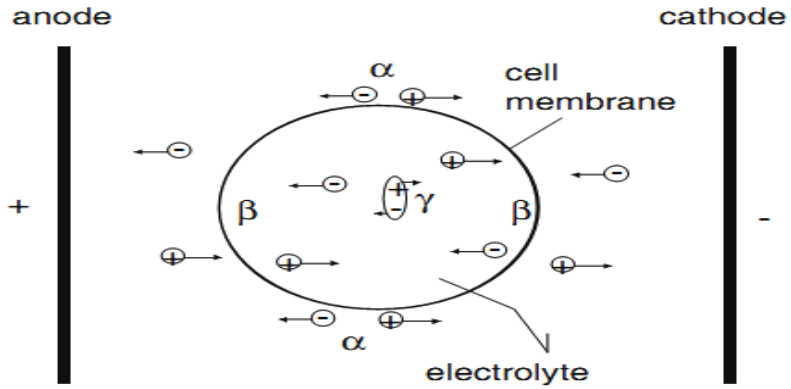

Fig. 2. Polarisation mechanisms for a cell situated between two electrodes*. Movement of ions along the cell membrane gives α a-dispersion. β-dispersion occurs as the cell membrane is depolarised. The γ-dispersion is recognised as polarisation of macromolecules (figure used with permission from Pliquett, 2010).*

Impedance-based methods have an advantage when compared to traditional methods because they allow ”in situ” real-time recordings without the use of markers, as well as monitoring of the dynamics in cell growth and viability[54]. In NANoREG, the xCELLigence system (ACEA Biosciences) was used for real-time monitoring of adherent cells (UiB and CEA)”in situ” without the

use of markers. For cells in suspension, a microfluidic chip-based impedance flow cytometer Ampha Z30 (Amphasys AG) was employed for the first time in NANoREG (UiB). Furthermore, the prototype of a microfluidic impedance-based biomimetic chip has been designed and produced (UiB), and preliminary studies using NM-110 indicate that under dynamic exposure, the toxic response is significantly reduced compared to static exposure.

Cytotoxic methods such as **AlamarBlue®** measure cytotoxicity through a colorimetric response to the intracellular reducing metabolism of living cells. The conversion of resazurin (oxidised form) to resorufin (reduced form) results in colorimetric and fluorescence changes; resazurin is blue and non-fluorescent whereas resorufin is red and highly fluorescent. As other colorimetric methods also AlamarBlue may be prone to interference thus additional control should be included as previously suggested[58,59].

The ultimate index of cytotoxicity is loss of cell viability, and this can be measured by their ability to survive and form colonies in the **Colony forming efficiency assay (CFE)**. CFE is a label-free method and thus is suitable for cytotoxicity testing of NMs without interference with the readout – a common problem with colorimetric assays. The CFE assay was optimized and standardized for MNM testing, validated in an interlaboratory comparison and shown to be sufficiently sensitive to detect potential MNM toxicity[102,198]. The assay was modified within the NANoREG project by NILU within this task for higher throughput by reducing the number of cells to 50 per well and applying a 6-well plate format. CFE is a quantitative clonogenic assay measuring the ability of single, adherent cells to survive and form colonies. The test allows for detection of cytotoxic effects (reduction in number of colonies) as well as cytostatic effects (reduction in colony area).

Genotoxicity endpoints are crucial in assessing the safety of MNMs and same principles as for chemical safety that all genotoxicity endpoints should be covered, are also applied for NM safety evaluation. Main genotoxicity endpoints include DNA damage as indication for potential mutagenicity, gene mutation, chromosomal breaks (clastogenicity) and numerical chromosomal change (aneuploidy). For assessment of genotoxicity it is crucial to know cytotoxicity, thus always cytotoxicity is performed together with genotoxicity.

One of the most used test for detecting DNA damage generally as well as for measurement of DNA damage induced by MNMs is **the Comet assay**[123]. The assay is relatively simple, fast, sensitive to measure DNA breaks at the level of single cells and was recently miniaturized and developed as medium- , high- throughput assay[68, 191, 195]. Within the NANoREG project we also measured DNA base oxidation by inclusion of a post-lysis incubation with Fpg (prepared as a crude extract from *Escherichia coli* with an over-producing plasmid) as the modified comet assay. Fpg converts oxidised purines to DNA strand breaks.

Mammalian gene mutation tests detect point mutations (alteration of one single base pair) or small delitions. Two in vitro mammalian gene mutation tests detecting mutations in Hprt and Tk genes are most commonly used (OECD). HPRT is a purine salvage enzyme, which phosphorylates 'waste' purines and adds them to the cellular DNA precursor nucleotide pool[68,87]. The *HPRT* gene is X-linked, with only one active copy per cell, so that a mutation in only one allele is needed for phenotypic expression. Both can detect small deletions. However, the in Tk gene deletions can be detected with higher efficiency compared with the *HPRT* gene mutation test[86].

The in vitro micronucleus test is a genotoxicity test that measures micronuclei in the cytoplasm of interphase cells. Micronuclei may originate from acentric chromosome fragments (i.e. lacking a centromere), or whole chromosomes that are unable to migrate during the anaphase stage of cell division. Micronuclei represent damage that has been transmitted to daughter cells. The micronucelus test can provide information on potential chromosomal damage and can detect both aneugens and clastogens in cells that underwent cell division during or after exposure to MNMs. In the case of the *in vitro* micronucleus test, when cytochalasin B is used the interaction between cytochalasin B and NMs is a limiting factor. Cytochalasin B inhibits cytokinesis and is used to

generate the binucleated cells but it also inhibits endocytosis, an important mechanism of uptake of MNMs into the cell thus cytochalasin B is recommended after ensuring that NMs were taken up by cells[123, 199, 200].

Reverse transcription-polymerase chain reaction (RT-PCR) is a relatively rapid, sensitive and simple technique to determine the mRNA expression level of different target genes and is widely used in biomedical research including toxicity studies. Real-time PCR allows for the detection of PCR amplification in the exponential growth phase of the reaction and is much more quantitative than traditional RT-PCR. Reverse-transcribed RNA (cDNA) is used as the template for amplification and combined with TaqMan probe for detection. TaqMan PCR which is a Probe-based real time PCR requires a pair of PCR primers and an additional fluorogenic oligonucleotide probe with both a reporter fluorescent dye and a quencher dye attached.

A recent review on nanogenotoxicity shows that the most frequently used genotoxicity tests are the comet assay followed by the micronucleus test, chromosome aberrations test[196, 197]. The Ames test was also used in many studies but is not recommended due to size of bacteria and limited or no uptake of MNMs across the bacterial wall and size of bacteria[197]. There are several Overall, the most promising battery of assays for nanogenotoxicology testing *in vitro* covering all genotoxicity endpoints seem to be comet assay, mammalian gene mutation and micronucleus tests.

Combining automated image acquisition and powerful algorithms designed to quantify and extract a maximum of information from individual cells, **High Content Analysis (HCA)** generates great quantities of data for a large number of cellular characteristics, including changes in fluorescence intensity and distribution of intracellular targets, as well as detailed information on cellular and nuclear morphology. The speed of analysis, the multiparametric nature of the analysis, combined with the quantity and quality of data, make HCA an efficient and powerful approach to study a wide range of cellular processes and responses. The miniaturization of cellular toxicity assays greatly increases the number of MNMs that can be analyzed within a single assay. In addition, automated image analysis and quantification of markers of cellular toxicity in individual cells makes HCA a powerful tool for the evaluation of the mechanisms of toxicity of MNMs.

The miniaturization and automation of fluorescence based cellular assays, coupled with the automated image analysis and quantification of cellular markers in individual cells has increased considerably the amount of information generated when compared to standard methods. Limitations associated with the time required for the dispersion protocol do not allow high throughput screening. The use of an HCA approach, however, generates multiparametric data for a number of cellular parameters in individual cells. While the approach may not be high throughput, the use of HCA generates high content data.

High Content Analysis is perfectly adapted for the testing and quantification of markers of cytotoxicity, genotoxicity, oxidative stress, etc. providing that the appropriate controls are in place to evaluate possible interference artifacts with certain MNMs. A large number of MNMs can be tested in a single assay, and multiple markers of cellular toxicity pathways can be analyzed with individual cells, thereby allowing the correlation of toxicity endpoints. The results obtained from the HCA methodology in this project were reliable and reproducible.

All methods and cellular toxicity markers were developed prior to the start of the NANoREG project. Apart from additional controls to assess MNM interference, no considerable modifications were made to existing HCA protocols.

Confocal Raman Microspectroscopy (CRM) as a label-free and non-invasive imaging technique provides unique information about translocation and fate of nanoparticles at subcellular level. CRM allows the simultaneous visualization of NMs and their biological environment. CRM has a strong potential as a label-free, nondestructive technique for time-course imaging of individual cells and tracking of cell metabolism.

The combination of confocal microscopy with Raman spectroscopy provides very high content of molecular-spectroscopic information in every pixel of image at a singular cell level. CRM offers a label-free way to complement histopathology, diagnose and characterize culture cells and tissue sections. CRM provides 3D chemical composition images with a resolution of about 250 nm. CRM reveals not only the 3D NM distribution but also their co-localization within cell compartments.

Ion Beam Microscopy (IBM) techniques, such as micro-resolved proton-induced X-ray emission (μPIXE) and Rutherford backscattering (μRBS), are powerful tools for spatially resolved element analysis. IBM techniques were applied to quantify nanoparticles (NPs) uptake as well as cellular elements at the single-cell level.

A proton beam (2.25 MeV) is used for scanning the sample in the xy-plane at a resolution of about 1 μm. By combining μPIXE and μRBS it becomes possible to determine the concentration of cellular elements (for example, P, S, Ca, K, Zn, and Fe), with a sensitivity in the ppm range. The simultaneous application of μRBS and μPIXE methods delivers unique information on the genuine concentration and distribution of NMs down to the single-cell level. IBM allows visualization and quantification of a wide range of NMs in tissues and cells. Moreover, μRBS can reveal the distribution of NMs in the z-direction with an accuracy of about 100 nm. The method distinguishes between NMs that are internalized and those that are attached on the outside of the plasma membrane, owing to the loss of energy of back-scattered protons from NMs located inside cells.

2.3 Description of the work carried out

2.3.1 Methods used in task 5.6

Task 5.6 has investigated the cyto- and geno-toxicity of a total of 23 MNMs on cell lines representative of main organs of exposure and retention: a common cell line, i.e., A549 (alveoli), V79 (lung fibroblast), Calu-3 & BEAS-2B (bronchia), Caki-1 (kidney), Hep3B (liver), Caco-2 (intenstine), SaOS-2 (bone), primary gingival fibroblasts (GF) (oral), TK6 & L5178Y & THP-1 & U937 (immune response).

The three aims of task 5.6 ‘Develop a rapid high throughput screening methodology’ were to review and evaluate existing HTS/HCA methods, develop and applied them to assess toxicity of the MNMs in NANoREG and to develop a strategy/strategies for the use of HTS/HCA methodologies.

When collecting data, comparison of HTS methods and evaluation of their usefulness for MNM toxicity testing and to answering regulatory questions were performed to the extent possible within the project, and continued assessment of data is performed in NanoReg2.

The list of the methods used in this task and and experiments performed by the partners can be found in Table 2 (Annex 3) and the list of standard operating procedures as well as handbook of all SOPs in Annex 5.

2.3.2 Issues considered when performing the work

Accurate design and planning of HTS for assessing the toxicity of MNMs/NPs are essential; interlaboratory comparisons (before adopting a method for routine screening) help to reduce confidence variance and may identify possible sources of variability[11]. Adoption of automated and robotic liquid and sample handling is advisable since this will help to reduce systematic errors. To reduce such bias, the experimental design needs to be randomized.

High content analysis (HCA) and HTS approaches should deliver information on key biological indicators of NM-cell interactions, such as cell proliferation, cellular morphology, membrane permeability, lysosomal mass/pH, DNA and chromosome damage, activation of transcription factors, mitochondrial membrane potential changes, oxidative stress monitoring and post-translational modification[12].

Technical challenges can arise in HTS/HCA design, as toxicology screening needs to be coupled with characterization of NPs/NMs in the exposure medium. Characterisation is of necessity time-consuming and cannot be automated. This limitation is partially overcome if MNMs, once characterised, can then be tested (in an HTS/HCA mode) on a variety of cell lines, using different exposure times, a range of concentrations, etc.

To achieve statistical significance, experiments should be performed at least 3 times with replicate samples within each data point (three repeats).

Further basic requirements are:

a) clearly identified endpoints
b) assay-related as well as MNM-specific positive and negative controls
c) toxicologically relevant (extracellular) concentrations of MNMs
d) validated assays
e) multiparametric statistical analysis of data, e.g. using ANOVA with post Bonferroni analysis, or general linear models
f) well-designed graphical display of data (e.g. bar charts) and – in the case of multi-parametric datasets – various graphical plots to visualise associations between NP/NM exposure and different endpoints.

For example, a multilevel heatmap matrix has been used to illustrate effects of dose, concentration and time for multiple NMs[11-12] (Fig. 3).

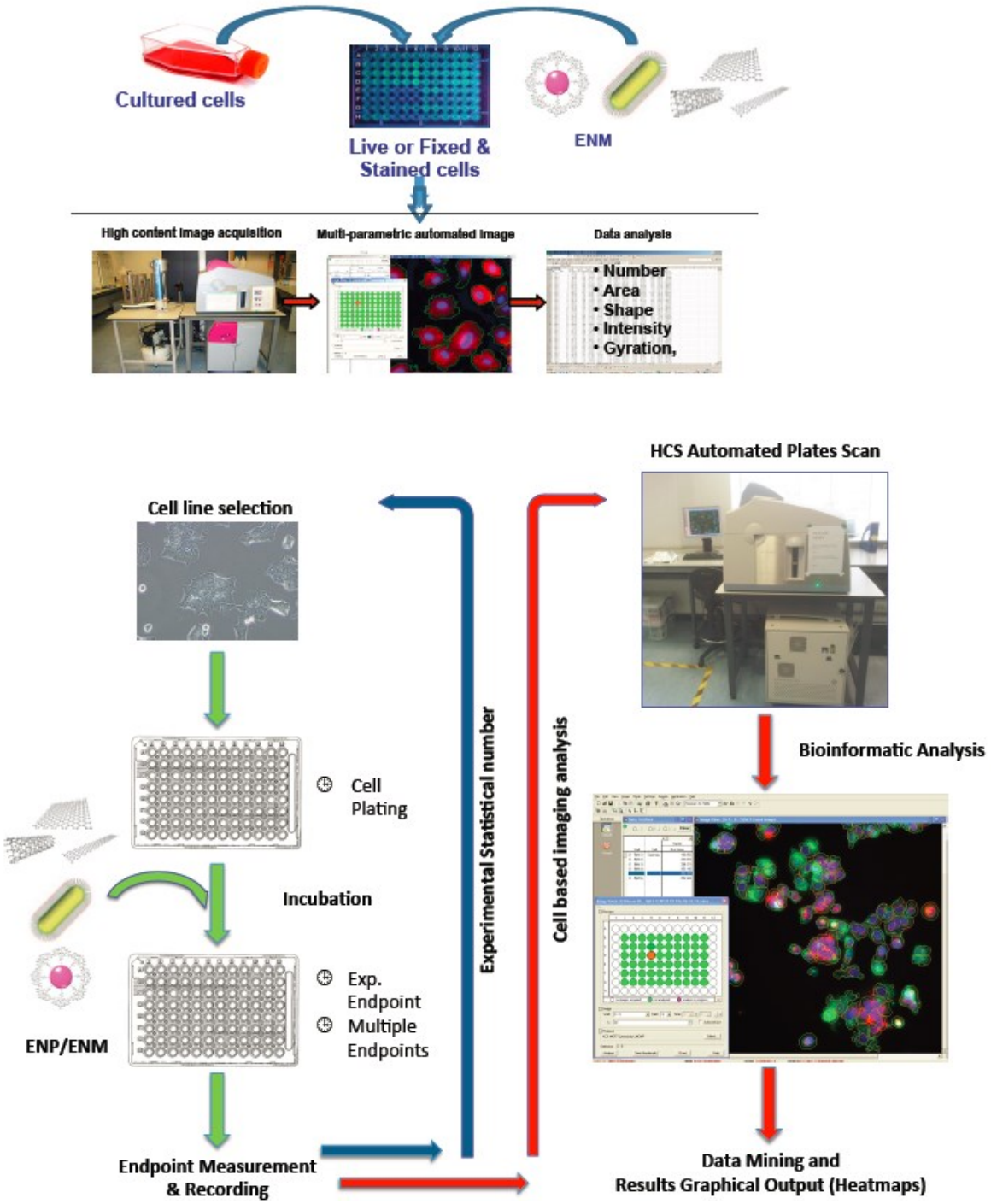

Fig.3. Experimental design for effective high-throughput screening

2.3.3 Literature review

This section provides the findings of the literature review performed in the task. This formed the basis for a scientific review paper that was published in 2016[191].

2.3.3.1 Methods for label-free cellular screening of MNM uptake

Various methods have been applied to the study of toxicity of MNMs, employing diverse physical, chemical and biological principles and endpoints; they will now be described in detail, with emphasis on high throughput adaptations. While the intracellular distribution pattern of MNMs is an important factor in investigating toxicological responses, it is generally difficult to predict and model, because it is the result of several translocation events. Flow cytometry as well as confocal laser scanning spectroscopy have been frequently applied for studying NM translocation and semi-quantitative estimation of MNM uptake. A potential problem with these methods is that they require fluorescently labelled MNMs. The comparatively large dye molecules may significantly change the surface properties of MNMs, and thus falsify the cellular distribution and uptake of MNMs. Clearly, label-free dosimetry and imaging techniques are advantageous in that they allow the study of authentic MNMs – a crucial requirement in the regulatory context. For this reason, this section focuses on label-free techniques.

Atom emission spectroscopy (AES) has been shown to be a useful tool for the quantification of a large range of elements. AES is based on the emission of radiation, which is characteristic for every element. The method is capable of quantifying specific chemical elements of MNMs in cultured cells and tissues with ppb accuracy[14,15].

Mass spectrometry (MS) is another rather sensitive technique for cellular MNM quantitation. The elements of analysed particles are ionised and separated by their mass-to-charge-ratio. Predominantly, mass spectrometry with inductively coupled plasma (ICP-MS) is used for quantification of MNM uptake in cultured cells[16]. The specimen to be investigated is either a suspension of cultured cells or a tissue sample, which needs to be dissolved prior to ICP-MS. Studying the uptake of organic or inorganic MNMs requires a comparatively large number of cells[17]. ICP-MS was further developed as single particle ICP-MS (sp-ICP-MS). This technique is able to record pulses related to a single MNM. sp-ICP-MS has the advantage of being able to distinguish between the dissolved and particulate form of NMs,[18] because the dissolved analyte does not generate pulses.

A disadvantage of these techniques is that there is no possibility to distinguish between MNMs that are internalised into the cells, extracellularly associated and/or just located between cells or within the extracellular fluid[19]. It has been shown that there is a significant difference between uptake measured by means of ICP-MS and uptake based on the analysis of individual cells [17].

Ion beam microscopy (IBM) techniques, such as micro-proton-induced X-ray emission (μPIXE) and micro-Rutherford backscattering (μRBS), are powerful tools for spatially resolved elemental imaging and quantitative analysis at the single cell level. A proton beam is used for scanning the sample in the xy-plane at a resolution of about 1 μm. With the combination of PIXE and RBS it becomes possible to determine the concentration of cellular elements (for example, P, S, Ca, K, Zn, and Fe), with a sensitivity in the ppm range[20,21]. Recently, IBM was applied to quantify MNM cellular uptake in cultured cells[17,22]. The simultaneous application of μRBS and μPIXE methods delivers unique information on the genuine concentration and distribution of MNMs down to the single cell level. IBM allows visualisation and quantification of a wide range of MNMs in tissues and cells (Fig. 4). Moreover, μRBS can reveal the distribution of MNMs in the z-direction with an accuracy of about 100 nm. The method distinguishes between MNMs that are internalised and those attached on the outside of the plasma membrane, owing to the loss of energy of back-scattered protons from MNMs located inside cells.

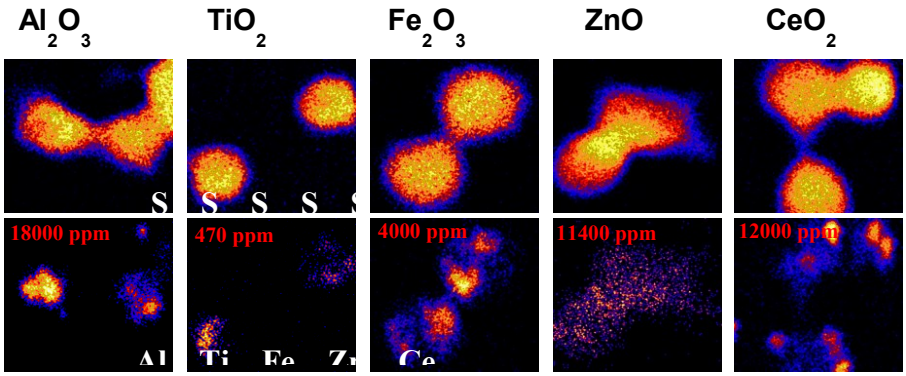

Fig. 4. µPIXE elemental mapping of A549 cells exposed to different metal oxide NMs at a concentration of 30 µg/ml for 48 h*. Top and bottom images demonstrate S and NM related element distributions, respectively. The colour code is as follows: yellow is the maximum, black represents the minimum. The size of all images is 50x50 µm.*

Electron microprobe analysis (EMPA) is a technique similar to µPIXE. Here a scanning electron beam is used instead of a proton beam. EMPA is able to quantify and visualise single elements in biological specimens[23,24,25,26] in a spatially resolved manner.

The advantage of PIXE/RBS over electron-based X-ray emission is that proton beams can analyse a much higher probe thickness and so can quantify the total cellular NM concentration in cells and tissues. Moreover, the protons offer a better signal/noise ratio allowing the accurate detection of cellular trace elements at very low concentrations.

Magnetic resonance imaging (MRI), positron emission tomography (PET) and single photon emission computer tomography (SPECT) are commonly used in clinical imaging applications as well as for the detection of MNMs in the whole organism with a resolution of about 1 mm. The activation of oxygen by the 16O(p,α)13N reaction within metal oxide NMs avoids the undesired surface modification of MNMs. Therefore, it becomes possible to study the distribution of Al_2O_3 MNMs in tissues and organs of rats by PET[22].

Transmission electron microscopy (TEM), time-of-flight secondary ion mass spectrometry (ToF-SIMS) and confocal Raman microspectroscopy (CRM) are methods which allow the simultaneous visualisation of MNMs and their biological environment at a sub-cellular level. These techniques can be considered as semi-quantitative space-resolved imaging methods. TEM visualises the intracellular localization of MNMs in ultra-thin (50-100 nm) sections of tissue or cultured cells[28,29]. Chemical identification of MNMs can be done by X-ray energy-dispersive spectrometry (EDS) and electron energy-loss spectrometry (EELS) in TEM. The 3D reconstruction of MNMs internalized by tissues and cells with suitable contrast and high depth resolution has been accomplished by tomography ("slice and view") using Focused Ion Beam - Scanning Electron Microscopy (FIB-SEM)[30]. With ToF-SIMS it is possible to measure the 3D distribution of MNMs in cells and tissues by means of a layer-wise high energy beam raster technique. The lateral resolution is about 300 nm. Pathological changes in the pattern of cellular lipids following MNM exposure have been detected[31,32]. TEM and ToF-SIMS methods are relatively cost-intensive and time-consuming, and so might not be useful as high throughput techniques for MNM screening. CRM, in contrast, is an economical and relatively fast technique, which could well be adopted for regulatory purposes in the future. CRM provides 3D chemical composition images with a resolution of about 200 nm at tissue and cellular levels. CRM reveals not only the 3D MNM distribution but also their co-localization within cell compartments. CRM is especially suitable for the detection of manufactured MNMs, as the nanostructures show a specific Raman signal, which distinguishes the NMs from the signals of their chemical constituents. Biochemical changes in cells that have been exposed to

toxic chemical agents, drugs or MNMs can be detected, identified and quantified[33,34]. CRM imaging was used to follow the different stages of the cell cycle[35], DNA condensation in late stages of apoptosis and also for the assessment of cell viability[36,37]. DNA damage, lipid changes and protein denaturation were analyzed as a response to drugs and chemicals[38,39]. However, the spatial resolution and sensitivity of CRM are limited compared with TEM which typically has a threshold of ~60 nm[40].

The power of CRM regarding cell imaging, subsequent analysis of biochemical and cell physiological processes as well as diagnostic power has been demonstrated in a number of studies with cells and tissues. Label-free imaging of cell organelles[41.42], uptake and intracellular fate of drug carriers[43-45] and MNMs inside individual cells[31,46,47,63] have been studied. CRM has a strong potential as a label-free, non-destructive technique for time-course imaging of individual cells and tracking of cell metabolism. It may become a useful tool for *in vitro* toxicological studies for estimation and prediction of cell response to agents at the cellular level. This qualifies CRM as an innovative high throughput technique for *in vitro* toxicity/uptake studies.

2.3.3.2 High-throughput screening and High Content Analysis for MNM-induced cytotoxicity

Assays for cellular metabolic activity, oxidative stress evaluation, apoptosis detection, and cell membrane integrity[48-54] have been developed for analysing cytotoxicity of chemicals and these are widely used also in NM-induced cytotoxicity screening. The methods are time-consuming, labour-intensive, complex, and in some instances unreliable owing to MNM interferences[52]. The reagents employed in such methods may interact with some of the tested MNMs or may interfere with spectrophotometric readings, leading to unreliable results[48,49,54]. Conventional assays focus on specific endpoints, without providing information about the dynamic biological processes leading to those endpoints, or the specific time points and concentrations at which different toxic effects are induced by MNMs[53,55]. Walker and Bucher[56] suggested that, owing to the unpredictable behaviour of many NMs, HTS approaches based on conventional methods may only be applicable for a few classes of MNMs that are compatible with the available test systems. However, these issues do not preclude the use of HTS approaches to screen for MNM-induced cytotoxicity[57]. Assay interferences can be avoided by using label-free methods[58,59]. Impedance-based spectroscopy is suggested as a method that does not need markers or dyes, and that has enhanced sensitivity compared to traditional assays[60,61]. In addition, live cytotoxicity screening provides information at any given point throughout the progress of an experiment – based on which, relevant time-points and concentrations can be identified for further mechanistic studies.

Combining automated image acquisition and powerful algorithms designed to quantify and extract a maximum of information from a population of cells, High Content Analysis (HCA) generates great quantities of data for many cellular characteristics, including changes in fluorescence intensity and distribution of intracellular targets, as well as detailed information on cellular and nuclear morphology. From its debut in the mid-1990s, developments in cellular imaging have rendered HCA an important tool for understanding biological processes induced by diverse xenobiotic molecules. Originally an approach used almost exclusively in the pharmaceutical industry to screen potential drug candidates aimed at specific targets, this technology is now widely used by researchers in many disciplines to study a wide range of cellular responses. Although a relatively new approach, the development of HCA technology has been accelerated by advances in optics, automated imaging, and great improvements in fluorescent molecular probes and reagents. In addition, rapid advances in information technology, including image analysis software, and increases in computing power and memory for storage of vast amounts of images and results have been a driving force in the success of HCA.

Quantitation of fluorescence corresponding to relevant molecular targets in cellular compartments allows researchers to characterise and quantify biological responses at the level of the individual cell as well as for whole cell populations. Moreover, since high content imaging allows multiparametric analyses of several markers at the same time, correlations between cellular

markers can be readily analysed on the same cell populations. The speed of analysis, the multiparametric nature of the analysis, combined with the quantity and quality of data, make HCA an efficient and powerful approach to study a wide range of cellular processes and responses.

Several commercial bench top HCA instruments are currently available, each offering specific advantages for imaging and analysis. These systems are equipped with powerful image analysis software based on the automatic identification of cells, and – depending on the instrument – they offer considerable flexibility for analysis. Currently, most HCA microscopes have optional environmental control systems, which can regulate temperature, atmosphere and humidity, thereby allowing live cell imaging in real time. Although with most instruments HCA can be performed on histological samples, the approach is best adapted to studies using cultured cell lines in multi-well plates (6-1536 wells) where multiple conditions (various compounds, range of concentrations, etc.) can be tested in a single experiment.

The wide selection of high quality primary antibodies and specific fluorescent molecular probes has given rise to limitless possibilities for analysis of biological responses. In addition, a broad range of fluorescent secondary antibodies with relatively narrow excitation and emission characteristics allows the multiplexing of several markers simultaneously. Many cell-permeable fluorescent probes are currently available which allow the visualisation of changes in membrane permeability, reactive oxygen species (ROS), mitochondrial and lysosomal functions, among many other cellular processes, in fixed or living cells. Indeed, the vast array of possible analyses of specific cellular endpoints has made HCA a key approach in various domains including toxicology, genotoxicology, oncology, neurobiology, and research on metabolic disorders[62].

High content analysis approaches offer a number of advantages regarding assay cost and data output. Miniaturization of HCA runs on 96-, 384- or 1536-well plates increases the number of compounds analysed, and reduces the volumes of reagent used. The incorporation of robotic handling systems into the workflow, combined with automated image and data analysis, permit a significant reduction in hands-on time in the laboratory. Furthermore, the throughput, speed and the number of cells analysed using HCA approaches generate great quantities of statistically robust quantitative data in considerably less time when compared to manual image acquisition and analysis.

HCA approaches have been widely used for many years by the biotech and pharmaceutical industries in drug discovery and toxicity testing[63] of extensive libraries of chemical compounds[64], and have accurately predicted the toxicity of novel compounds. Indeed, a multiparametric assay quantifying oxidative stress, mitochondrial membrane potential and intracellular glutathione levels was capable of accurately predicting hepatotoxicity with a low false positive rate[65].

There is an urgent need to develop HCA assays to evaluate the toxicity of manufactured MNMs. The sheer number of MNMs currently being used in consumer products means that HCA-based approaches will undoubtedly be key tools for safety testing, as suggested by the growing number of published HCA studies in the field of nanotoxicology. HCA can provide detailed information concerning the pathways of cellular responses to treatment with MNMs[66-68]. Recently, several studies have applied high content imaging to hazard characterization of MNMs[10,69,70].

High content imaging represents a promising approach in the prediction and evaluation of MNM toxicity. Combined with complementary HTS methods as described in this article, HCA will provide valuable information on the mechanistic pathways involved in toxicity and cellular responses.

2.3.3.3 High-throughput flow cytometry

From simple cell-based fluorescent, colorimetric, luminescent, and radiologic plate reader assays, to high-content fluorescent imaging systems, the ability to screen MNMs in the context of living cells is essential in toxicology-screening programs. The emerging field of high throughput flow

cytometry extends the capabilities of cell-based screening technologies[71]. The process involves the rapid introduction of multiple samples through a single length of tubing, and it is even possible to process samples from microplates through a flow cytometer. This allows the implementation of large screening campaigns using assays with multiple readouts per well. High throughput flow cytometry is an ideal tool for cell-based applications involving screening of cells in suspension, where multiple readouts are desired[72]. Potential applications include cell viability, intracellular incorporation of MNMs, and ROS detection. However, careful consideration should be given to the selection of appropriate flow cytometry assays in the light of possible MNM interference with fluorescent markers.

2.3.3.3.1 Cell death (apoptosis/necrosis determination)

Cellular death may be divided into programmed cell death, commonly referred to as apoptosis, and necrosis, which indicates accidental cell death. Cellular apoptosis occurs in a sequential manner, starting from cell shrinkage, increased cellular permeability, membrane asymmetry and chromatin condensation. Flow cytometry analysis coupled to a high throughput system allows investigation of several parameters in one sample, producing a complete picture of the cell death profile. Collapse of the mitochondrial membrane, an early stage in apoptosis, can easily be assessed by positively charged fluorescent probes, which are easy to locate inside the negatively charged mitochondria. As mitochondrial potential is lost, the emission of the fluorescent probe changes, indicating the onset of apoptosis in affected cells. Intermediate apoptotic events include the activation of caspases, which can be easily detected in permeable cells upon incubation with non-fluorogenic substrates.

Loss of membrane asymmetry can be studied by incubating cells with Annexin-V conjugated with green-fluorescent dye – apoptotic cells giving a positive fluorescent signal. Subsequent incubation with propidium iodide detects necrotic cells. Proportions of apoptotic and necrotic cells are estimated by flow cytometry[73]. However, unpublished experiments[55] indicate that Annexin V may not be a reliable assay, as false negatives were obtained; the more TiO_2 MNMs were added, the lower was the apparent percentage of apoptotic (Annexin V-positive) cells. Obviously, some type of interference occurred: cell membrane attached NMs masking PS, or adsorption of Annexin V to the MNMs (possibly both). Final steps in apoptosis usually include chromatin condensation and fragmentation. At this stage, cells are smaller and can be detected with the traditional UV-excited Hoechst 33342.

2.3.3.3.2 Reactive oxygen production

Reactive oxygen species (ROS) occur as by-products of mitochondrial respiration and inflammation processes. In addition, xenobiotics can induce ROS production, either directly or via inflammation. The physicochemical characteristics of MNMs enable them, in many cases, to catalyse ROS production and oxidative damage to biomolecules, with potential pathological consequences. Most of the commercially available probes to monitor ROS production by flow cytometry in living cells are cell-permeating chemicals that undergo changes in their fluorescence spectral properties once oxidised by ROS. Two such probes are represented by dihydroethidium (DHE, also called hydroethidine) and CM-H2DCFDA (chloromethyldichlorodihydrofluorescein diacetate). DHE emits blue fluorescence in the cytoplasm until oxidized by superoxide to 2-hydroxyethidium, which intercalates within the DNA staining the cell nucleus a bright fluorescent red. On the other hand, the nonfluorescent CM-H2DCFDA is first hydrolysed to DCFH by intracellular esterases and DCFH is then oxidised to form the highly fluorescent DCF in the presence of ROS[74] (Fig. 5).

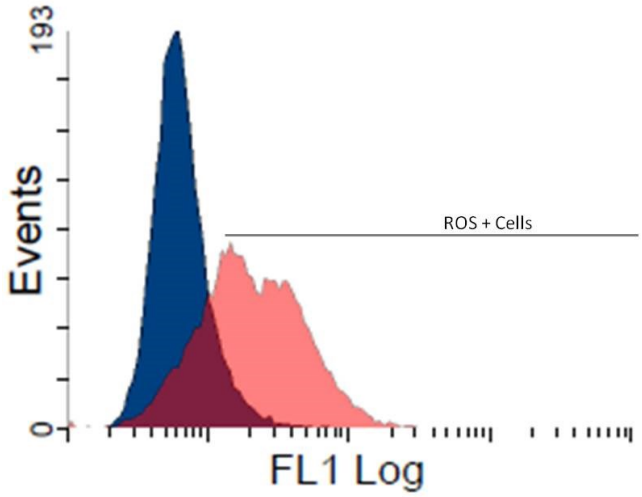

***Fig. 5**. CM-H2DCFDA (FL1) plots to determine **ROS production in 3T3 cell line** after 24 h CeO_2 NP exposure. **Blue Area**; Control group without CeO_2 NP exposure. **Red Area**; 0.1 mg/ml CeO_2 NP exposure.*

Detection of ROS species by flow-cytometry coupled to a high-throughput system allows the detection of several early intracellular indicators at much lower MNM concentrations than those needed for standard cytotoxicity assays. This system is also very flexible, allowing for the study of several MNMs in one single experiment, or alternatively, a few NMs in cell lines representing different tissues susceptible to MNM exposure.

2.3.3.3.3 Specific cellular uptake

Uptake of MNMs labelled with Rhodamine fluorescent probe is measured by flow cytometric detection of Rhodamine-positive cells. In the case of non-labelled MNMs, it is possible to analyse the specific cellular uptake through forward scatter (FS) (size) and side scatter (SS) (Fig. 6). Higher side scatter can also be indicative of apoptosis, and so additional methods such as microscopy should be used for validation.

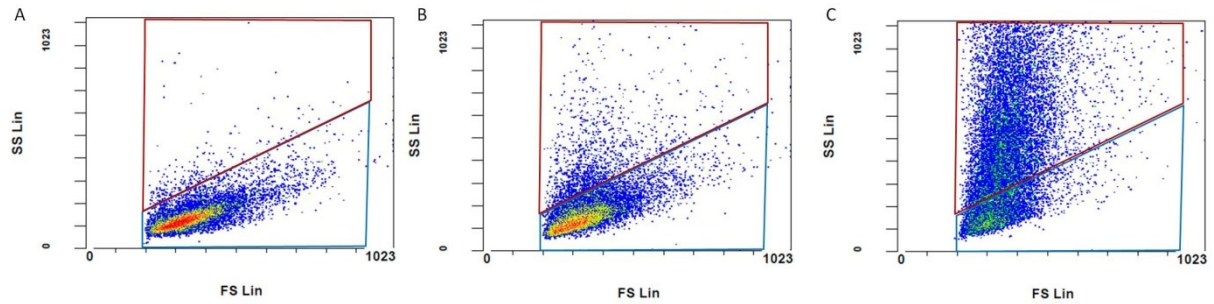

***Fig. 6. Forward Scatter (FS) / Side Scatter (SS) plots to determine NP uptake in 3T3 cell line** after 24 h CeO_2 NP exposure. **Blue box**; Cells with no NP incorporation. **Red box**; uptake of NPs by 3T3 cells. **A**) Control group with no CeO_2 NPs. **B**) CeO_2 NP exposure at 0.01 mg/ml. **C**) CeO_2 NP exposure at 0.1 mg/ml.*

Properties of MNMs can interfere with conventional cytotoxicity assays and induce bias. Regarding uptake, iIt was demonstrated that TiO_2[75-77] and Ag[78] MNMs induce an increase of SS signal in cell populations after exposure to the MNMs. SS indicates the granularity of the cells and is strongly linked to their content of MNMs. As few as 5-10 NMs per cell can be detected[76]. Recently, SS signal analysis was successfully applied for detecting carboxylated nanodiamonds and tungsten carbide-cobalt (WC-Co) MNMs in cells, results being validated by Raman and confocal microscopy

associated with 3D reconstruction[79,80]. However, care should be taken in the interpretation of the results because in some biological processes, such as apoptosis, SS (granularity) is also increased. Finally, imaging flow cytometry (an integrative approach combining flow cytometry analyses with confocal microscopy) relates the physicochemical characteristics of MNMs to their uptake, with a view to designing safe MNMs[81]. Flow cytometry appears to be a good alternative method to detect MNM internalization compared to TEM which is very time-consuming and requires heavy equipment.

2.3.3.4 Impedance-based monitoring

2.3.3.4.1 Real-time cell monitoring

Real-time cell monitoring uses electrical properties (electric cell-substrate impedance sensing, or ECIS) and was introduced by Giaever and Keese over 20 years ago[82]. As a label-free, non-invasive biophysical assay detecting dynamic cell responses, it provides a valuable tool for the investigation of MNM toxicity and early stage efficacy testing of NP-linked drugs. Impedance-based methods have been used in applications ranging from food processing to clinical research[83-87] and recently have been adapted to HTS techniques to examine the impedance characteristics of cell monolayers after exposure to certain bio-reactive agents, for instance in the pharmaceutical industry[83].

Impedance-based devices used for adherent cells consist essentially of electrodes attached to cell culture vessels. When cells are grown on the electrodes, their growth, attachment and proliferation result in changes in the measured impedance output, as growing cells – with their insulating bilipid membranes – act as dielectric objects[54,82,88]. An alternating electrical current (AC) is applied through the electrodes and the extent to which the cells impede that current is measured[55,86]. When the cells grow and attach to the electrodes at the bottom of the culture vessels the impedance increases; this provides information about the cell count, cell morphology, attachment to the substrate and viability. When cells die, they detach from the electrode surface, causing a drop in the recorded impedance, which indicates a reduction in the number of viable cells[52,55].

Commercially available impedance-based instruments for *in vitro* analysis on cell monolayers monitor the changes in impedance properties of cells after exposure to bioactive agents. The xCELLigence®, CellKey and ECIS systems, probably the most used such instruments, work on essentially the same principle. They utilise cell culture well plates with gold-plated electrodes attached to the bottom of the wells and measure the real-time opposition of the seeded cells to the applied electric current, providing information about the cells' attachment to the well, their proliferation and their reaction to the bioactive agent in question[83,88]. The format of cell culture plates that these instruments employ varies from 16-well to 96-well and 384-well plates, allowing the live screening of a large number of materials[83,90,91]. A limitation of such impedance-based devices is that they observe cellular responses to effectors without giving any indication of how the effects took place. However, they enable real-time observations to be made of cell changes throughout an experiment without the need for destructive cell sampling. They collect data about both short-term and long-term responses of cells to MNMs[92], facilitating the identification of key time-points and concentrations (Figs. 7 and 8). Toxicity assays with other endpoints can then be applied to investigate the underlying mechanisms. Impedance-based methods, being easy to implement, can also be used in HTS fashion to test several MNMs at different concentrations simultaneously[53,93].

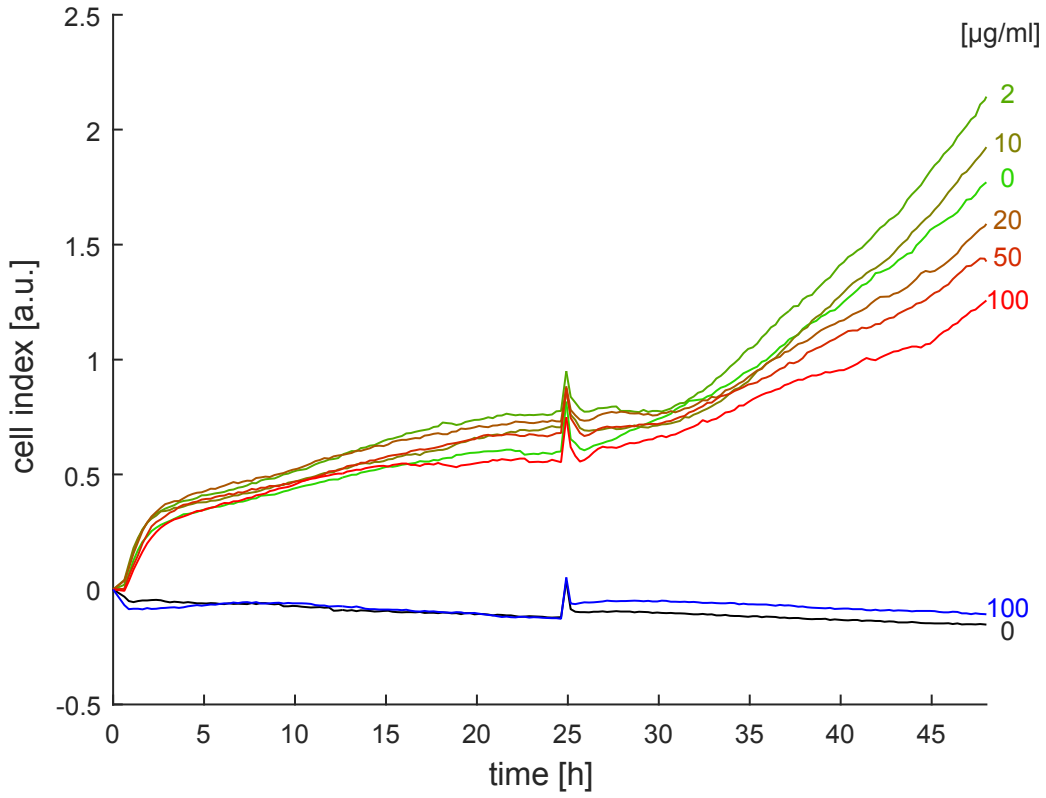

Fig. 7.Impedance-based measurements of A549 cells exposed for 24h to NM-100 TiO_2 particles (110 nm diameter, anatase)*: Representative data collected with the xCELLigence instrument (ACEA Biosciences Inc., USA). The figure shows the plot of the cell index (CI) which reflects real time cellular proliferation. Exposure of cells started at 24 h after cell seeding and lasted 24 h. The conditions are colour coded from green to red in concentrations 0, 2, 10, 20, 50 and 100 µg/ml. Medium only (black) or with100 µg/ml NM-100 (blue) are included for reference*.

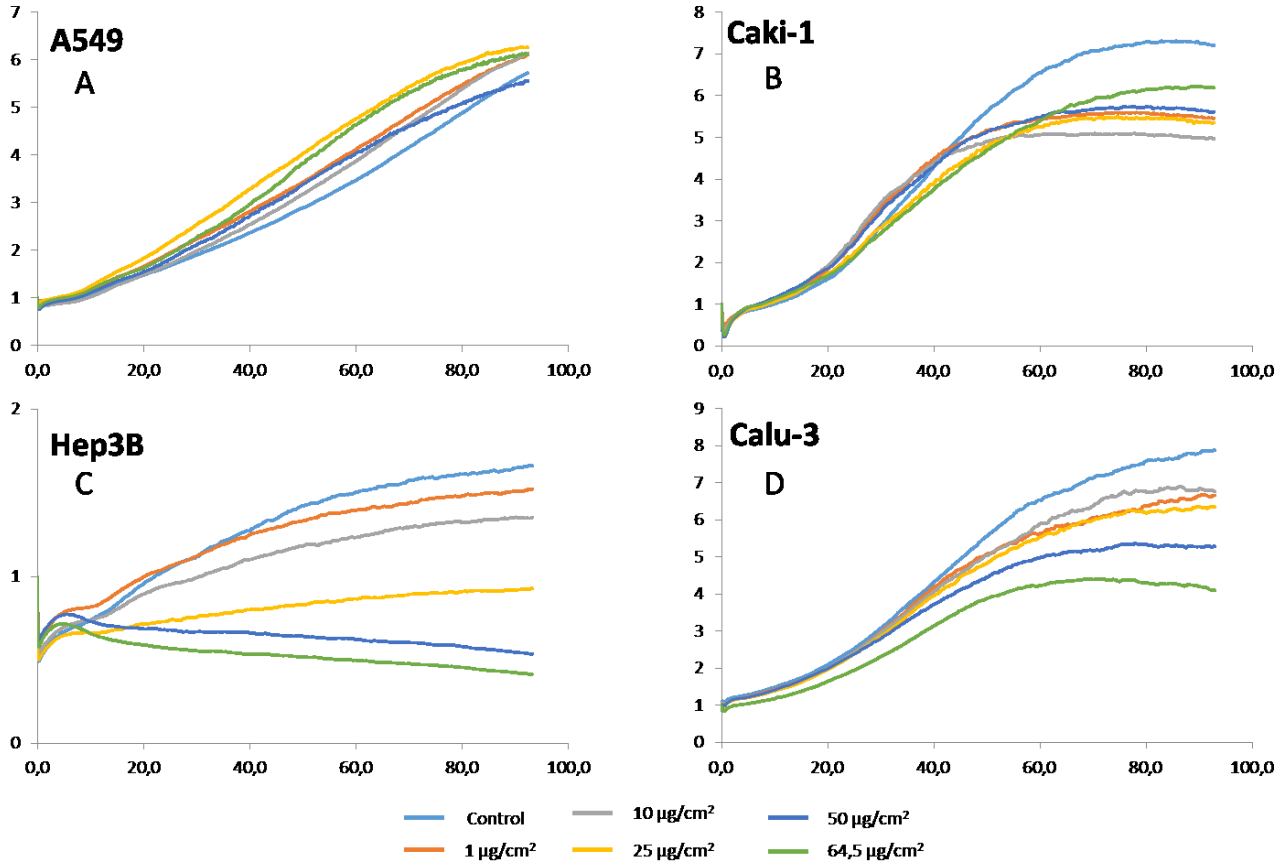

Fig. 8. Impedance-based measurements: Cell index for real-time monitoring and viability *of A549 (A), Caki-1 (B), Hep3B (C) and Calu-3 (D) cells exposed to TiO_2 NM-100. One representative experiment among three independent experiments whcih were carried out for 96 h and cell indices were normalised at time 0 to ensure no inter-well variability prior to the addition of NMs. Control cells were not exposed to TiO_2 NMs. The curves correspond to CI values at four endpoints (24, 48, 72 and 96 h). Statistical analysis was performed for each exposure condition compared to non-exposed cells (Student's t-test, *p < 0.01; **p<0.001; ***p<0.0001).*

Real-time measuring of cellular impedance is a useful and sensitive method for screening effects of MNMs, at different concentrations, on a range of cell lines simultaneously[94], without variation due to artefacts affecting the measured signal[79,95-97]. It can also be used to assess changes in cellular motility and adhesion in physiological conditions[98].

2.3.3.4.2 Impedance-based flow cytometry

In contrast to the real-time impedance methods, impedance-based flow cytometry (IFC) is an endpoint assay for cells in suspension that examines the impedance characteristics directly for each single cell. A microfluidic chip-based IFC developed by Amphasys AG (Switzerland) can analyse single cells without any specific sample preparation prior to measurement[94,98,99]. Compared to other impedance-based cytometers, e.g. Z series Coulter Counters or the CASY from Roche, the microfluidic chip-based IFC can cover impedance measurements at a broader frequency range, and thus yield information regarding the size and number of cells and, in addition, their membrane capacitance and cytoplasmic conductivity[53,100]. IFC gives a snapshot of the cellular state of single cells based on the changed resistance within the chip-channel caused by the passing cells[99]. The advantages of microfluidic chip-based IFC are that it measures the dielectric properties of cells directly; it can analyse the state of each single cell (Fig. 9); and it is suitable for

cells in suspension[99]. Additionally, it can apply multi-frequency impedance measurements to obtain diverse information regarding the state of the cells and cellular identity.

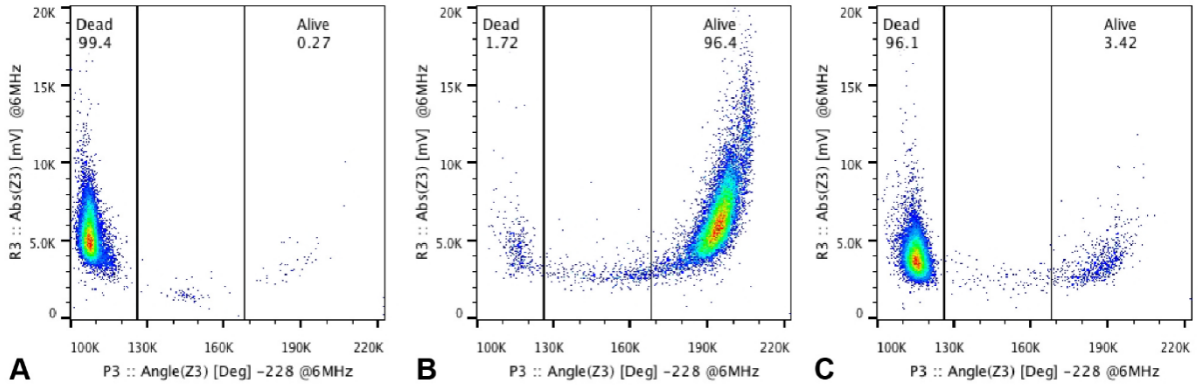

Fig*. 9. Impedance-based measurements by microchip-based flow cytometry.* *U937 monoblastoid cells were exposed to NM-300K Ag particles (15 nm, spherical): Representative data collected with the Ampha Z30 microchip-based flow cytometer (Amphasys AG, Switzerland). The figure shows dotplots of (A) necrotic cells (heated at 70ºC), (B) unexposed cells, and (C) cells exposed for 24 h to100 µg/ml NM-300k.*

Impedance-based methods have been compared with conventional cytotoxicity assays, examining effects on various types of cells induced by MNMs as well as other chemicals. Toxicological information obtained by impedance-based methods were found to be consistent with results obtained via conventional methods, and impedance-based methods have been recommended as a fast and reliable alternative to conventional methods for cytotoxicity testing[52,53,55,101]. Recently, impedance-based monitoring was used to screen TiO_2 MNM-induced cytotoxicity on fibroblasts[55]; the authors suggested that the method has merit when addressing MNM-induced cytotoxicity. In another study, Moe et al.[100] investigated the cytotoxic effects of nano-TiO_2 and nano-Ag on three cell lines simultaneously. The authors recommended such techniques for the initial assessment of the potential cytotoxic effects of MNMs and to direct further toxicological testing. A chip-based system measuring electrochemical impedance was used to monitor cytotoxicity in human hepatocellular carcinoma cells (HepG2) and immortalized mouse fibroblasts (BALB/3T3). The results were consistent with findings from the traditional MTT assay[102].

In summary, impedance-based methods for cytotoxicity testing are simple, cost-effective, label-free, lend themselves to HTS, and importantly allow in situ monitoring of not just cell death but also other aspects of cell physiology such as proliferation, morphology, attachment and intercellular adhesion. These methods are widely used in pharmaceutical research, oncology, cardiology and other fields of biomedicine and clinical research, to investigate responses of cells to exposure to bioactive chemical agents and toxicants. However, further validation of HTS applications of impedance-based instruments/techniques is advisable. To date, several studies using cell impedance have demonstrated its ability to discriminate cytostatic from cytotoxic effects [103] and also to predict different outcomes in cell-based functional assay[89]. Various cell types have already been tested: astrocytes[104], cardiomyocytes[91,105], cervix cells[106,107], eye cells[91], intestinal cells[96,108], lung cells[79,91,96,97,100], hepatocytes[79,90,91,96], kidney cells[79,96], macrophages[97], fibroblasts[55], breast[80] and neuronal cells[109].

In conclusion, besides eliminating interferences and allowing continuous follow-up measurement, cellular impedance provides qualitative and quantitative cytotoxicity data, and also directs further studies into the mode of action (toxicity) of a MNM[100].

2.3.3.5 Multiplex analysis of secreted products

Cytotoxic effects induced by MNMs may be detected by conventional methods. Besides the possibility of interference effects of certain NMs that impact on interpretations of gytotoxicity, these methods only focus on specific endpoints and do not consider relevant intracellular biological events. Secreted proteins such as cytokines, chemokines and growth factors are the largest class of soluble factors, and are generally determined by enzyme-linked immunosorbent assays (ELISA). ELISA allows the quantification of a single protein in serum, supernatants of cultured cells and tissue lysates. ELISA depends on an enzymic reaction, for instance between hydrogen peroxide and horseradish peroxidase (HRP), which means that possible interference by NMs in the reaction could affect the estimation of protein levels[58,110,111].

Multiplex analysis of soluble factors has emerged as the 'next generation' of ELISA and can be applied in different systems such as flow cytometry and chemiluminescence and fluorescence measurements. The purpose of this HTS technology is to quantify several analytes in the same sample at the same time, avoiding enzymic reactions and minimising eventual biochemical interferences. Instruments are available that analyze up to 500 analytes in the same assay kit. Multiplex panels comprise polystyrene or magnetic beads developed by biotechnology companies, where each capture antibody is conjugated to a specific bead. In general, a common biotinylated detection antibody is added to the samples (beads plus analytes) followed by incubation with phycoerythrin-labelled streptavidin. Beads and binding events are recognised and quantified by red and green lasers or LEDs, respectively. Advantages of this technology include the reduced use of reagents and sample volume, the possibility to perform repeated measures of the multiplex panels in the same experimental assay condition, detection of analytes in a broad range of concentrations, and customization of analytes in the assay plates. In addition, there is a considerable positive impact in reduced time and cost for the assay development[122,113]. Proteins related to intracellular signalling pathways are also covered by multiplex assay kits, and it is possible to study the effect of an exogenous effector on multiple pathways in the same cell population.

The multiplex analysis of secreted products is important for identification of alterations that conventional methods would not detect efficiently. For instance, gold NMs are considered nontoxic, non-immunogenic and have biocompatibility relevant to applications in nanomedicine[114-116]. A recent study demonstrated that PEGylated gold nanoparticles did not affect viability in C2C12 muscle cells determined by conventional methods (MTT conversion into formazan or altered intracellular calcein activity). However, multiplex analysis based on magnetic beads for several soluble factors contained in the cell supernatant showed a sharp increase of IFN-γ, a pleiotropic cytokine related to induction of pro-inflammatory mediators as well as differentiation of T and B cells, macrophages, granulocytes, endothelial cells, fibroblasts and NK cells. Also, levels of TGF-β1 increased, suggesting an involvement in fibrosis induction in muscle cells. These data suggest that this MNM has the potential to induce inflammation and fibrosis, promoting cell vulnerability and susceptibility to death stimuli[117]. It is unlikely that these results would have been obtained if analytes had been chosen at random for conventional analysis.

2.3.3.6 High-throughput Comet assay

The mismatch between the speed with which new MNMs appear on the market and the current low-throughput, time-consuming and laborious approaches for evaluating their genotoxicity[70] has led to the development of rapid, efficient and high-throughput genotoxicity testing strategies for safety/risk assessment of MNMs. It is important to identify and distinguish the existing genotoxicity testing methods that are amenable to HTS/HCA approaches.

The Comet assay is the method of choice for measuring DNA damage in cellular DNA. Briefly, cells in suspension are embedded in a thin layer of agarose on a microscope slide, lysed, and electrophoresed. Lysis removes membranes, releases soluble cell components, strips histones from DNA, and leaves compact structures known as nucleoids in which the DNA is attached at intervals to the nuclear matrix. The DNA is in effect a series of supercoiled loops. Under

electrophoresis (normally at alkaline pH), the DNA is attracted to the anode, but only those loops that contain breaks, relaxing supercoiling, are able to extend significantly. They form comet-like structures when viewed by fluorescence microscopy, and the relative intensity of the tail ('% tail DNA') reflects the frequency of DNA breaks. While the basic comet assay detects strand breaks, a common modification – incorporating digestion with a lesion-specific endonuclease after the lysis step – allows detection of damaged bases. Formamidopyrimidine DNA glycosylase (FPG) has been particularly useful; its primary substrate is the oxidised base 8-oxoGua, and it has therefore been employed to measure the effects of oxidative stress on DNA.

The Comet assay is popular on grounds of sensitivity, accuracy, simplicity and economy. However, it has limitations. The number of samples that can be analysed in one experiment is limited by the size of the electrophoresis tank, typically accommodating 20 slides with one or two gels each. Also, it is relatively labour-intensive, especially at the stage of scoring; normally 50 or 100 comets per gel are selected by the operator for analysis of % tail DNA using dedicated comet image analysis software. Various approaches have been used to increase the number of samples per experiment; the higher throughput entails a commensurate increase in scoring time, and fully automated scoring becomes a necessity.

2.3.3.6.1 Increasing throughput

Options for increasing throughput include increasing the size of tank, for instance incorporating a stack of platforms for slides, and reducing the size of gels. The latter approach has been more popular to date. The standard gel of 70-100 µL, covering an area of about 4 cm^2, contains thousands of cells, of which only a tiny fraction are actually scored. Reducing the gel to a volume of 4 or 5 µL, with just a few hundred cells, allows twelve gels to be set on a standard slide, or 96 as a standard 8x12 array. Such formats are available commercially (Fig. 10). For the 12-gel format, standard slides pre-coated with agarose are placed on a metal template and gels are set on the positions marked on the template. If gels are to be treated with different reagents or enzymes, the slides are clamped in a chamber device creating individual wells above the gels. The throughput is further increased with the 96 gel arrays, four of which can be fitted into one tank. The gels can be set on films of GelBond, which are then held under slight tension in special frames.

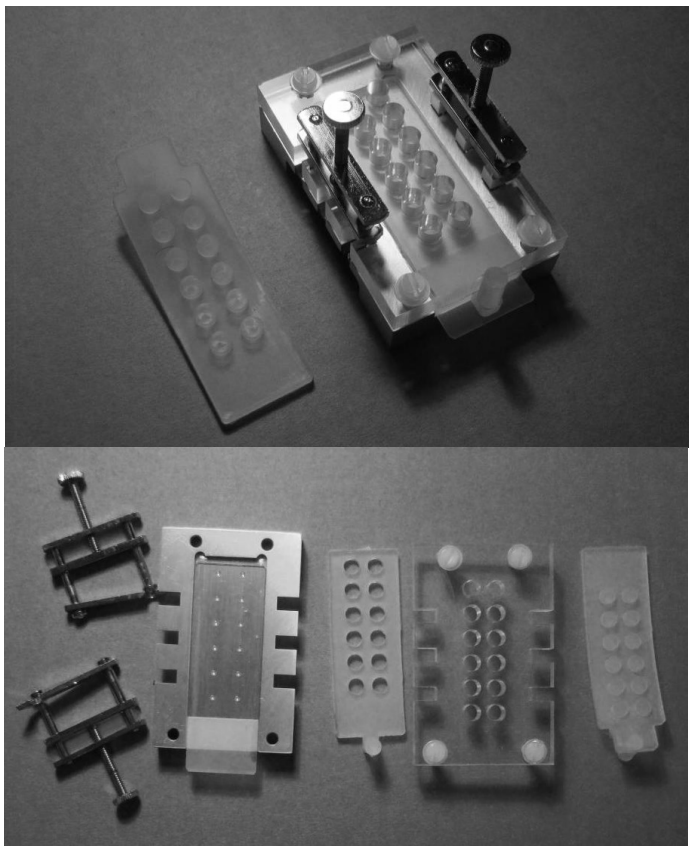

Fig. 10. Medium throughput Comet assay: 12 mini-gels on a slide. *Top: Component parts of 12-gel chamber unit (Severn Biotech), including metal base with marks for positioning gels on slide, silicone rubber gasket, plastic top-plate with wells, and silicone rubber seal. Bottom: chamber unit assembled.*

These HTS approaches were developed in the EC-FP6 project COMICS, and for nanogenotoxicity in the FP7 NanoTEST[68,118]. The performance of the 12-gel and 96-gel formats was compared with that of the standard Comet assay[119]; the damage induced in cultured cells by X-rays or methylmethanesulphonate (MMS) was detected equally well by the three formats – and with very similar coefficients of variation between replicate experiments. Further characterisation of the 96-gel format has been published[120].

The HTS Comet assay, together with FPG, has recently been applied to study the potential induction of ROS by MNMs. Cos-1 fibroblast-like kidney cells were treated with different concentrations of iron oxide MNMs, and cells embedded in minigels (12 per slide) Subsequent incubation with FPG revealed damage not seen with the basic assay for strand breaks (without FPG)[68]. Further, Huk *et al*. used the 12 gel system to study genotoxicity of nine well-defined nanosilvers in relation to their size and surface properties[121,122]. Reservations have been expressed about the use of the Comet assay, because of potential interference of MNMs with the assay. However, recent studies[123,124] showed that this is unlikely for most MNMs; the Comet assay can therefore be considered reliable and useful for testing MNM genotoxicity, especially in the HTS version.

2.3.3.6.2 Automated scoring

Automated scoring systems are dependent on accurate positioning of gels on slide or GelBond film, optimal intensity of comets and low background fluorescence, and a density of embedded cells such that few comets overlap. The gels are located and comet images focused automatically; images are captured, and later the comets are analysed one by one to obtain % tail DNA. Non-comet fluorescence, from cell debris, fibres, etc. must be recognised and eliminated from the analysis. Automated scoring is fraught with difficulties, but has been successfully developed by a few companies, notably Imstar with the Pathfinder system, and MetaSystems with Metafer. (High content imaging systems have also been adapted for automated comet scoring.) In the COMICS project the Pathfinder system of Imstar was compared with semi-automated image analysis

(comets selected by the operator for analysis), and also with manual scoring (comets categorised by visual examination into one of 5 classes). While there were differences between the three methods, all were capable of accurate damage measurement, with comparable sensitivities[125]. The 'CometChip' integrates a HTS Comet assay with automated scoring in a novel way; cells are deposited at predefined positions stamped in a micro-array on an agarose-coated plate, so that it is possible to locate comets precisely for image capture and analysis[126,127].

The Comet assay is currently the most used method for genotoxicity testing of MNMs/NPs. The need for MNM-specific positive and negative controls (reference standards) should be met with the candidate materials identified in projects such as FP7 NanoTEST and Nanogenotox[118,128].

2.3.3.7 High-throughput in vitro micronucleus assay

The *in vitro* micronucleus assay is a likely choice among a battery of genotoxic assays for rapid and effective screening of MNMs using HTS/HCA platforms. Different approaches have been proposed to increase the speed of this assay. Classically, the long and tedious visual scoring of slides has been relieved by using automated platforms scoring many slides in each run[129-131]. Different commercial automatic scoring devices are now on the market and the time saving, based on person-hours, due to the automation is approximately 70%.

Another high-throughput change in the micronucleus assay includes the use of flow cytometry, based on the pioneering work of Nüsse and Kramer[132]. The standard protocol involves 1) the lysis of membranes by a non-ionic detergent; 2) the use of one or more nucleic acid dyes that can permit discrimination between the liberated nuclei and micronuclei, according to their DNA-dye associated fluorescence intensities; 3) the separation of micronuclei and nuclei by flow cytometry. Further modifications use a 96-well format in conjunction with a robotic auto-sampling device. This adaptation requires less test material than conventional test methods, and has a greater compatibility with high throughput screening instrumentation[133-136].

The use of Chinese Hamster Ovary K1 (CHO-K1) and human hepatocarcinoma (HepG2) cells in a HCA approach has demonstrated its potential as an alternative to labour-intensive manual scoring of micronuclei[137-140]. The micronucleus assay on this HTS platform has proved to be an efficient methodology with high sensitivity and specificity to detect genotoxic compounds. Cells are cultured in 96-well plates pre-loaded with a dye that stains the cytoplasm. After incubation with the test compounds the cells are fixed and their DNA is stained with a Hoechst dye. The visualization and scoring of the cells are done using an automated fluorescent microscope coupled with proprietary automated image analysis software.

Until now, these approaches have not been applied to evaluating the genotoxic potential of MNMs. However, a recent collaboration between Flinders University, University of South Australia, CSIRO and Safe Work Australia has developed an automated HTS procedure for assessing the genotoxic potential of NMs[141]. As a proof of concept, the development and validation of the method was carried out in several steps. A mixture of B-lymphocytes (HR1K cells) stained with Vybrant™ DiO Cell-labelling, and T-lymphocytes (Jurkat cells) with Hoechst-33342, was separated on an antibody microarray slide printed with different antibodies. Three monoclonal antibodies that can differentiate between human leukocytes were used; anti-CD2 (specific for T lymphocytes), anti-CD20 (specific for B lymphocytes), and anti-CD 45 (common for T and B lymphocytes). Silver NPs (citrated and PVP-capped), and H_2O_2 as a positive control were used in the genotoxicity assay. Results showed the usefulness of the method; 10 nm citrate-capped AgNPs induced a strong genotoxic effect after 24 h exposure, double that induced by 70 nm citrate-capped AgNPs, and greater than the effect of treatment for 1 h with 20 µM H_2O_2. In addition, 10 nm citrate-capped AgNPs induced much greater genotoxicity than did 10 nm PVP-capped AgNPs.

A crucial aspect of the HTS micronucleus assay – as with other assays – is the choice of suitable NM-based positive and negative controls. This has been a focus of many European Union funded

projects including NANOGENOTOX and FP7 QualityNANO or FP7 NanoTEST. Overall, we can conclude that the micronucleus assay can be the subject of HTS approaches and that this can be applied to the testing of the genotoxic potential of MNMs. Nevertheless these different approaches need to be validated with a wide range of MNMs.

2.3.3.8 The γH2AX assay

A number of studies have proposed C-termini phosphorylated histone protein, γH2AX, as a potential biomarker of DNA double strand breaks (DSB) caused by genotoxicants[142-145]. After DSB formation large numbers of γH2AX molecules accumulate around the break site, making possible their detection. The importance of this biomarker arises from the fact that DSB are considered the most critical kind of DNA damage, initiating genomic instability and, potentially, leading to cancer[146,147]. Paradoxically, DSB can also help to kill cancer cells[148]. Thus, this method is used in different fields ranging from cancer chemo- and radiotherapy[149] or drug discovery[10] to *in vitro* toxicology testing of environmental pollutants[145].

Two types of methods are often used for γH2AX detection; those counting foci or other γH2AX-containing structures in images of cells and tissues (by immunofluorescence microscopy), and those measuring overall γH2AX protein levels (by immunoblotting or flow cytometry). Although both methods are currently used, counting γH2AX foci is several orders of magnitude more sensitive, and allows the distinction between pan-nuclear staining and focus formation, and it is this approach that is being employed in efforts to develop high throughput techniques[142].

Although initially this biomarker was used to identify ionizing radiation effects, several studies have already used the γH2AX phosphorylation technique to measure DSB caused by different MNMs, including carbon nanotubes[151,152], zinc oxide[144], gold[153], silica[154], nanodiamands[80,96], tungsten cobalt[79], polystyrene[97], TiO_2 NPs[155,156] and WC-Co NPs (Fig. 11) showing that this technique can be a useful tool to assess the genotoxic potential of NMs. However, counting γH2AX foci is usually done manually by microscopy, which is time-consuming and cumbersome.

Therefore, efforts have been made to improve this method, based on microscopy techniques such as imaging modalities in cell culture and in tissues[157], and computer-assisted approaches[158]. The computational approaches are supported by image analysis software such as NIH Image and its Windows counterpart ScionImage, ImageJ, HistoLab, AutoQuantX or Image Pro, among others, which rely on different computational algorithms for foci identification or the calculation of quantitative foci parameters[159-161]. High content imaging systems are also capable of γH2AX quantitation. Specialised software for counting foci (FociCounter) has been developed[162]. The latest development is the incorporation of focus counting into an automated high throughput image acquisition and processing platform[163]. Recently, Harris *et al.*[68] have analysed the H2AX phosphorylation induced by iron oxide NPs using a high content platform, demonstrating the possibility of using this technique with exposures such as NPs. These different computational approaches render conventional γH2AX assay as a highly efficient HTS technique. At the same time they allow the analysis of other parameters in a cell population, while avoiding possible operator manipulation error. These are some of the several options that could contribute to utilising the full potential of the γH2AX assay for assessing the DSB produced by MNMs.

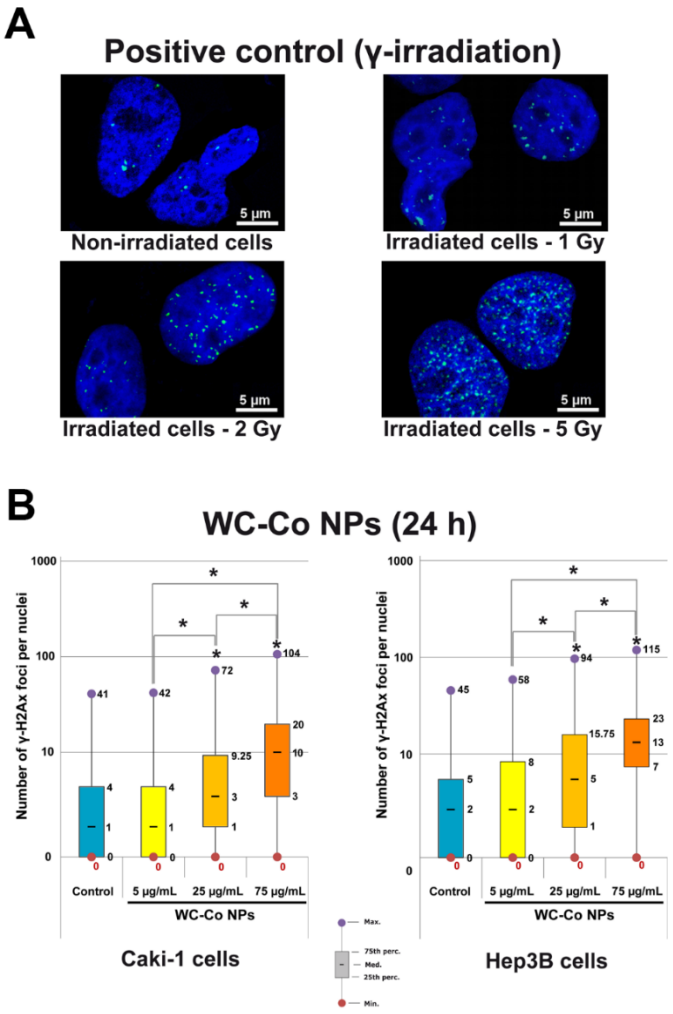

Fig. 11. ***WC-Co NP genotoxicity determined by measuring γ-H2Ax foci.*** *Counts of γ-H2Ax foci were performed on at least 200 cells per condition and the results are depicted as box plot distribution values [minimum (min), maximum (max), median, 25th and 75th percentiles] of the number of foci obtained for each tested condition. A Wilcoxon rank test was performed for statistical comparisons (i.e. versus control cells not exposed to NPs; *p<0.01). For both cell lines Caki-1 and Hep3B, WC-Co NPs were found to be genotoxic in a dose-dependent manner (B). For γ-H2Ax positive control, Caki-1 cells were exposed to gamma irradiation (A).*

2.3.3.9 High-throughput omics assays

Omics-based methods have the potential broadly to indicate toxicity of MNMs on a systems biology level. Recent studies have shown that data from such methods, in combination with phenotypical HTS results, can be integrated to reveal complex physiological and toxicological effects of MNMs as well as of chemicals, drug molecules, or the complex mixtures in consumer products (reviewed in [164, 165]. Omics analysis is normally classified as a form of HCA, but is relatively costly and slower than typical robotics-assisted HTS methods. Typically, omics testing involves the use of chip-based or sequencing technologies for genome-wide profiling of gene activities, e.g. measuring mRNA levels following a toxic insult. However, reduced sets of toxicity-associated genes can be assayed at higher throughput and lower cost, e.g., with Luminex® technology[166]. Future high-throughput transcriptomics platforms, e.g. in the LINCS and the Tox21 Phase III projects, enable rapid gene profiling experiments with both several doses and biological replicates using multiple model of 800-1500 genes[167,168]. MNM effects analysed using traditional microarrays, such as Affymetrix GeneChips®, form the basis for most existing gene profiling analyses of MNMs[169,170], providing

reference values for recent next-generation sequencing (e.g.,[171] and future generation of HTS data from selected toxicity-reflective gene sets. Open source or commercial bioinformatics tools, such as – respectively – InCroMap or Ingenuity Pathway Analysis (Ingenuity® Systems, www.ingenuity.com), rapidly sort omics-derived data into mechanistically meaningful results, enabling grouping of MNMs into clusters by gene or pathway activation levels[172]. Connectivity mapping, i.e. grouping for similarities in gene expression profiles, can be viewed as a form of biological read-across[173]. Modelling efforts have indicated a need for investigating more than 200 and even thousands of agents, whether MNMs or chemicals, to effectively characterise toxicity mechanisms through omics analysis[174]. The well-known Connectivity Map project[175], and its successor LINCS, have addressed this issue with over 1.5 million gene expression profiles covering over 10^5 variables to date[168]. Overall, data integration across high-throughput, high-content, pathway-based cellular assays and omics profiling will enable a diversified view of the potential toxicological activity of a MNM. Tiered HTS approaches including toxicity assessment and immunochemical assays followed by omics analysis, lead to gradually broader characterization of intoxicating concentrations of selected, potentially class-representative MNMs[164,165]. Such efforts promise efficiently to define relevant toxic modes-of-action of MNMs, via comprehensive evaluations of existing omics data collections aimed at systems toxicology.

2.3.4 Cost-effectiveness of high-throughput screening of nanomaterials

Even though only safe NPs/MNMs should reach the market place, the conventional methodologies for conducting hazard assessment have not been able to keep pace with innovation, leading to the urgent need for innovative high throughput and cost-effective technologies. It has recently been estimated that the time taken to complete evaluation of existing MNMs would be more than 30 years and the costs for testing them on an individual basis would be prohibitive[176]. The HTS approaches for hazard assessment of MNMs described above clearly allow a reduction of the time required for toxicity testing while increasing data outcomes, but the cost-effectiveness of those approaches needs also to be considered. Analyses of cost-effectiveness involve complex economic indicators and have been used to measure the relative value of a new or modified technology in terms of the cost per benefit gained. This type of analysis takes into account short-term costs, e.g. the cost per new endpoint identified or per time saved, and long-term costs, e.g. the cost per hazardous MNM identified versus the gains in terms of human disease prevention and environment protection. Thus, while short-term costs comprise mainly the direct costs associated with laboratory expenditure, the long-term costs are related to the societal costs and are much more complex to measure. Focusing merely on direct costs, HTS for toxicity is expected to reduce the costs of MNM development, as has happened in drug discovery[177], as a result of the greater number of NPs/MNMs and experimental conditions simultaneously assayed, and the lower amounts of test samples and consumables required, provided that the adequate equipment or accessories are available in the laboratory. There should also be savings related to direct labour (e.g. decreased time required to complete each task and lower degree of expertise or training necessary) (Figures 1 and 10).

These advantages have been realised in an integrated study of iron oxide NP toxicity in which high-content-imaging endpoints for cell viability, oxidative stress and DNA damage (double-strand breaks) were employed, as well as the HTS Comet assay[68]. Three laboratories using the Comet assay have estimated the time taken to process one sample in the form of a mini-gel (excluding scoring) as between 4 and 9 times less than the time taken to process a sample in the conventional large gel format. Scoring time per gel using non-automated image analysis was roughly halved with minigels compared with standard gels, as time was saved on changing slides and refocusing. However, scoring is still the main bottleneck, and it needs to be made fully automatic.

Another example is the replacement of traditional microscopy by automated imaging in the micronucleus assay, also contributing to time saving and consequent decrease in labour costs. Moreover, the faster scanning of micronucleus slides using an automated platform has given the

possibility of increasing the statistical power of results, through maximising the number of cells scored, while still saving time compared with visual scoring[178]. Furthermore, the flow cytometric micronucleus assay allows the possibility of scoring tenfold more cells in the same period of time compared with the conventional microscopic evaluation, also increasing the statistical power of the assay.

Despite the unequivocal direct gains from applying HTS to nanotoxicology, the costs incurred by the laboratory can be prohibitive if the acquisition of expensive laboratory equipment (e.g. fully automated equipment for image analysis), and sophisticated tools for data analysis or on-line data storage capacity are needed for its implementation[179]. The investment can, however, be justified depending on the number of tests and samples to be analysed, among other factors related to laboratory management.

Finally, regarding long-term costs versus societal benefits, the promotion of more robust, diverse and adaptable HTS techniques for the safety assessment of MNMs, providing information early in the process of MNM development, will further minimise the costs resulting from a delayed finding of potential harm to human health and/or the environment, thus maximising the benefits of innovation.

With the growing numbers of engineered MNMs, there is a huge demand from the scientific community as well as the legislative institutions to come up with ways of accurate and rapid testing of MNM safety *in vitro*. The adoption of HTS techniques for this task not only allows the examination of large numbers of different materials at different concentrations and on different types of cells, but also makes substantial savings in time and cost, as well as reducing the effect of experimental variation.

Validation of *in vitro* HTS tests is essential, with regard to their relevance to *in vivo* conditions. Also, validated HTS approaches to assess dose- and time-dependent toxicity that are predictive of *in vivo* adverse effects are required. HTS/HCA methods for studying cellular uptake and intercellular transfer, with automated imaging and image analysis, and reduced-feature gene sets and biomarkers predictive of toxicity effects should be developed. The crucial toxicity endpoints include cytotoxicity, oxidative stress, genotoxicity and markers indicative of cell transformation and carcinogenicity.

Automation should further streamline testing procedures, and – linked with appropriate standard operating procedures – this should contribute substantially to reducing variability and operator bias. HTS is bound to generate large data collections, and to encourage research groups to establish databases on relevant toxicological determinants of MNMs. The availability of a bank of reliable information about MNM toxicity will facilitate grouping approaches and the selection of class-representative materials that require animal testing. Finally, future efforts of HTS and HCA should also consider means of potentially automating the preparation and dispersion of MNMs, as this task is so far mostly manually performed, leading to a less than desirable output of data from the increasingly growing array of HTS approaches reviewed here.

MNMs display singular physicochemical properties that can bias the results of conventional toxicity assays [58, 180, 181] depending both on the assay and on the MNM. Positive and negative controls should be systematically included in experiments, in order to confirm the sensitivity of the techniques used, to assess potential NM interferences with assays or detection systems, and to benchmark the cytotoxic/genotoxic effects of tested MNMs. Recently, several suitable candidate control NMs have been described. Iron oxide was suggested as a positive control for cytotoxicity, oxidative stress and genotoxicity endpoints and PLGA-PEO as a negative control[118,128]. Also aminated polystyrene nanobeads were suggested as a positive control for acute toxicity[96,105], including cytotoxicity and membrane damage[182] but also activation of the inflamasome pathway[183,184], while carboxylated nanodiamonds (as negative control) were found to be neither cytotoxic nor genotoxic on several human cell lines[96]. These last two kinds of MNMs have already

been assessed on the xCELLigence® system, and results were very close to (i) those obtained by cell mortality detection using flow cytometry[96], and (ii) results using conventional toxicity evaluation methods[105, 105-187].

2.3.5 Overview of applicability of HTS/HCA methods

Within this task partners reviewed the state of the art of high throughput methods used in pharma industry and other fields. We evaluated the usefulness of HTS/HCA methods for hazard and risk assessment of MNMs. The review paper was published in 2016[191] (see Annex 1). The advantages and disadvantages of the HTS approaches and available HTS/HCA methods are listed in Table 1 (see Annex 2).

2.3.6 MNMs characterisation

The following MNMs were used in task 5.6: TiO_2 NM-100, NM-101, NM-103 and NM-104; ZnO NM-110, NM-111; SiO_2 NM-200, and NM-203; CeO_2 NM-212; $BaSO_4$ NM-220; Ag NM-300K and NM-302; carbon nanotubes NM-400, NM-401, NM-411; red and green fluorescent negatively or positively charged SiO_2 (provided by IIT) SiO_2@IIT 50 red(+), SiO_2@IIT 50 red(-), SiO_2@IIT 50 green(+), SiO_2@IIT 50 green(-), SiO_2@IIT 115 red(+), SiO_2@IIT 115 red(-), SiO_2@IIT25 red(+), and SiO_2@IIT25 red(-).

Eleven MNMs were common for the partners in task 5.6:
TiO_2 NM-100, NM-101, NM-103; ZnO NM-110, NM-111; SiO_2 NM-200, and NM-203; CeO_2 NM-212; $BaSO_4$ NM-220; Ag NM-300K and NM-302.

All MNMs were dispersed according to the NANOGEONOTOX protocol, starting with the including preparation of a water- 0.05% BSA stock solution at 2.56 mg/ml, which was then diluted into appropriate culture media before exposure to cells. Data regarding the size distribution and morphology of NMs in stock solution and in culture media at different incubation times were obtained by dynamic light scattering (DLS), Nanotracker and TEM and can be found in the NANoREG results repository (ISA-TAB tables, or CIRCABC).

2.4 Results

Results obtained in this task are described by methods and endpoints measured.

During the course of the project several HTS/HCA methods were developed, established and adjusted for hazard assessment of MNMs (see Annex 3, Table 2 and excel file) in parallel with standard methods (see Annex 5, SOP Table and handbook with 19 SOPs).

The NMs dispersions for the *in vitro* assays were prepared per the NANOGENOTOX dispersion protocol[201].

Task 5.6 has investigated the cyto- and geno-toxicity of a total of 23 MNMs on cell lines representative of main organs of exposure and retention: a common cell line, i.e., A549 (alveoli), V79 (lung fibroblast), Calu-3 & BEAS-2B (bronchia), Caki-1 (kidney), Hep3B (liver), Caco-2 (intenstine), SaOS-2 (bone), primary gingival fibroblasts (GF) (oral), TK6 & L5178Y & THP-1 & U937 (immune response).

The following MNMs were used altogether in task 5.6: TiO_2 NM-100, NM-101, NM-103 and NM-104; ZnO NM-110, NM-111; SiO_2 NM-200, and NM-203; CeO_2 NM-212; $BaSO_4$ NM-220; Ag NM-300K and NM-302; carbon nanotubes NM-400, NM-401, NM-411; red and green fluorescent negatively or positively charged SiO_2 (provided by IIT) SiO_2@IIT 50 red(+), SiO_2@IIT 50 red(-), SiO_2@IIT 50 green(+), SiO_2@IIT 50 green(-), SiO_2@IIT 115 red(+), SiO_2@IIT 115 red(-), SiO_2@IIT25 red(+), and SiO_2@IIT25 red(-).

Of the 23 MNMs, 11 MNMs were common in task 5.6: TiO_2 NM-100, NM-101, NM-103; ZnO NM-110, NM-111; SiO_2 NM-200, and NM-203; CeO_2 NM-212; $BaSO_4$ NM-220; Ag NM-300K and NM-302.

Stable dispersions have been obtained for the 23 MNMs tested with HTS/HCA methods (overview see Table 2) and an enormous amount of data has been generated. These studies show the robustness of HTS assay. All results have been uploaded into the NANoREG/TNO database. Preliminary comparison with standard assays show that both standard as well as HTS/HCA approaches are giving similar results (see D5.6). An example of standard versus HTS method for endpoint of DNA damage based on the Comet assay and number of MNMs tested can be seen is in Table 3.

Most of the HTS/HCA assays address cytotoxicity and genotoxicity.

For a reliable and fast screening of cytotoxicity of MNMs one of the assays with great potential is real time bioimpedance assay.

The Comet assay is a robust technique which has been successfully adapted for high-throughput. Based on the experience gained in NANoREG, further enhancement of throughput is being done.

HCA techniques have provided valuable structural and mechanistic data with high amount of information per each condition (cell type, MNM) tested.

The results were in concordance with those obtained by standard, or low throughput methods (see D5.6). Many results performed within task 5.6 were already reported in other Deliverables, especially in D5.05 (Report on cell type and in vitro-in vivo correlation studies for inhalation toxicity) and D5.06 (Identification and optimization of the most suitable in vitro methodology) as both HTS and HCA were used in D5.05 and D5.06 such as Ion beam microscopy (IBM) techniques as micro-proton induced X-ray emission (μPIXE) and micro-Rutherford backscattering (μRBS). These methods were applied to quantify the intracellular concentration of MNMs in cells under *in vitro* and *in vivo* conditions. Knowledge of cellular uptake under *in vivo* conditions is the basis for addressing the question of the *vitro-vivo* relevance on a quantitative basis (also reported in Task 4.4) – D4.04 Organ burden and particle detection pattern in other organs after subacute exposure. Flow cytometry for ROS, DNA damage, gene mutations, micronucleus and inflammation analysis were largly reported in D5.06.

Deliverable D5.06 reports on the use of “standard” toxicity assays applied to safety assessment of MNM such as genotoxicity, generation of oxidative species or expression of interleukins. Several such assays have been adapted to medium-high throughput by the incorporation of multiwell plates (96, 386 wells). Following this reasoning, several partners from task 5.5 took advantage of expertise from task 5.6 to carry out traditional assays in a time efficient and cost efficient manner. Results from such assays, though reported in D5.06, were carried out in a high throughput fashion without need to adapt the phys-chem protocols since, in all cases, the dispersion of one particular MNM was used to study toxic responses on several cell lines.

2.4.1 Stable MNM dispersion were obtained using the NANOGENOTOX protocol

Analyses of size distribution of MNMs in water-BSA stock solution and in complete cell culture media at the beginning and at the end of exposure were performed by DLS (Z-sizer) and Nanoparticle Tracking Analysis (NTAer. Additionally transmission electron microscopy (TEM) was performed.

A total of 23 MNMs were used in task 5.6, 11 of which were common. The NANOGENTOX dispersion protocol was used by all partners. For the common 11 materials, the DLS measurements performed by UiB (39) using a Zetasizer Nano ZSP device (Malvern Instruments, Malvern, UK) in batch solution and in complete McCoys and DMEM cell culture media are presented in the panel below (t0= time of exposure, t24 = at end of exposure, i.e., 24h).

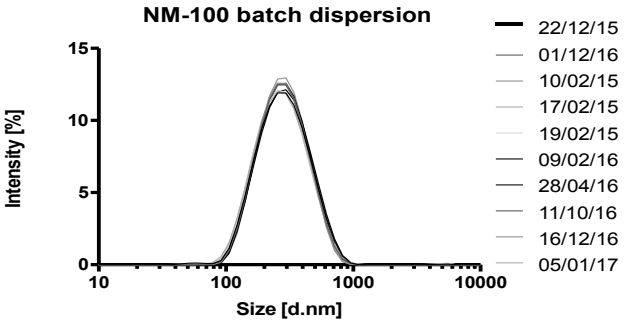
NM-100 batch dispersion
Intensity [%]
Size [d.nm]
22/12/15
01/12/16
10/02/15
17/02/15
19/02/15
09/02/16
28/04/16
11/10/16
16/12/16
05/01/17

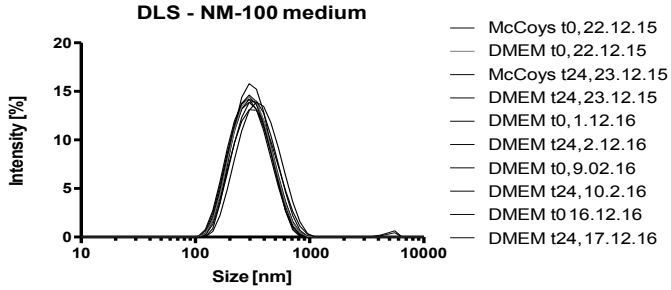
DLS - NM-100 medium
Intensity [%]
Size [nm]
McCoys t0, 22.12.15
DMEM t0, 22.12.15
McCoys t24, 23.12.15
DMEM t24, 23.12.15
DMEM t0, 1.12.16
DMEM t24, 2.12.16
DMEM t0, 9.02.16
DMEM t24, 10.2.16
DMEM t0 16.12.16
DMEM t24, 17.12.16

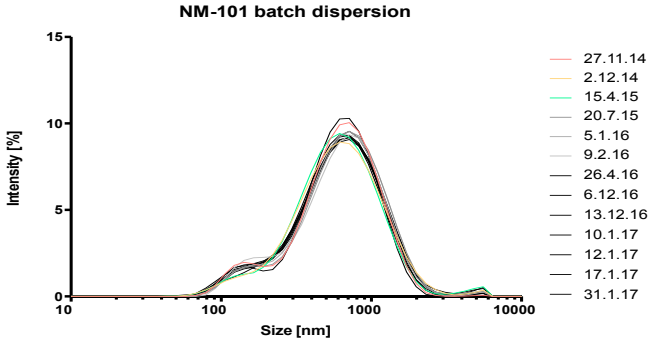
NM-101 batch dispersion
Intensity [%]
Size [nm]
27.11.14
2.12.14
15.4.15
20.7.15
5.1.16
9.2.16
26.4.16
6.12.16
13.12.16
10.1.17
12.1.17
17.1.17
31.1.17

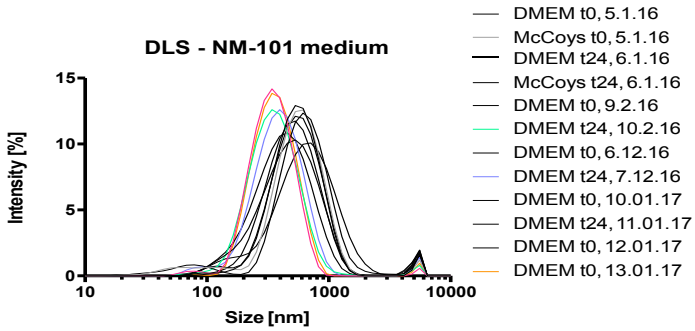
DLS - NM-101 medium
Intensity [%]
Size [nm]
DMEM t0, 5.1.16
McCoys t0, 5.1.16
DMEM t24, 6.1.16
McCoys t24, 6.1.16
DMEM t0, 9.2.16
DMEM t24, 10.2.16
DMEM t0, 6.12.16
DMEM t24, 7.12.16
DMEM t0, 10.01.17
DMEM t24, 11.01.17
DMEM t0, 12.01.17
DMEM t0, 13.01.17

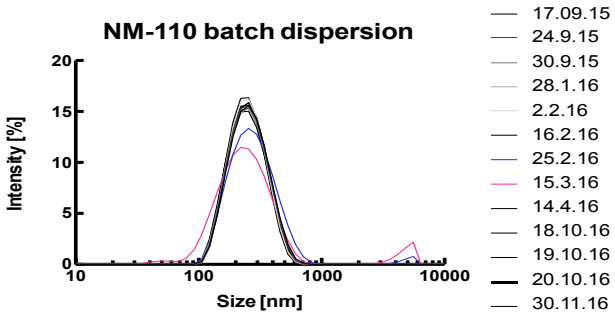
NM-110 batch dispersion
Intensity [%]
Size [nm]
17.09.15
24.9.15
30.9.15
28.1.16
2.2.16
16.2.16
25.2.16
15.3.16
14.4.16
18.10.16
19.10.16
20.10.16
30.11.16

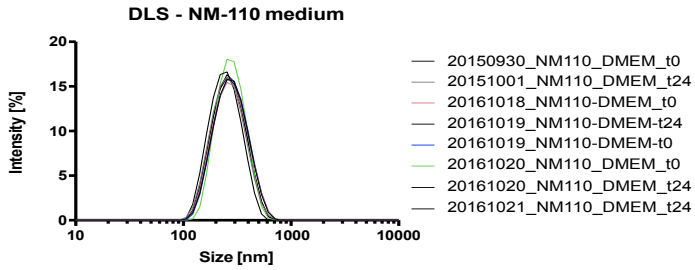
DLS - NM-110 medium
Intensity [%]
Size [nm]
20150930_NM110_DMEM_t0
20151001_NM110_DMEM_t24
20161018_NM110-DMEM_t0
20161019_NM110-DMEM-t24
20161019_NM110-DMEM-t0
20161020_NM110_DMEM_t0
20161020_NM110_DMEM_t24
20161021_NM110_DMEM_t24

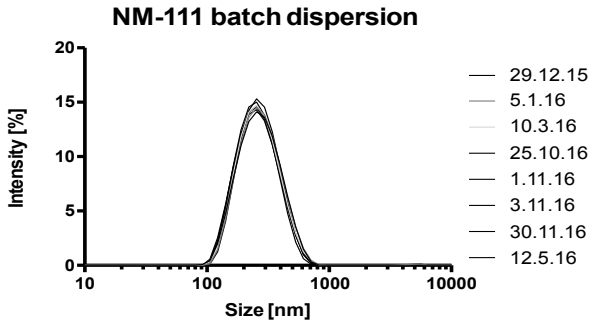
NM-111 batch dispersion
Intensity [%]
Size [nm]
29.12.15
5.1.16
10.3.16
25.10.16
1.11.16
3.11.16
30.11.16
12.5.16

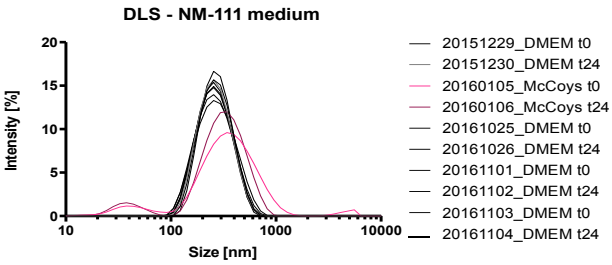
DLS - NM-111 medium
Intensity [%]
Size [nm]
20151229_DMEM t0
20151230_DMEM t24
20160105_McCoys t0
20160106_McCoys t24
20161025_DMEM t0
20161026_DMEM t24
20161101_DMEM t0
20161102_DMEM t24
20161103_DMEM t0
20161104_DMEM t24

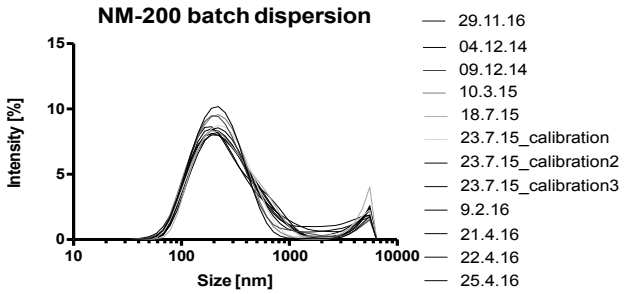
NM-200 batch dispersion
Intensity [%]
Size [nm]
29.11.16
04.12.14
09.12.14
10.3.15
18.7.15
23.7.15_calibration
23.7.15_calibration2
23.7.15_calibration3
9.2.16
21.4.16
22.4.16
25.4.16

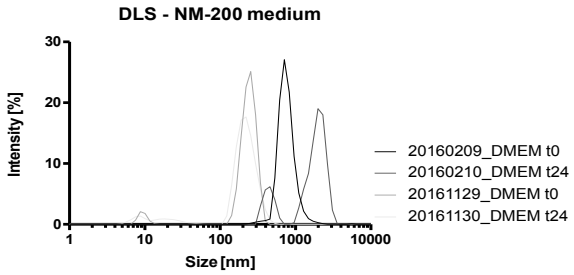
DLS - NM-200 medium
Intensity [%]
Size [nm]
20160209_DMEM t0
20160210_DMEM t24
20161129_DMEM t0
20161130_DMEM t24

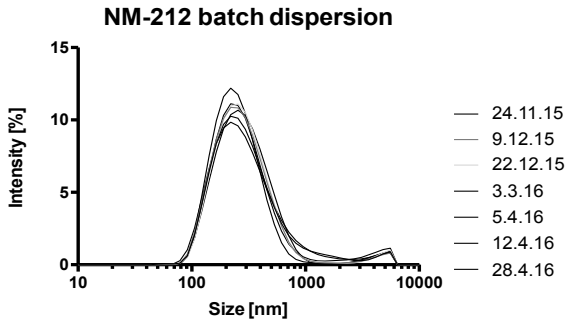
NM-212 batch dispersion
Intensity [%]
Size [nm]
24.11.15
9.12.15
22.12.15
3.3.16
5.4.16
12.4.16
28.4.16

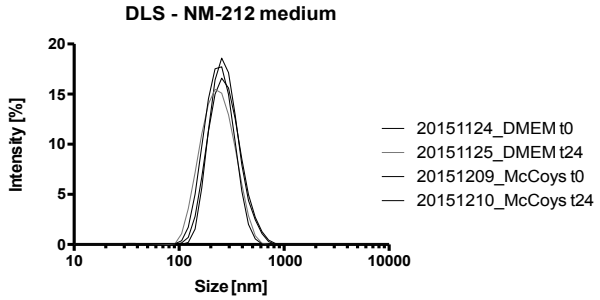
DLS - NM-212 medium
Intensity [%]
Size [nm]
20151124_DMEM t0
20151125_DMEM t24
20151209_McCoys t0
20151210_McCoys t24

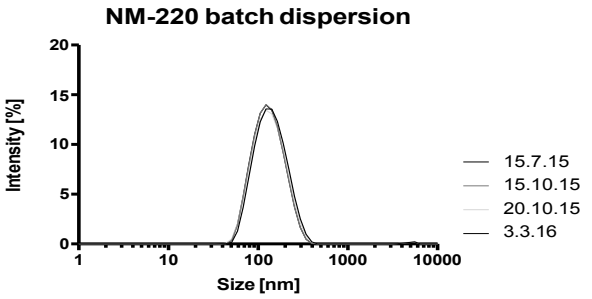
NM-220 batch dispersion
Intensity [%]
Size [nm]
15.7.15
15.10.15
20.10.15
3.3.16

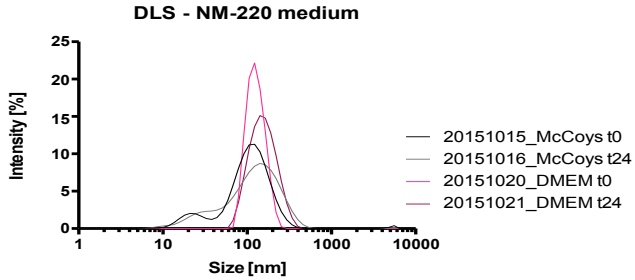
DLS - NM-220 medium
Intensity [%]
Size [nm]
20151015_McCoys t0
20151016_McCoys t24
20151020_DMEM t0
20151021_DMEM t24

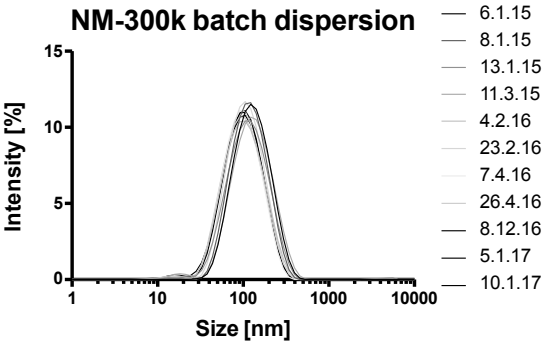
NM-300k batch dispersion
Intensity [%]
Size [nm]
6.1.15
8.1.15
13.1.15
11.3.15
4.2.16
23.2.16
7.4.16
26.4.16
8.12.16
5.1.17
10.1.17

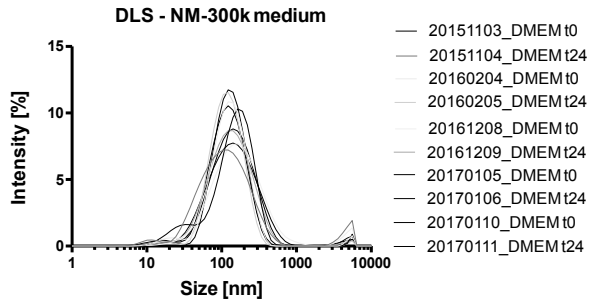
DLS - NM-300k medium
Intensity [%]
Size [nm]
20151103_DMEM t0
20151104_DMEM t24
20160204_DMEM t0
20160205_DMEM t24
20161208_DMEM t0
20161209_DMEM t24
20170105_DMEM t0
20170106_DMEM t24
20170110_DMEM t0
20170111_DMEM t24

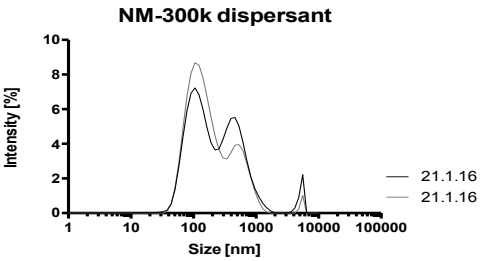
NM-300k dispersant
Intensity [%]
Size [nm]
21.1.16
21.1.16

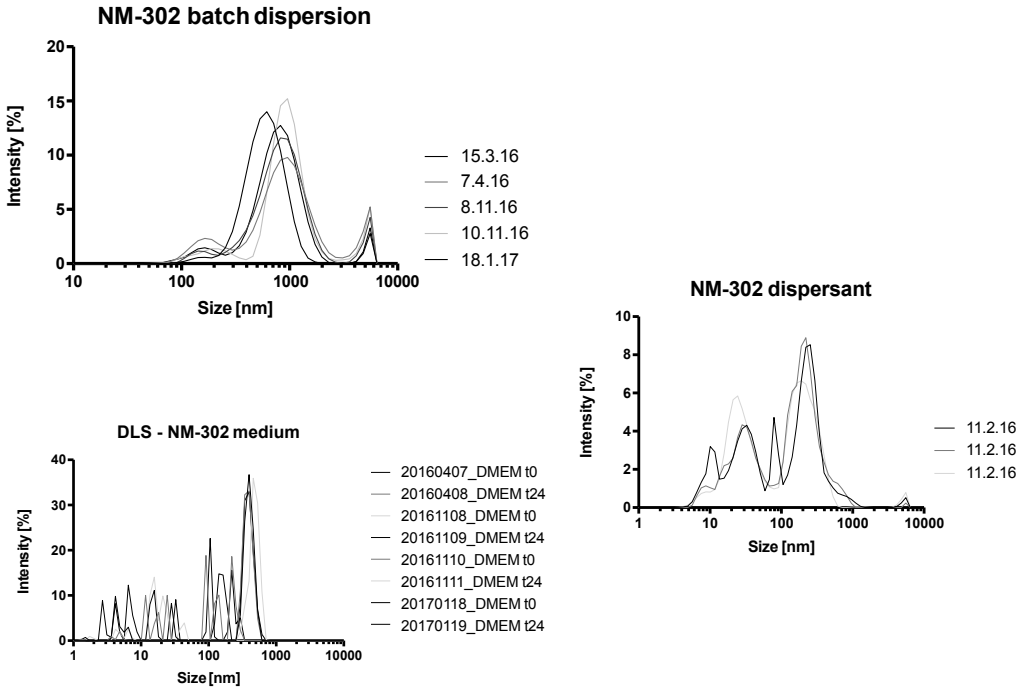

NILU characterized MNM dispersion with Nanoparticle Tracking Analysis (Nanosight 500) in stock dispersion as well as in medium in time 0 as well as after 3 and 24h exposure with all 20 MNM dispersion. Below there are summary data for 11 MNMs.

		STOCK (0h)		DMEM 0h		DMEM 3h		
NM code	**NM**	**Mean size**	**Mode size**	**Mean size**	**Mode size**	**Mean size**	**Mode size**	**Shape**
NM100	TiO_2	194,6	158,1	195,7	163,0	189,0	152,0	Spherical
NM101	TiO_2	179,6	122,4	175,5	102,5	231,7	197,0	Spherical
NM103	TiO_2	229,0	202,8	210,5	177,8	200,0	172,0	Spherical
NM104	TiO_2	244,0	214,4	179,3	150,8	186,8	160,3	Spherical
NM110	ZnO	188,5	169,2	148,0	140,8	230,7	192,3	Spherical
NM200	SiO_2	192,3	150,5	237,0	188,5	260,0	194,3	Spherical
NM212	CeO_2	216,4	191,3	174,2	120,4	214,0	163,7	Spherical
NM220	Ba_2SO_4	131,8	98,5	130,3	114,3	134,5	113,5	Spherical
NM300K	Ag	65,1	42,4	65,4	46,2	65,7	41,7	Spherical
NM302	Ag	172,4	83,6	172,8	84,8	133,0	58,5	Fiber
NM401	CNT	285,0	151,0	266,0	142,0	296,0	144,0	Fiber

Images from transmission electron microscopy performed by UiB (39) on the common 11 MNMs in batch solution are presented in the panel below:

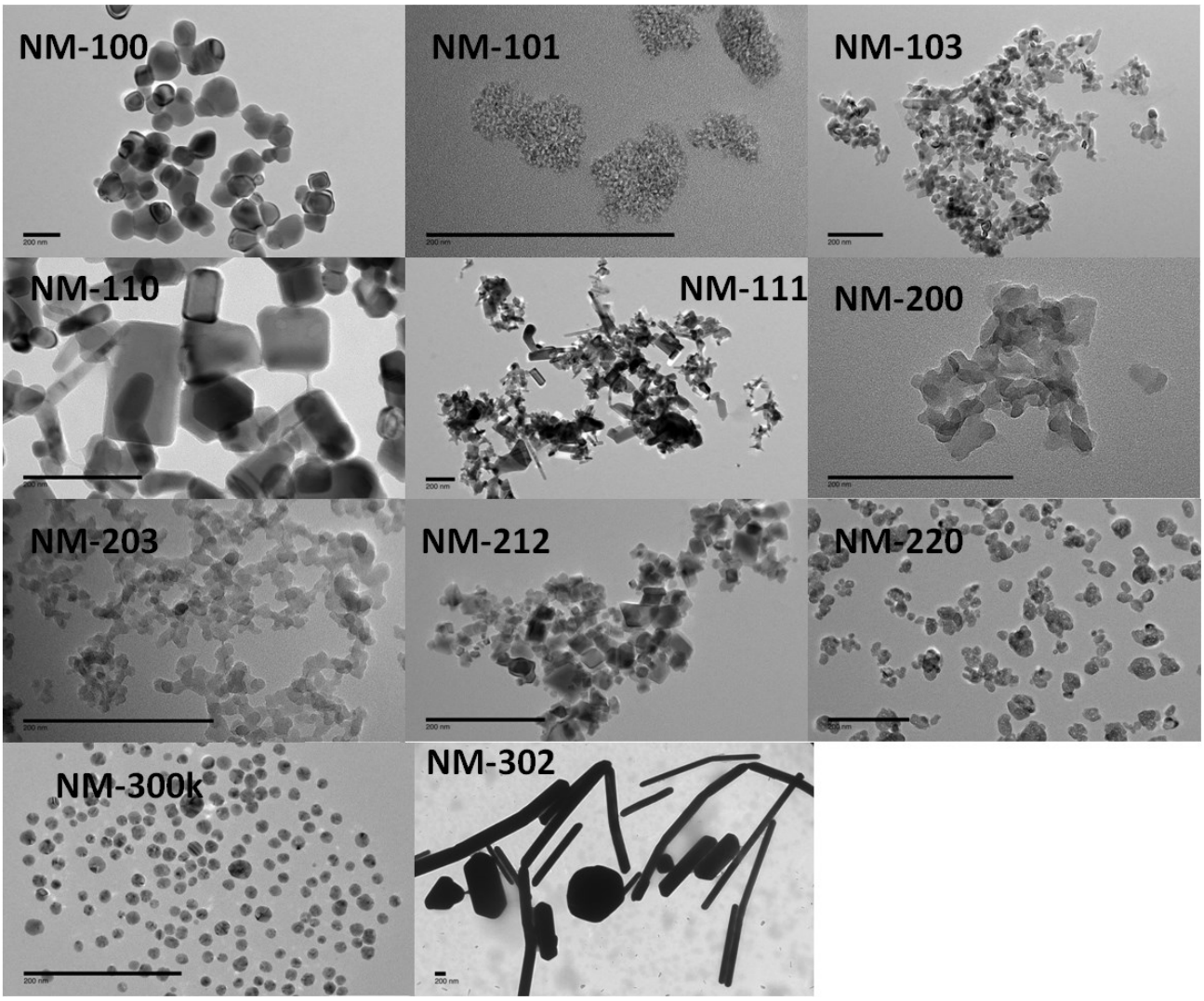

Fig. 12. Transmission electron microscopy of the common 11 MNMs used in task 5.6 dispersed in batch solution following the NANOGENOTOX protocol: *2.56 mg/ml powder dispersion in 0.05 wt% BSA-water (UiB 39).*

2.4.2 *Impedance-based real- time monitoring* (UiB 39 and CEA 23)

Cell viability, attachment and proliferation were assessed by impedance-based monitoring.
A common protocol was designed by the partners (UiB 39 and CEA 23) using the xCELLIgence system (ACEA Biosciences Inc), employing a common cell line (A549) at identical cell density. In addition, GF and SaOs-2 (UiB), Caki-1, HEP3B and Calu-3 (CEA) cells were also used. The cells were exposed to five MNM concentrations, of which four common (1, 10, 25, 50 µg/cm^2 corresponding to 2, 20, 50, 100 µg/mL) for 24 h (common expsoure time). CEA has additionally exposed cells up to 96 h. A total of 18 MNMs were tested, of which ten were common (NM-100, NM-101, NM-103, NM-110, NM-200, NM-203, NM-212, NM-220, NM-300k, NM-302).

Analysis protocol:

UiB and CEA defined a joint analysis procedure in order to facilitate inter-comparison.
To summarize, the following procedure was adopted:

1) Remove instrument errors: remove data of wells which can be rejected as instrument readout failure
2) Hose a normalization point: the corresponding Cell Index will be considered as the reference for all following measurement. It is the last measure before exposure start.
3) Calculate ratio by dividing the median of each condition (quadruplet), by the median of the corresponding control.
4) Calculate the SD from each quadruplet of each condition.
5) Upload the calculated ratio and corresponding SD on the online TNA database.

The preliminary toxicity rankings were:

A549, GF, SaOs-2 cells- overall ranking - (UiB 39): NM-300k > NM-111 > NM-110 > NM-302 >> NM-101, NM-103 > NM-220 > NM-203, NM-212, NM-100, NM-200 > SiO_2@IIT-25nm-green(-), SiO_2@IIT-115nm-red(+) > SiO_2@IIT-50nm-red(+), SiO_2@IIT-50nm-red(-), SiO_2@IIT-50nm-green (-), SiO_2@IIT-50nm-green(+), SiO_2@IIT-115nm-red(-) (Fig. 13).

A549 cells (CEA 23): NM-300k, NM-110 > NM-302, NM-200 > NM-100, NM-203 > NM-212, NM-220, NM-103.

Caki-1 cells, (CEA 23): NM-300k, NM-110 > NM-302 > NM-100, NM-203, NM-212, NM-220 > NM-103, NM-200 > NM-101 (Fig. 13).

HEP3B cells (CEA 23): NM-302, NM-300k, NM-110 > NM-212, NM-203 > NM-200, NM-103 > NM-220, NM-100.

Calu-3 cells (CEA 23): NM-300k > NM-302, NM-100 > NM-200 > NM-103, NM-220 > NM-203, NM-212.

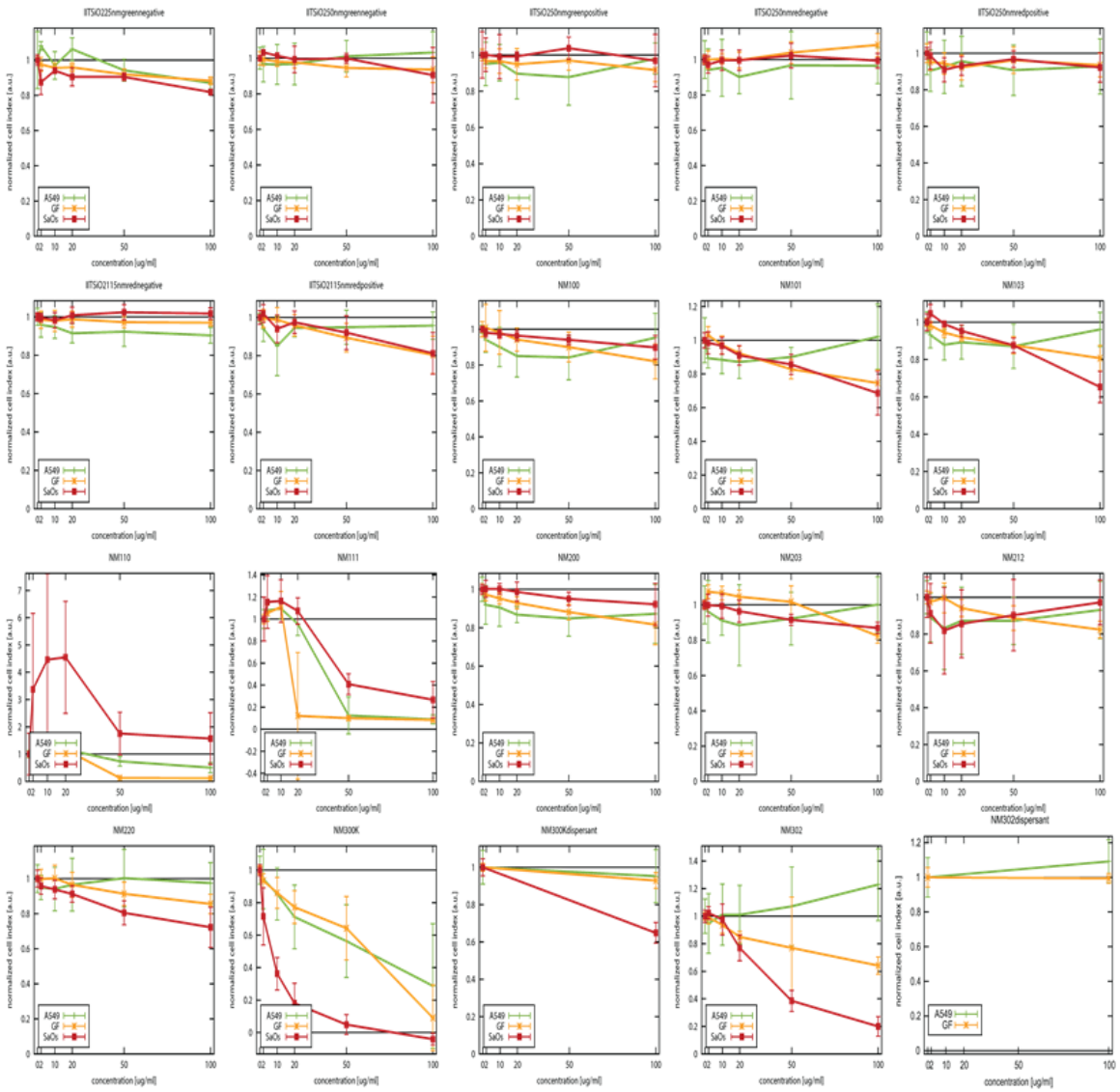

Fig. 13. Real-time impedance results (xCELLIgence system) *(UiB 39). Assessment of cell viability and proliferation on A549, GF,and SaOs-2 cells, exposed to 20 MNMs/dispersants at 1, 5, 10, 25, 50 µg/cm^2 (i.e., 2, 10, 20, 50, 100 µg/mL), for 24 h. Data points represent median with error bars. The cell index is normalized to the median of the control (0 µg/ml). Increased proliferation can be correlated to values over 1 and cell death to values below 1.*

Conclusion: The different cell lines (A549, GF, SaOs-2) reacted differently to different MNMs and MNM-concentrations. The most toxic MNMs were NM-110, NM-111, NM-300k and NM-302. NM-101 had a stronger effect on A549 cells at small concentrations than at higher concentrations. SiO_2 particles appeared to be generally mildly toxic or non-toxic.

A toxicity ranking can be suggested as follows: NM-300k > NM-111 > NM-110 > NM-302 >> NM-101, NM-103 > NM-220 > NM-203, NM-212, NM-100, NM-200 > SiO2-25nm-green(-), SiO2-115nm-red(+) > SiO2-50nm-red(+), SiO2-50nm-red(-), SiO2-50nm-green(-), SiO2-50nm-green(+), SiO2-115nm-red(-).

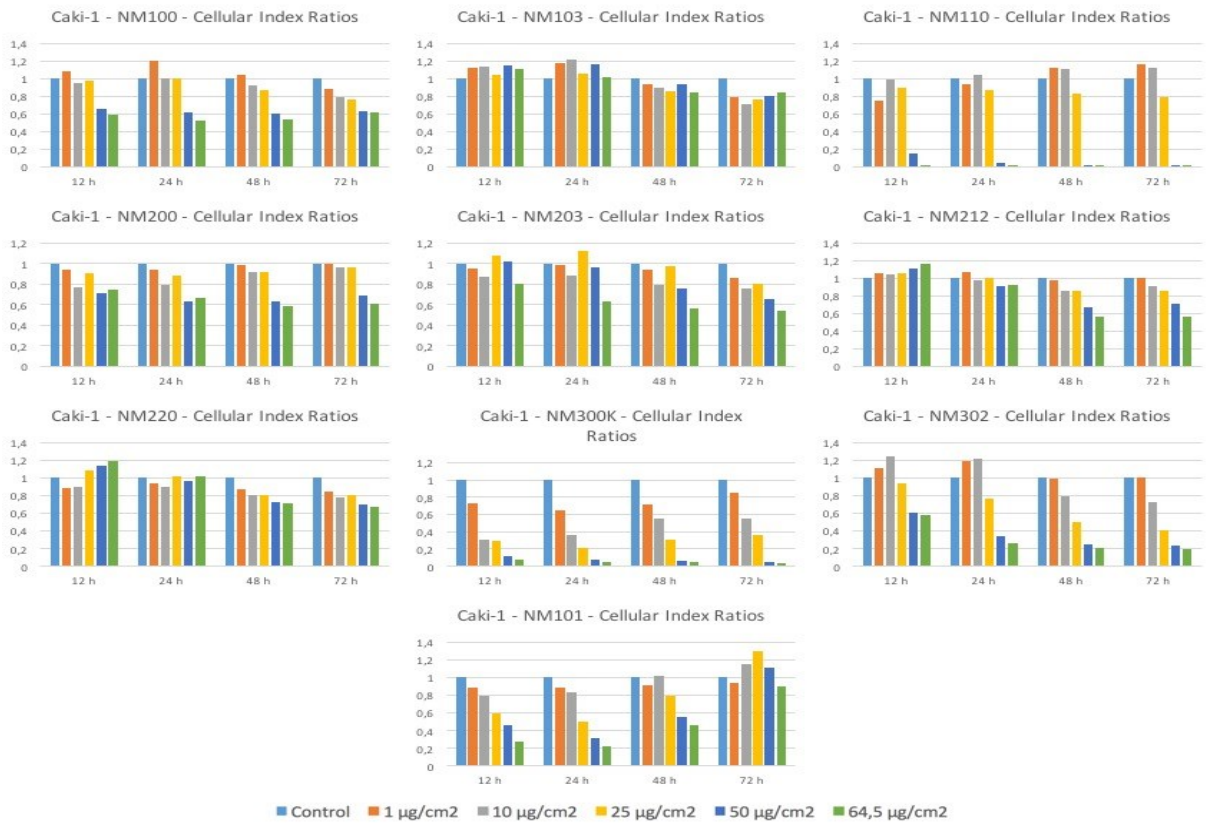

Fig. 14. Real-time impedance results (xCELLIgence system) *(CEA 23) for Caki-1 cells.*

By using a "Grouping Strategy" a ranking of the MNMs based on their physico-chemical characteristics and toxicity was made (Fig. 15). The grouping was made for 24 h exposure.

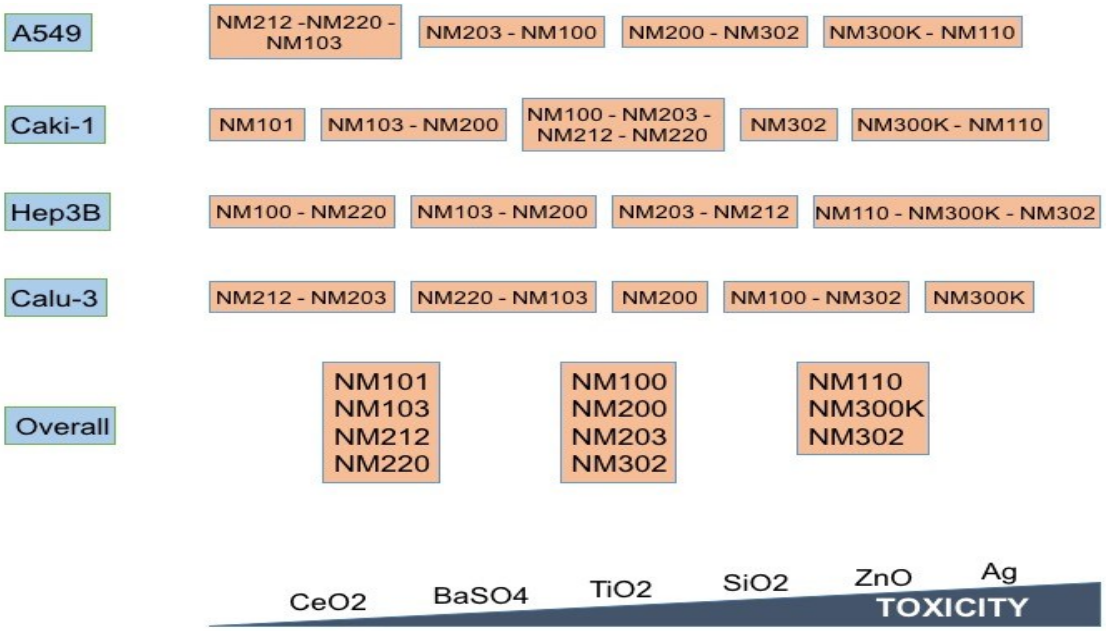

Fig. 15. Preliminary grouping and ranking of MNMs *based on real-time impedance monitoring (xCELLIgence) at 24 h exposure (CEA 23).*

When performing grouping and ranking after different times of exposure (12, 48 or 72 h), the classification changes. Indeed, it becomes apparent that the evolution of toxic effects of the MNMs is a dynamic process depending on the time of exposure (Fig. 16).

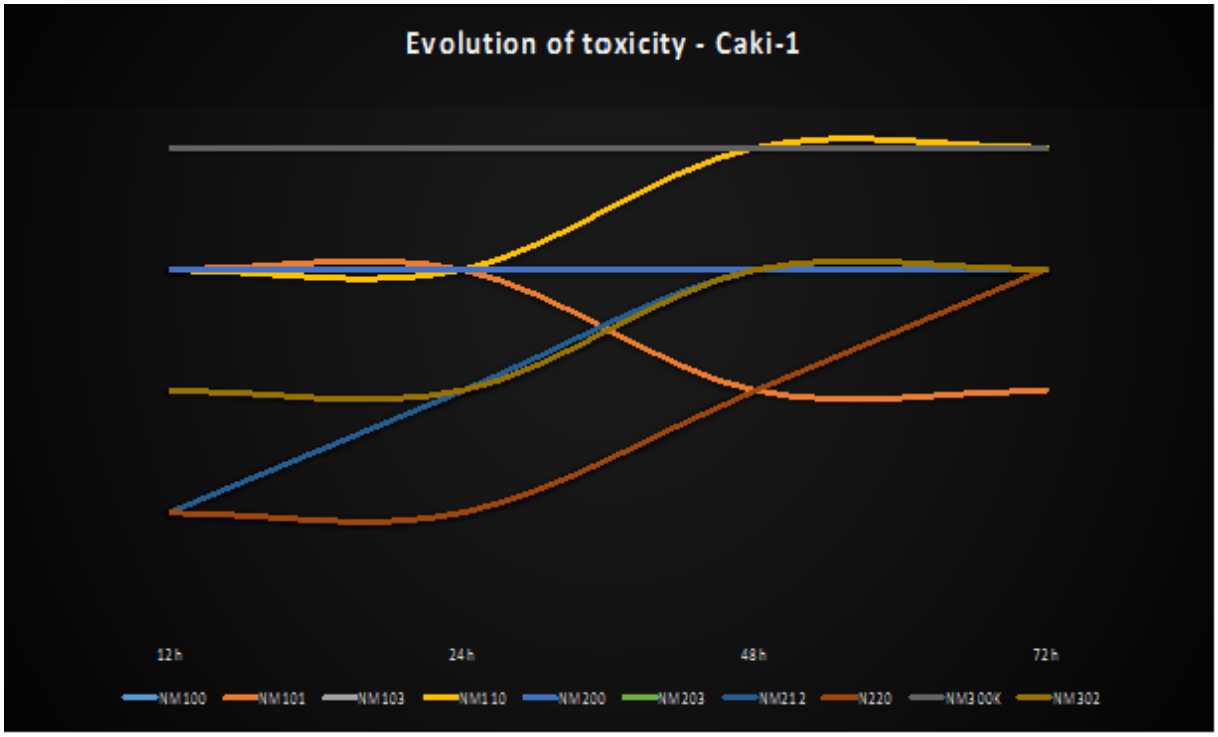

Fig. 16. MNM effects according to time of exposure: *Caki-1 cell line exposed to 10 MNMs for 72 h (CEA 23).*

The classification of the MNMs is not the same at 12 h and at 72 h (Fig. 17).

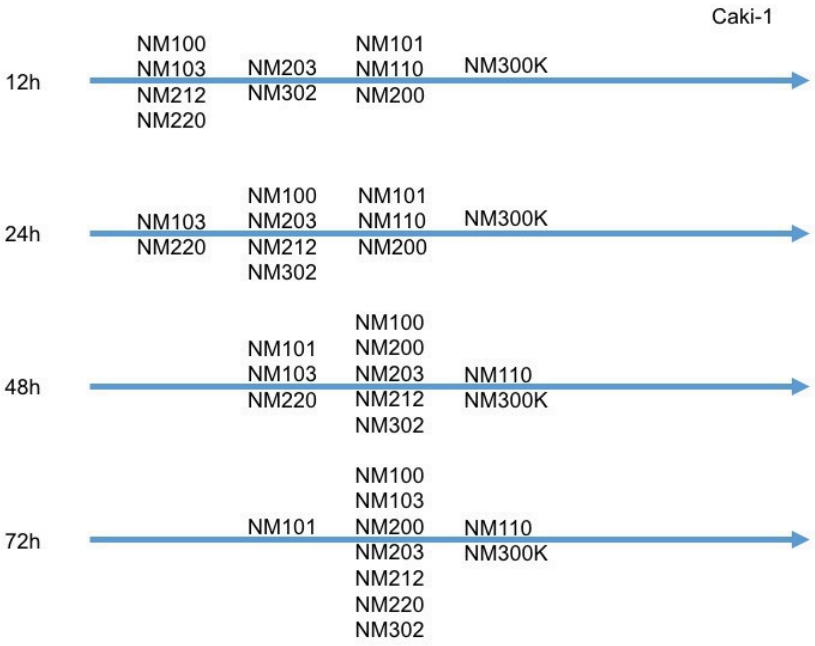

Fig. 17. Ranking of MNMs according to exposure time *(CEA 23).*

Extended analyses are currently being performed by CEA and UiB on data obtained by using the xCELLIgence system. The toxicity rankings obtained above are preliminary, the final ranking will be given after data analyses and method validations will be finalized.

2.4.3 Microfluidic-chip impedance-based flow cytometry

(UiB 39)

A microfluidc-chip impedance-based flow cytometer was used (Ampha Z30, Amphasys AG) to assess the viability and mode of cell death (apoptosis vs. necrosis) on U937 cells exposed for 24 h to 2, 10, 20, 50, 100 µg/mL (i.e., 1, 5, 10, 25, and 50 µg/cm^2) (Fig. 18).

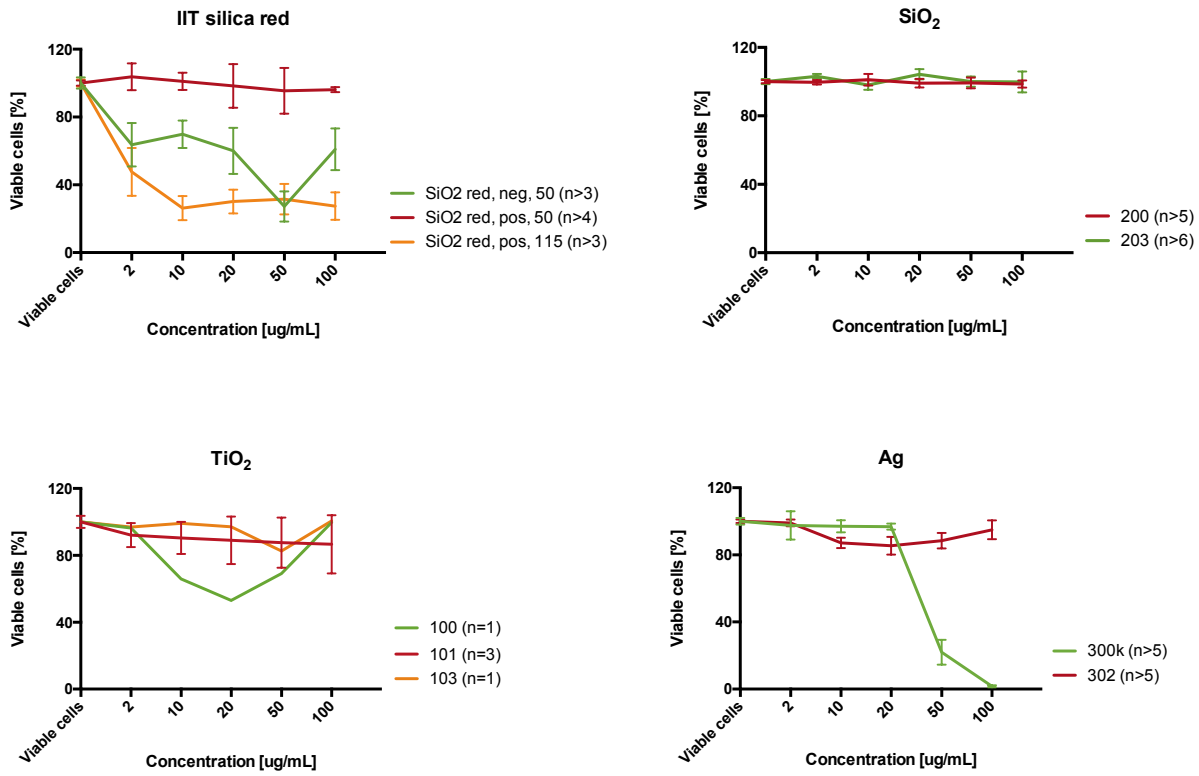

Fig. 18. Viability assessment by Ampha Z30 *(UiB 39). U937 cells, 10 NMs at 5 concentrations and 24 h exposure time. Data points represent the median normalised to viable cells plus SE bars.*

Conclusion: U937 cells reacted differently to different MNMs and MNM-concentrations. The most toxic NM was NM-300k (Ag). SiO_2 particles (NM-200 and NM-203) appeared to be mildly toxic or non-toxic. However, the SiO_2 particles 115nm red (+) from IIT showed a toxic effect on U937.
The following toxicity ranking can be suggested: NM-300k > SiO_2@IIT 115nm red(+), SiO_2@IIT 50nm red(-) > NM101, NM-302 > NM-100, NM-103, SiO_2@IIT 50nm red(+) > NM-200, NM-203.

2.4.4 Real time RT-PCR (UiB 39)

The mRNA expression level of different target genes (IL-6, IL-6, Bcl-2, Bax, RIPK1, FAS, SOD1, SOD2, NFKb1) was assessed in A549 (common cell line) and GF for the 10 common MNMs at 2 and 100 µg/mL (corresponding to 1 and 50 µg/cm^2) and 24 h exposure time.

The following overall preliminary toxicity ranking was obtained: NM-300k > NM-110 > NM-103 > NM-302 >> NM-101 > NM-203 > NM-212, NM-220 > NM-100, NM-200 (Fig. 19).

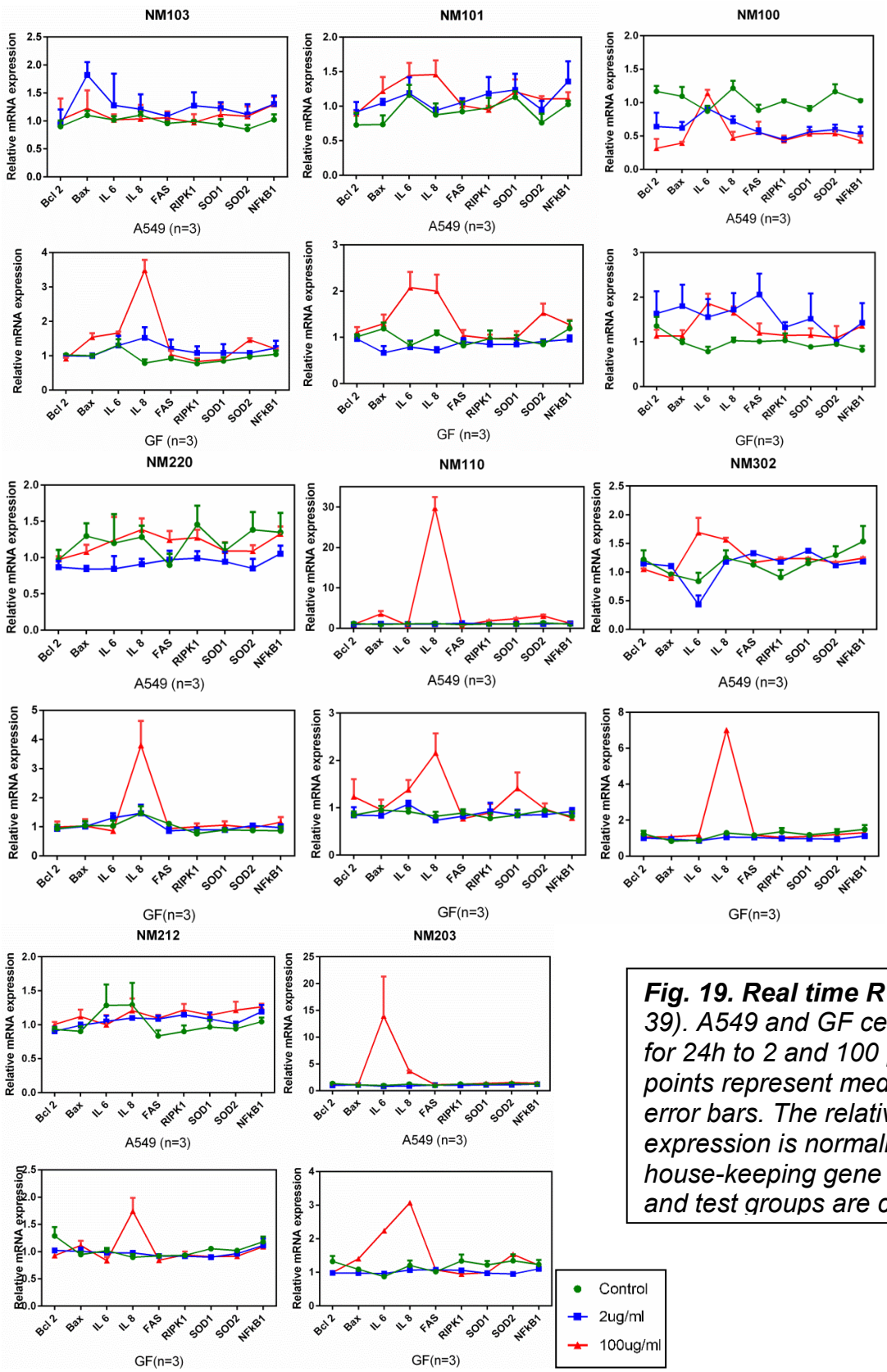

Fig. 19. Real time RT-PCR *(UiB 39). A549 and GF cells exposed for 24h to 2 and 100 µg/ml. Data points represent median with error bars. The relative mRNA expression is normalized to house-keeping gene GAPDH and test groups are compared*

Conclusion: The two cell types A549 and GF reacted differently to different MNMs and MNM-concentrations. The NMs which induced strongest effects were NM-110, NM-103, NM-300k and NM-302.

The following ranking can be suggested: NM-300k > NM-110 > NM-103 > NM-302 >> NM-101 > NM-203 > NM-212, NM-220 > NM-100, NM-200.

Overall conclusion on Impedance-based and real time RT-PCR results:
Although differences could be seen with regard to the sensitivity of each cell type, method (xCELLigence, AmphaZ30, real time RT-PCR) and laboratory performing the tests, the overall toxicity ranking was concordant for all three methods and partners involved, indicating that the methods are robust and can be employed in nanotoxicity testing. The most toxic particles at the tested concentrations and timepoints were NM-300k, NM-302, NM-110, and NM-111.

2.4.5 Cytotoxicity and Genotoxicity

Genotoxicity was always tested with cytotoxicity. The AlamarBlue (NILU, CBT) and MTS (IEM) have been used to investigate viability of A549 cells after exposure to 23 MNMs (AlamarBlue) or 11 MNMs (MTS assay). Additionally the *CFE assay* (NILU, INSA) was used together with the comet assay. For gene mutation test cell proliferation and plating efficiency was used and for the mucronucleus test proliferation index was used.

For the Comet assay non-cytotoxic concentrations of MNMs as determined in the MTS, AlamarBlue, and/or CFE. For mammalian gene mutation tests SOP12 and SOP13 and the micronucleus assay range of non-cytotoxic to cytotoxic concentrations was used.

2.4.5.1 Cytotoxicity and the Comet assay

Cytotoxicity was evaluated in A549 cells after 3 (AlamarBlue, NILU), 24 hour (AlamarBlue NILU, MTS, UAB, IEM) and continuous exposure (CFE, NILU) and are largely reported in D5.6.
IEM used MTS assay in 5 concentrations of NMs ranging from 1 µg/ml (= 0,3 µg/cm2) to 100 µg/ml (= 31,3 µg/cm2). Cytotoxicity was only observed in NM-110 and NM-300K (Figure 1).
Ranking NMs in the MTS assay (A549 cells): NM110 (LC50 = 35 ± 6 µg/ml) > NM300k (LC50 = 78 ± 2 µg/ml) > NM-200 = NM-203 = NM-212 = NM-220 = NM-302 (non-cytotoxic).

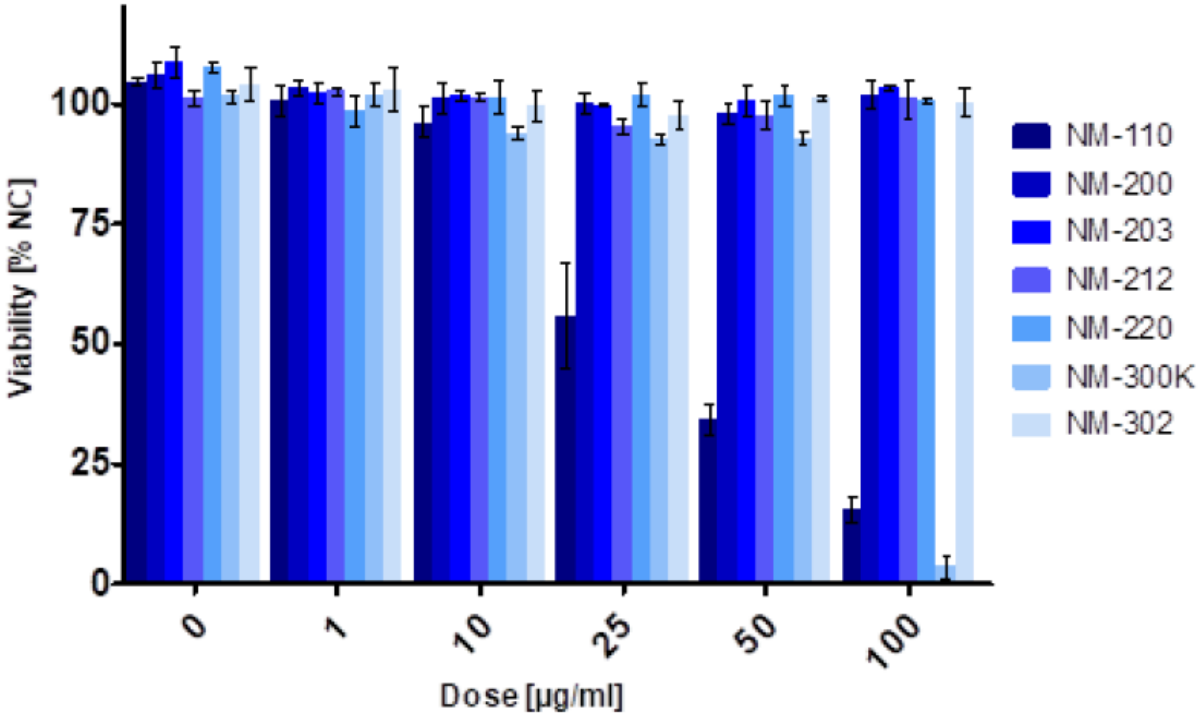

Fig. 20. *Viability of the A549 cells exposed to selected NMs for 24 h. Viability is expressed as % of negative control values that were assumed 100% viability. Bars represent average values (±SD) of three independent experiments (partner IEM).*

Within the Comet assay NILU and CBT tested over 20 MNMs. Comparison within 7 laboratories both using standard comet assay (2 gels) or HTS comet assay (12 or 20 mini gels) shows good concordance.

Altogether 11 NMs have been tested for *gene mutation by NILU, UAB and INSA SOP12 and SOP13*): NM-100, 101, 103, 104, 110, 300, 302, 401, 200, 203, 220. Among them carbon nanotubes NM-401 and silver nanorods NM-302 showed strong positive mutation potential. In this case, the effect was most likely due to shape rather than to chemical composition. Results are reported in D5.6 and several are already published[193,194].

The alkaline version of the Comet assay was performed in A549, TK6 and Beas2-B and Caco2 cells (for 2, 12 and 20 mini-gel slides) after 3 and 24h exposure with and without FPG to assess DNA strand breaks as well as oxidized purines. To increase the performance of the assay, 12 (developed within the COMICS project) and 20-mini gels slides (CometSlide™ 20 Well, Trevigen) were used. Several scoring systems Perceptive, and automated slide-scanning platform Metafer with the MetaCyte CometScan software were used to scan the slides.

Two protocols for the slide format has been used: 12 mini-gels (NILU SOP (HEALTH EFFECTS LABORATORY SOP code HEL11T005)) and 20-minigel slides (CometSlide™ 20 Well, Trevigen, Cat No 4252-02K-01). For 20-well slide experiments the assay was performed according to the manufacturer's instructions (Trevigen, 2016) following by the protocol for the comet assay provided to the NANoREG project partners by NILU, Comet assay with and without repair enzymes.

Preliminary NILU *genotoxicity* ranking based on the Comet assay on *A549* cells:

after *3h exposure*: NM111 > NM302 > NM110 > NM300K > NM203 > NM100 > NM220 > NM103 > NM104 > NM212 > NM101 > NM200

24h exposure: NM110 > NM302 > NM111 > NM300K > NM100 > NM200 > NM203 > NM101 > NM220 > NM103 > NM104.

Table 3: An overview of the comet assay experiments *using both standard (UAB, IEM, FIOH, GAIKER, KI) as well as HTS version (NILU, CBT, UAB, IEM). Preliminary results are rported in D5.6.*

Comet assay	
NILU (Norway) –	18 NMs including 2 fluorescent silicas tested with A549 cells: DNA strand breaks and oxidised purines (Fpg-sensitive sites)
CBT (Norway) –	17 NPs tested with TK6 cells: DNA SBs and Fpg-sites
UAB (Spain) –	8 NMs tested with BEAS-2B cells: DNA SBs and Fpg-sites
IEM (Czech Rep) –	8 NMs tested with A549 cells: DNA SBs and Fpg-sites
FIOH (Finland) –	5 cellulose NMs tested with BEAS-2B cells
Gaiker (Spain) –	4 NPs tested in Caco2 cells: DNA SBs and Fpg-sites
Karolinska (Sweden) –	3 TiO_2 NMs tested with BEAS-2B cells: DNA SBs and Fpg-sites

In the Comet assay (A549 cells, 24h exposure), an increase in % tail DNA was observed especially after NM-110, NM-300K and NM-203. Oxidative DNA damage represented by net FPG values was increased in NM-110 and NM-300k, but the increase was not dose-dependent (Fig. 20). The results were in concorance with those obtained by standard, or low throughput methods (see D 5.6).

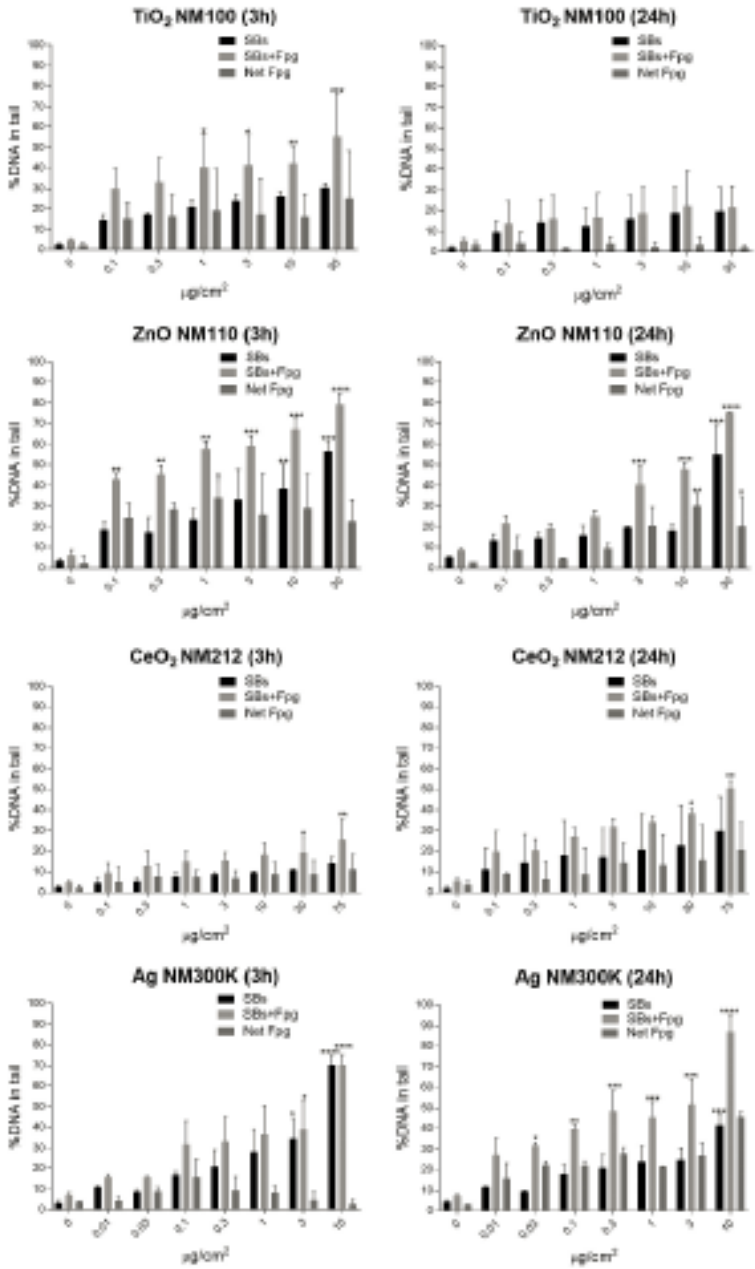

Fig. 21. Comet assay *after 3 and 24h exposure to TiO_2, ZnO CeO_2 and Ag NMNs in A549 cells.*

Partner IEM tested 7 MNMs with 20 gel format Comet assay (A549 cells, 24h exposure, IEM), an increase in % tail DNA was observed in NM 300K and NM 110 exhibiting cytotoxicity at concentrations of 100 µg/ml or lower (NM-110 cytotoxic at 25 µg/ml and NM-300K cytotoxic at 100 µg/ml) even at non-cytotoxic concentrations. A dose-dependent increase in DNA strand breaks was also observed in NM-203, but not in other tested samples, namely NM-200, NM-212, NM-220 and NM-302 Figure 22).

Oxidative DNA damage represented by net FPG values was increased in NM-110 and NM-300K, but the increase was not dose-dependent (Figure 22).

Ranking NMs in the Comet assay (Strand breaks) (A549 cells): NM-110 > NM-300K > NM-203 > NM-200 = NM-212 = NM-220 = NM-302.

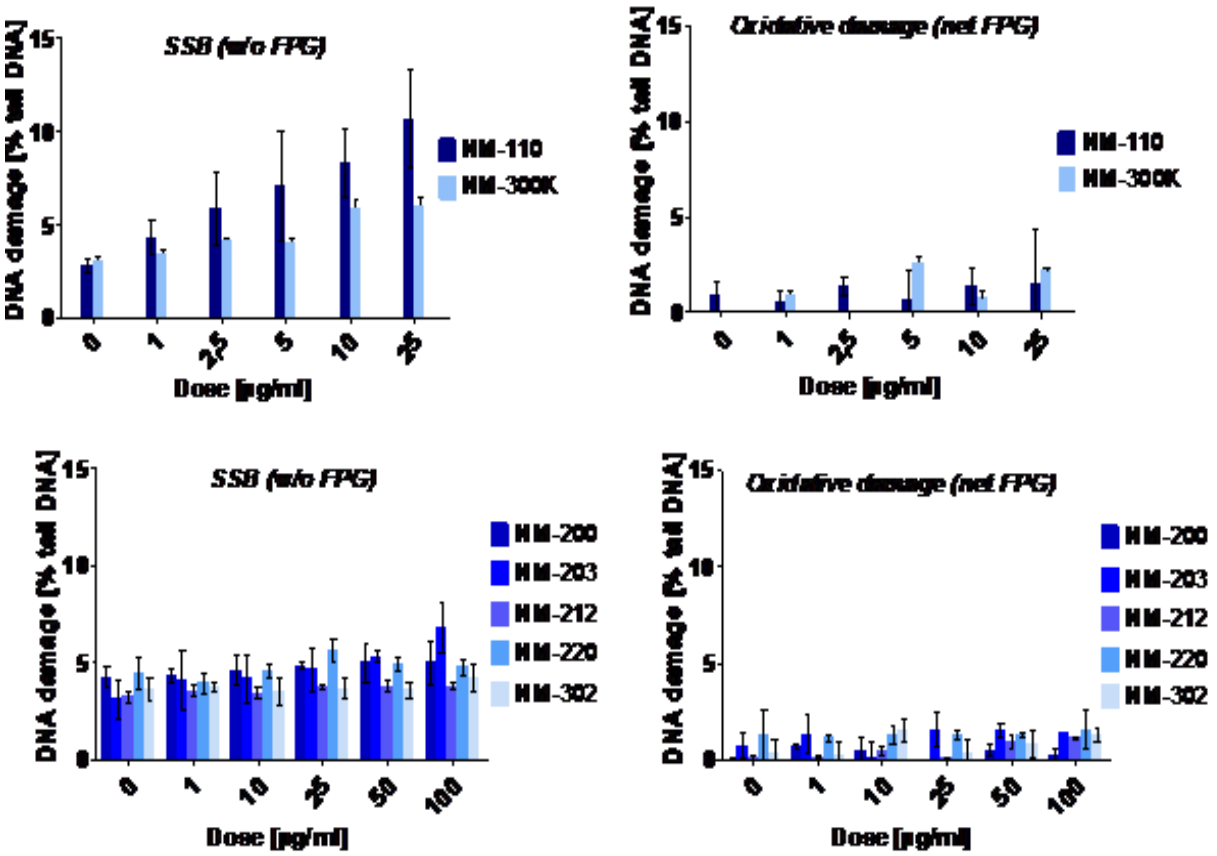

***Fig. 22**: DNA damage in A549 cells exposed to selected MNMs for 24 h. NM110 and NM300k were tested in doses ranging from 1 to 25 µg/ml and for NM200, 203, 212, 220 and 302 in non-cytotoxic concentrations up to 100 µg/ml. Strand breaks as well as oxidised DNA damage were assessed. Bars represent average values (±SD) of medians obtained from three independent experiments.*

2.4.5.2 Micronucleus assay

The Micronucleus assay was performed by UAB according to the SOP15 and by IEM according to the protocol published by Fenech[192] using 8-well Lab-Tek™ Chamber Slide System (Nalge Nunc International). We consider this method to be medium-to-low throughput (preparation of the slides using Lab-Tek™ Chamber Slide System is medium throughput, manual scoring of micronuclei is low throughput)[192].

In the micronucleus assay (IEM, BEAS-2B cells, 28 and 48h exposure), the number of micronuclei was always higher at 48h exposure than at 28h exposure. Negative controls were very stable with an average number of 1.99% (+/- 0.05%) micronuclei (Fig. 23).

Ranking NMs in the micronucleus assay (BEAS-2B cells): NM-200 > NM-302 > NM-101.

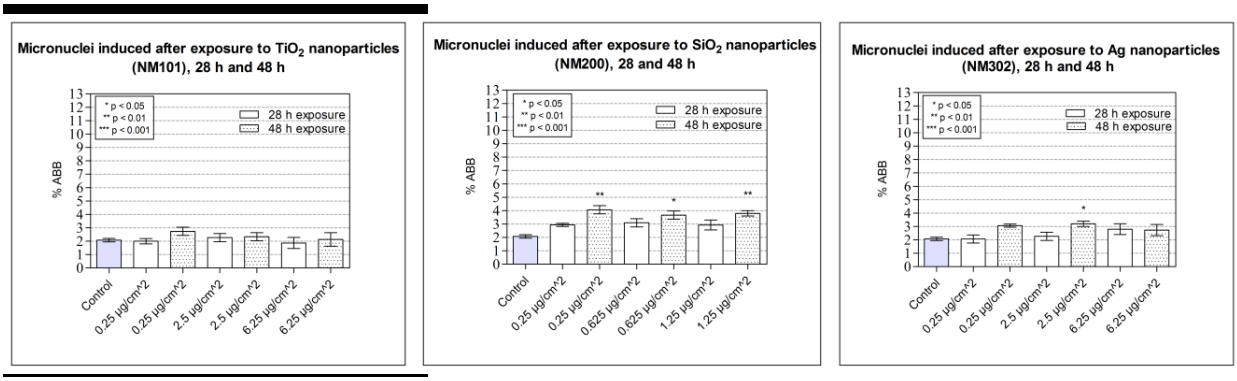

Fig. 23. Micronuclei in BEAS-2B cells exposed to selected NMs for 28 and 48 h.

2.4.5.3 Strategy for increased throughput testing for cyto- and geno-toxicity

The limitation is based on the number of MNMs that are possible to be tested, thus throughput is increased with number of cell lines and time endpoints. The experiments performed with reference MNMs showed great potential for HTS/HCA methods with high capacity to test several dozen MNMs per day (depending on type of HTS/HCA method). However, this appeared not be practically possible.

The reason for not being able to fully explore the HTS/HCA methods for MNM testing is the time consuming, low throughput MNM characterisation. One of the requirements in the NANoREG project was to characterise NMs always before, during and after the treatment of cells and thus in vitro HTS/HCA testing should be coupled with characterisation. Characterisation methods, however, are not yet developed for HTS. This is the biggest challenge for MNM testing with HTS/HCA approaches. To at least partially overcome this, for cytoxicity/genotoxicity HTS we modified study design to be able to test four MNMs in one run, including characterisation of NMs before during and after the treatment and using 2 methods for cytotoxicity, several endpoints for genotoxicity, two cell lines and two treatment time points (Fig. 22).

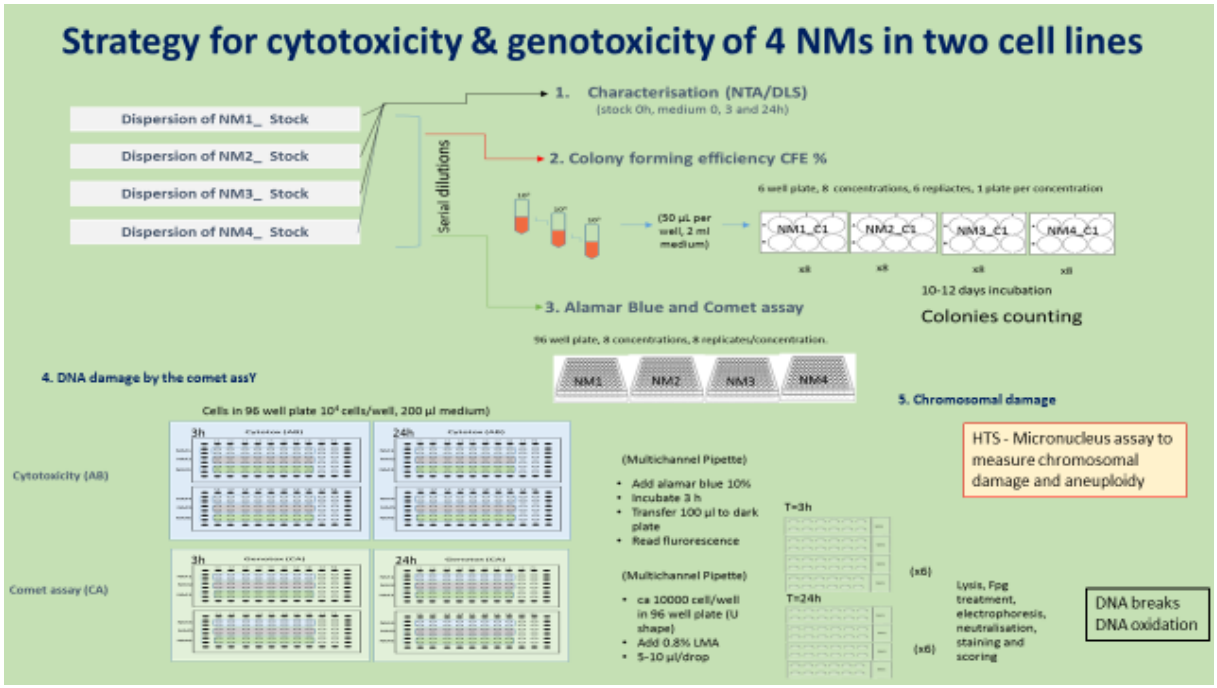

Fig. 24. Suggested strategy with increased throughput for cytotoxicity (AlamarBlue and Colony forming efficiency – CFE) and genotoxicity (DNA damage by the Comet assay and Micronucleus assay by flow cytometry) for testing four MNMs.

2.4.6 MNM cellular translocation and uptake quantification by means of label-free dosimetric and imaging techniques

2.4.6.1 Molecule-based imaging technique: confocal Raman microspectroscopy (CRM)

Intracellular uptake and distribution pattern of CeO_2 (NM-212), $BaSO_4$ (NM-220), ZnO (NM-110) and TiO_2 (NM-103, NM-104) were monitored in human epithelial lung A549 and Caco-2 cells. Quantification of NP uptake weighted to cellular protein content, internalization as well as their co-localization with different cell components and biomolecules were studied with respect to the toxic effects of these MNMs observed *in vitro* and *in vivo* studies (WP4). The monitoring of MNMs in A549 and Caco-2 cancer cells showed different uptake and intracellular processing for the various MNMs.

ZnO (NM-110) were observed to be attached to the cell membrane and internalized only peripherally in the cell remaining in close vicinity to the plasma membrane. The phonon bands, which are characteristic for the crystalline structure of internalized particles, disappeared completely after very short time. This result proves a fast dissolution of ZnO (NM-110) after passing through the cell membrane within a time of 20 min. ZnO (NM-110) which were observed during the whole exposure time were found to be accumulated at the membrane surface from the outside. The very high rate of Zn^{2+} release explains the high toxicity ranking of ZnO NPs.

Different uptake and translocation were monitored for CeO_2 (NM-212) and $BaSO_4$ (NM-220). CeO_2 were found in peripheral cytoplasm close to the cell membrane (early endosomes) and in perinuclear regions (late endosomes/endolysosoms). Instead, $BaSO_4$ were almost entirely accumulated in the endoplasmic reticulum (ER) and also in the close vicinity of the nucleus membrane. A specific co-localization of $BaSO_4$ (NM-220) with ribosomes associated with the ER was observed.

Additionally, quantification of CeO_2 (NM-212) and $BaSO_4$ (NM-220) uptake weighted to cellular protein content at the single cell level was performed. Uptake rate was ca. 3.5 times higher for CeO_2 compared to $BaSO_4$ NP in the A549 cells exposed to NPs up to 100 µg/ml concentration.

2.4.6.2 Element based dosimetric/imaging techniques

The comparison of in vivo and in vitro uptake based on the knowledge on intracellular effective dose in culture cells and tissues was performed. The question of vitro-vivo relevance was addressed.

IBM method supports the CRM results showing the high uptake rate of CeO_2 (NM-212) in spite of their very low toxicity ranking.

The following uptake ranking was obtained in A549 cells exposed over 24h: NM-212 >> NM-110 > NM-103 > NM-104.

The element content and intracellular distribution of CeO_2 NPs were studied and compared to the cellular uptake from the 28 day CeO_2 inhalation study of Wistar rats at a single cell level. The average concentration of Ce in cells exposed to 10 µg/ml CeO_2 NM-212 amounted to ca. 17000 ppm. The mean cerium concentration in the septum of single alveoli was by a factor of 10 lower then as in in vitro experiments. Even the concentration in "hot spots" in alveolar septum was by a factor 3 times lower.

2.4.7 High Content Analysis

A total of six MNMs were tested in two cell lines, Caco-2 and A549 cells, using a High Content Analysis based approach. The MNMs evaluated included NM-103, NM-104, NM-203, NM-200, NM-110 and NM-300K. Eight markers of cellular toxicity were analyzed in each cell line and for each nanomaterial (Cytotoxicity (cell count, nuclear size and nuclear intensity), Apoptosis (active Caspase-3), genotoxicity (γH2AX, ATM phospho S1981, p53 phospho S15), and cell cycle (Ki-67).

Of the MNMs tested, only NM-300K and NM-110 generated cytotoxic responses in either cell line. In Caco-2 cells, NM-300K was the most cytotoxic, whereas in A549 cells, NM-110 was slightly more cytotoxic. Interestingly, in both cell lines, treatment with NM-300K resulted in a significant increase in nuclear size and nuclear intensity at non-cytotoxic concentrations.

NM-300K appeared to induce considerably greater genotoxic effects in Caco-2 cells compared to A549 cells, as seen by significant increases in γH2AX, ATM phospho S1981 and p53 phospho S15 levels at relatively low concentrations. In A549 cells however, it was NM-110 that induced the markers of genotoxicity, whereas NM-300K induced these markers only at cytotoxic concentrations.

2.4.8 Human in vitro whole blood assay (WBA) to determine MNM contamination with endotoxin.

The whole blood assay was performed by CNR who has applied the WBA assay to MNMs after having determined their contamination with endotoxin. CNR has examined the ability of 16 of the NANoREG core materials of which 11 used in task 5.6, all at 100 µg/ml, to induce an inflammatory response in human blood leukocytes, by using the standardised WBA assay adapted to NANoREG requirements. At this concentration, some of the NPs were still measurably contaminated with endotoxin, although at low levels (Table 4).

Table 4. ENDOTOXIN CONTAMINATION OF NANoREG CORE MATERIALS at 100 μg/ml

1	NM-100 (JRCNM1000a)	TiO_2	<0.10 EU/ml
2	NM-101 (JRCNM1001a)	TiO_2	0.05 EU/ml
3	NM-103 (JRCNM1003a)	TiO_2	0.05 EU/ml
4	NM-110 (JRCNM1100a)	ZnO	<0.04 EU/ml
5	NM-111 (JRCNM1101a)	ZnO	<0.01 EU/ml
6	NM-200 (JRCNM2000a)	SiO_2	0.03 EU/ml
7	NM-203	SiO_2	<0.10 EU/ml
8	NM-212 (JRC2102a)	CeO_2	<0.08 EU/ml
9	NM-220	$BaSO_4$	0.01 EU/ml
10	NM-300K <20 nm	Ag	<0.32 EU/ml
11	NM-302	Ag rods	<0.01 EU/ml

Most the MNMs had no direct inflammation-inducing effect in the WBA, except for MNM-110- (uncoated ZnO particles), as compared to the positive control (LPS 2.5 ng/ml).

In addition to their possible direct inflammatory effect, we did also examine the capacity of MNMs to interfere with the inflammation-inducing capacity of LPS. The results indicate that several NMs had little/no effect on the LPS capacity of inducing IL-1β production (NM-100, NM-103, NM-200, NM-212, NM-220, NM-300K, NM-302), while a few had some enhancing effect (NM-101, NM-110, NM203, the latter very pronounced). On the other hand only one NM had an appreciable inhibitory effect, *i.e.*, NM-111 (ZnO particles with a triethoxicaprylsilane coating).

2.4.9 Advantages and challenges of HTS/HCA approaches in MNM safety evaluation

A thorough literature review and analysis of HTS/HCA methods used in nanotoxicity testing, including the ones used in NANoREG, have been done by the task 5.6 partners and presented in a review article[191]. Advantages and challenges pertaining to HTS/HCA approaches in MNM safety evaluation have been identified and are summarised in Table 1 (Annex 2).

2.4.10 Methodological considerations

2.4.10.1 Genotoxicity vs. Cytotoxicity

An important part of genotoxicity testing is that each assay has to be performed within a specific toxicity range. This is crucial especially for the comet assay where nontoxic up to mild toxic concentrations should be used to avoid false positive results that might occur when toxic concentrations are applied. The *clonogenic assay (CFE),* as one of the earliest cytotoxicity test, gives an overview on both cytotoxic as well as cytostatic effect and can be used for calculation of lethal concetration 50% (LC50). This assay is not prone to interference and thus is specifically useful for testing MNMs. The assay is time consuming, however during the NANoREG project the throughput of this assay was increased by using a 6-well format and currently a 24-well format assay is under development. The *Alamar Blue* assay was successfully applied and its robustness increased in combination with the comet assay.

NB! AlamarBlue and other spectroscopic methods must be checked for the interference with MNMs.

For *in vitro* genotoxicity assessment, all major endpoints should be covered: DNA damage, gene mutations, chromosome breakage and/or rearrangements (clastogenicity), and numerical chromosome aberrations (aneuploidy) should be evaluated. Representative assays that can measure these endpoints are the Comet assay, mammalian gene mutation and micronucleus

assays. The standard low throughput genotoxicity assays applied for hazard assessment of chemicals are also applied for MNMs. Within the task 5.6 we adopted, developed, applied and standardized medium/high throughput genotoxicity assays based on standard already accepted tests, namely *mini-gel comet assay* for detection of DNA strand breaks and DNA oxidation lesions (oxidized purines), medium throughput gene mutation assay on 96 well format (Mouse lymphoma tests) and flow cytometry micronucleus assay.

Within the comet assay we tested over 20 MNMs. Comparison within 7 laboratories both using standard comet assay (2 gels) or HTS Comet assay (12 or 20 mini gels) shows good concordance.

For *point gene mutation*, the most commonly used assay the Ames test could not be applied especially because of bacteria as biological model, the bacterial wall and limited or no uptake of MNMs. Thus, the mammalian gene mutation test was the only option. Two gene mutation assays have been used, the point mutation in Hprt and Tk locus using V79 or mouse lymphoma L5178Y cells. Both assays are still very laborious but Mouse lymphoma assay in Tk locus has the advantage that a 96-well format can be used. This assay can be further adapted towards increasing of throughput. However, p53 competent cells should be preferably applied.

Impedance-based assays have the advantage of being label-free, non-invasive and less prone to interferences from MNMs. They can be used as a first line of cytotoxicity screening, especially the ones that perform continuous monitoring of the cells and which can give indications regarding relevant time-points and concentrations for more in depth mechanistic investigations.

2.4.10.2 MNM cellular translocation and uptake quantification by means of label-free dosimetric and imaging techniques

Confocal Raman microscopy as a fast, label-free and non-invasive imaging technique provides unique information about translocation and fate of NPs at subcellular level. The living cells as well as formaldehyde-fixed cells were investigated with the CRM at an excitation wavelength of 532 nm and a spatial resolution of about 260 nm.

Ion beam microscopy (IBM) as label-free imaging technique represents a unique possibility to perform the spatial resolved element analysis at single cell level. Two IBM techniques, as micro-resolved proton induced X-ray emission (μPIXE) and Rutherford backscattering (μRBS) analysis, were applied to quantify the intracellular concentration of NPs in alveolar cell under *in vitro* and *in vivo* condition. The comparison of in vivo and in vitro uptake based on the knowledge on intracellular effective dose in culture cells and tissues was performed. The question of vitro-vivo relevance was addressed. IBM method supported the CRM results showing the high uptake rate of CeO_2 NM-212.

The comparison of *in vitro* and *in vivo* intracellular concentrations has a fundamental meaning for addressing the question of the *vitro-vivo* relevance on quantitative basis. There could be two ways for assessing the *in vitro-vivo* relevance question: i) intracellular concentration under in vitro condition can be matched to in vivo concentrations by means of adjusting the applied dose; ii) comparison of toxic effects in vitro and in vivo on the basis of knowledge on intracellular effective dose in culture cells and tissues.

2.4.10.3 Challenges related to high-throughput suitability of NANoREG protocols for dispersion and physico-chemical characterisation of MNMs.

A common bottleneck for most partners in task 5.6 was represented by the fact that only one MNM could be dispersed at a time and in addition by the hydrodynamic diameter measurements that had to be done in parallel. Some of the partners tried to circumvent this by exposing several cell lines to more concentrations of the same MNM in order to make the most of both the dispersion obtained and of the amount of MNM in each vial. However, the number of cell types that could be handled simultaneously was limited.

Some partners (e.g., ANSES 35) opted for testing several MNMs at a time, still only a maximum of 4 MNMs could be tested in a single test due to the time constraints of the dispersion protocol (approximately 25 minutes per MNM). Using HCA, while only a limited number of MNMs could be tested within a single test, several different cellular markers were analyzed in a single test. So, although the number of MNMs that could be tested was limited, large amounts of quantitative data were extracted for each MNM.

One partner (UAB 27) has tested the effect that freezing in liquid nitrogen of several aliquoted dispersions of metal oxides and MWCNT MNMs had and found out that they maintained their physico-chemical characteristics upon thawing[188]. This approach indicates that exposure to frozen pre-dispersed MNMs can be done. The method needs further testing for validation and to find out for which types of particles and dispersion media it is suited for.

General recommendations, though not for high throughput, were made by one partner (UiB 39): use of thicker probe, replaceable tip, beaker with stage (plate that keeps probe more stable and allows its immersion at same depth each time), hold vial by screw lock, and cooling-ice always on top/around vial via buoyancy. For calibration (optimization): mathematics for calibration of small vessels (including heat loss through vessel walls) and automatic temperature logging by (small) temperature probe(s).

2.4.11 Establisment, optimization and evaluation of the suitability of different HTS/HCA methods to assess toxicity of MNMs

Several methods have been improved prior to and during the NANoREG project by the task 5.6 partners and can be applied in hazard assessment of MNMs (uptake, quantification, real-time and endpoint impedance-based methods, colony forming efficiency, comet assay, micronucleus assay, HCA).

The use of a microchip-based bioimpedance flow cytometry method (Ampha Z30) for nanotoxicity testing was successfully established for the first time in the NANoREG project.

A microfluidic prototype for HTS impedance-based cell analysis of MNM-toxicity in biomimetic dynamic conditions was designed and produced.

Within the task 5.6, up to 23 NANoREG MNMs have been tested by different HTS/HCA methods addressing the main toxicity endpoints, especially cytotoxicity and genotoxicity. A considerable amount of data has been generated and all data have been uploaded to the ISA-TAB database and in CIRCABC for further analysis within NanoReg2 project (for overview of data available see the NANoREG Results Repository). The data obtained show that the HTS/HCA methods employed are faster, more economical, are of high quality and show lower variation. Preliminary cytotoxicity and genotoxicity rankings show good concordance between themselves and with standard approaches. These data will be used for further analysis within the NanoReg2 project and for grouping, read across and development of in silico methods.

The testing strategy for in situ characterization, cytotoxicity and genotoxicity was designed with increased throughput that allows to test several MNMs in several cell lines, either continuously or at specific time points in one experiment. Nevertheless, coupling HTS methods with in situ characterization appeared to be biggest challenge as characterization is time consuming and limits the efficiency and robustness of HTS/HCA.

Each of the abovementioned techniques has both advantages and limitations and combinations of techniques are needed to answer the specific questions related to hazard evaluation of MNMs.

2.5 Recommendations, evaluation, conclusions and future perspectives

Methods for HTS/HCA screening have been adapted (based on established exiting methods) and new methods have been developed and applied for MNM testing. The work in task 5.6 resulted in a large amount of valuable results. An overview of assays performed, cell types used and MNM tested is presented in the Table 2 (Annex 3) showing that 23 MNMs have been tested with 11 MNMs that were common for all partners. All the data can be found in ISA-TAB and CIRCABC. Currently, extensive data analyses and inter-laboratory comparisons are performed by the partners. Based on these the validity of methods will be assessed. Several articles have been already published and presentations were made national and international meetings and conferences. One e-poster presentation with data from NANoREG has received the prize for best presentation (UiB 39: M Ostermann, Miami 2017). Publications are in progress to show establishment of new methods, comparisons between HTS methods with the same endpoints, the same HTS methods versus standard method, comparison of several endpoints with same MNMs, ranking of MNMs and overall evaluation (for the plan for publication see Table 5, Annex 4).

To be able to fully evaluate all the data comprehensive biostatistical analysis is needed and work has to be shared among all partners. Plan for data comparison and dissemination of results in form of publications is presented in Table 5 (Annex 4). The results obtained are valuable and will be used to answer the regulatory questions, as well as to make recommendations regarding MNM toxicity and methods that can be used. The preliminary evaluation of data show that the HTS/HCA approach in NANoREG has great potential and methods are reliable, robust and complementary and can be used to test the toxicity of MNMs. Since all methods have both advantages and limitations (for overview see Collins et al. 2016[191] and Table 1, Annex 1 and 2), a combination of methods should be used for each tested endpoint, preferably based on different principle of measurements.

However, methods for characterization are not yet developed to be coupled with HTS approaches and to overcome this, a closer collaboration is needed between scientists performing and developing tests for physico-chemical assessment of MNMs and toxicologists.

The main outcome of the task 5.6 can be summarized:

- Several HTS/HCA methods have been established and adjusted for MNM testing including Label-free cellular screening of MNM uptake, HCA, HTS flow cytometry, Impedance-based monitoring, Multiplex analysis of secreted products, and genotoxicity methods – namely HTS comet assay, HTS in vitro micronucleus assay, and γH2AX assay (see Table 2, Annex 3).
- Several methods have been improved and can be applied in hazard assessment of MNMs (uptake, quantification, bioimpedance test, colony forming efficiency, micronucleus assay, HCA).
- The use of a microchip-based bioimpedance flow cytometry method (Ampha Z30) for nanotoxicity testing was successfully established for the first time in the NANoREG project. A microfluidic prototype for HTS impedance-based cell analysis of MNM-toxicity in biomimetic dynamic conditions was designed and produced. The preliminary results have shown lower toxicity under dynamic exposure than in static conditions (traditional testing).
- The SOPs of the main methods were uploaded in the CIRCABC system and can be found in the Results repository of the NANoREG project.
- It was shown that HTS/HCA methods are faster, robust, more economical. HTS/HCA methods are generally of higher quality and show lower variation.
- For genotoxicity the Comet assay was miniaturized and throughput increased.
- Impressive amount of data has been generated and all data have been uploaded to the database for further analysis within NANoREG2 (for overview of methods, cells, and MNM tested see Table 2, Annex 3). Data can be used for grouping and read across and development of in silico methods.
- Preliminary cytotoxicity and genotoxicity rankings show an overall good concordance with each other and with standard approaches.

- HTS methods coupled with in situ characterization appeared to be the biggest challenge. Partners have tried to overcome this by adapting the testing strategy to allows testing of four MNMs in two cell lines and two time points in one experiment (NILU). ANSES (35) opted also for testing several MNMs at a time, still only a maximum of 4 MNMs could be tested in a single test due to the time constraints of the dispersion protocol (approximately 25 minutes per MNM). To make the most of both the dispersion obtained and of the amount of MNM in each vial UiB (39) tried to circumvent this by exposing several cell lines to more concentrations of the same NM in order. However, the number of cell types that could be handled simultaneously was limited. One partner (UAB 27) has tested the effect that freezing in liquid nitrogen of several aliquoted dispersions of metal oxides and MWCNT MNMs had and found out that they maintained their physico-chemical characteristics upon thawing (Vila et al. 2017). General recommendations, though not for high throughput, were made by one partner (UiB 39.

Future perspectives

- Main technical challenge and limitation is still the low throughput of the physic-chemicla characterization methods. Progress in this field is urgently needed and for this a closer collaboration between physicists/chemists and toxicologists is needed.
- The HTS/HCA methods can be further developed as ISO or OECD guidance documents
- Research towards new approaches in in vitro toxicity testing to develop in vitro methods that mimic in vivo situation is needed. The focus should be on miniaturization, on increasing the throughput and on developing biomimetic methods that reflect more closely the dynamics of the in vivo situation.
- Chronic exposure models need further development also towards HTS.

2.6 Data management

Partners involved in the Task 5.6 participated in preparation of ISA-TABs templates related to all endpoints that were detected following the SOPs listed in Annex X.

All SOPs have been collected and data were reported in ISA-TABs. There were several delays in uploading data to the TNO database but all results are now available and are being trasfered to the NANoREG2 database.

3 Deviations from the work plan

There has been occasionally a late dispatch of the NANoREG MNMs. The delay in the validation of the probe sonicator and the requirement that additional DLS and TEM measurements should be done have also contributed to delays in accomplishing the work. These have determined a later start of the experiments in task 5.6. As a result, although initially the testing of all NANoREG MNMs was envisioned, it was agreed that only 11 MNMs will be tested as common MNMs in task 5.6.

Despite of the delayed start and additional requirements, a great effort has been made by the partners and the experimental work was finished on time with a total number of 23 MNMs being tested.

This first version of this deliverable was deliverd in time, and the final version was provided later after substantial revision.

4 Performance of the partners

All partners contributed sufficiently by providing information, reviewing endpoints relevant to them and provided necessary data.

List of partners:

- Comet Biotech AS, and Department of Nutrition, University of Oslo, Norway
- Grup de Mutagènesi, Departament de Genètica i de Microbiologia, Facultat de Biociències, Universitat Autònoma de Barcelona, Bellaterra, Spain
- CIBER Epidemiología y Salud Pública, ISCIII, Spain
- Institute of Biophysics and Medical Physics, University of Leipzig, Leipzig, Germany
- Department of Clinical Dentistry, Faculty of Medicine and Dentistry, University of Bergen, Norway; collaborator: Department of Electrical Engineering, Faculty of Engineering, Bergen University College, Norway
- Health Effects Group, Department of Environmental Chemistry, NILU- Norwegian Institute for Air Research, Kjeller, Norway
- Commissariat à l'Energie Atomique et aux Energies Alternatives (CEA) Direction des Sciences du Vivant, Institut de Radiobiologie Cellulaire et Moléculaire, Service de Radiobiologie Expérimentale et d'Innovation Technologique, Laboratoire de Cancérologie Expérimentale, 92265 Fontenay-aux-Roses cedex, France
- GAIKER Technology Centre, Bizkaia. Science and Technology Park, Zamudio 48170, Bizkaia, Spain
- ANSES Fougères Laboratory, Contaminant Toxicology Unit, France
- Institute of Experimental Medicine AS CR, Prague, Czech Republic
- Human Genetics Department, National Institute of Health Doutor Ricardo Jorge and Centre for Toxicogenomics and Human Health, NMS/FCM, UNL, Lisbon, Portugal
- Directory of Life Sciences Applied Metrology, National Institute of Metrology Quality and Technology, Rio de Janeiro, Brazil
- Nanomedicine Group, Trinity Centre for Health Sciences, Trinity College Dublin, Dublin, Ireland
- Institute of Environmental Medicine, Karolinska Institutet, SE-171 77 Stockholm, Sweden
- Nanotechnology Industries Association, Belgium.

5 References

1. Nel A, Xia T, Madler L, Li N. Toxic potential of materials at the nanolevel. *Science* 2006, 311:622-627.
2. Donaldson K, Poland CA. Nanotoxicity: challenging the myth of nano-specific toxicity. *Curr Opin Biotechnol* 2013, 24:724-734.
3. Cohen Y, Rallo R, Liu R, Liu HH. In silico analysis of nanomaterials hazard and risk. *Acc Chem Res* 2013, 46:802-812.
4. Nel A, Xia T, Meng H, Wang X, Lin S, Ji Z, Zhang H. Nanomaterial toxicity testing in the 21st century: use of a predictive toxicological approach and high-throughput screening. *Acc Chem Res* 2013, 46:607-621.
5. Arora S, Rajwade JM, Paknikar KM. Nanotoxicology and in vitro studies: the need of the hour. *Toxicol Appl Pharmacol* 2012, 258:151-165.
6. Dusinska M, Magdolenova Z, Fjellsbo LM. Toxicological aspects for nanomaterial in humans. *Methods Mol Biol* 2013, 948:1-12.
7. Dusinska M, Fjellsbø LM, Magdolenova Z, Ravnum S, Rinna A, E R-P. Safety of Nanomaterial in Nanomedicine. In: *Chapter 11. In: Nanomedicine in Health and Disease* Jersey, British Isles Enfield, New Hampshire: RJ Hunter, VR Preedy, Eds. CRC Press; 2011, 203-226.
8. Donaldson K, Stone V, Tran CL, Kreyling W, Borm PJ. Nanotoxicology. *Occup Environ Med* 2004, 61:727-728.
9. Lewinski N, Colvin V, Drezek R. Cytotoxicity of nanoparticles. *Small* 2008, 4:26-49.
10. George S, Xia T, Rallo R, Zhao Y, Ji Z, Lin S, Wang X, Zhang H, France B, Schoenfeld D, et al. Use of a high-throughput screening approach coupled with in vivo zebrafish embryo screening to develop hazard ranking for engineered nanomaterials. *ACS Nano* 2011, 5:1805-1817.
11. Prina-Mello A, Bashir M, Verma N, Namrata J, Volkov Y. Advanced methodologies and techniques for assessing nanomaterials toxicity from manufacturing to nanomedecine screening. In: *Chapter 9. In: Nanotoxicology: Progress toward Nanomedicine*: CRC Press, Taylor Francis Group; 2014, 155 - 176.
12. Prina-Mello A, Crosbie-Staunton K, Salas G, del Puerto Morales M, Volkov Y. Multiparametric Toxicity Evaluation of SPIONs by High Content Screening Technique: Identification of Biocompatible Multifunctional Nanoparticles for Nanomedicine. *IEEE Transactions on Magnetics* 2013, 49:377-382.
13. Mohamed BM, Verma NK, Davies AM, McGowan A, Crosbie-Staunton K, Prina-Mello A, Kelleher D, Botting CH, Causey CP, Thompson PR, et al. Citrullination of proteins: a common post-translational modification pathway induced by different nanoparticles in vitro and in vivo. *Nanomedicine (Lond)* 2012, 7:1181-1195.
14. Fischer HC, Fournier-Bidoz S, Chan WCW, Pang KS. Quantitative detection of engineered nanoparticles in tissues and organs: An investigation of efficacy and linear dynamic ranges using ICP-AES. *Nanobiotechnology* 2007, 3:46-54.
15. Albanese A, Tsoi KM, Chan WC. Simultaneous quantification of cells and nanomaterials by inductive-coupled plasma techniques. *J Lab Autom* 2013, 18:99-104.
16. Malugin A, Ghandehari H. Cellular uptake and toxicity of gold nanoparticles in prostate cancer cells: a comparative study of rods and spheres. *J Appl Toxicol* 2010, 30:212-217.
17. Zhou X, Dorn M, Vogt J, Spemann D, Yu W, Mao Z, Estrela-Lopis I, Donath E, Gao C. A quantitative study of the intracellular concentration of graphene/noble metal nanoparticle composites and their cytotoxicity. *Nanoscale* 2014, 6:8535-8542.
18. Laborda F, Bolea E, Jimenez-Lamana J. Single particle inductively coupled plasma mass spectrometry: a powerful tool for nanoanalysis. *Anal Chem* 2014, 86:2270-2278.
19. Allouni ZE, Gjerdet NR, Cimpan MR, Hol PJ. The effect of blood protein adsorption on cellular uptake of anatase TiO2 nanoparticles. *Int J Nanomedicine* 2015, 10:687-695.
20. Reinert T, Andrea T, Barapatre N, Hohlweg M, Koal T, Larisch W, Reinert A, Spemann D, Vogt J, Werner R, et al. Biomedical research at LIPSION – Present state and future developments. *Nuclear Instruments and Methods in Physics Research Section B: Beam Interactions with Materials and Atoms* 2011, 269:2254-2259.
21. Tanaka N, Kimura H, Faried A, Sakai M, Sano A, Inose T, Sohda M, Okada K, Nakajima M, Miyazaki T, et al. Quantitative analysis of cisplatin sensitivity of human esophageal squamous cancer cell lines using in-air micro-PIXE. *Cancer Sci* 2010, 101:1487-1492.
22. Llop J, Estrela-Lopis I, Ziolo RF, Gonzalez A, Fleddermann J, Dorn M, Gomez Vallejo V, Simon-Vazquez R, Donath E, Mao Z, et al. Uptake, Biological Fate, and Toxicity of Metal Oxide Nanoparticles. *Particle & Particle Systems Characterization* 2014, 31:24-35.

23. Gatti AM. Biocompatibility of micro- and nano-particles in the colon. Part II. *Biomaterials* 2004, 25:385-392.
24. Zelenik K, Kukutschova J, Dvorackova J, Bielnikova H, Peikertova P, Cabalova L, Kominek P. Possible role of nano-sized particles in chronic tonsillitis and tonsillar carcinoma: a pilot study. *Eur Arch Otorhinolaryngol* 2013, 270:705-709.
25. Pichler BJ, Kolb A, Nagele T, Schlemmer HP. PET/MRI: paving the way for the next generation of clinical multimodality imaging applications. *J Nucl Med* 2010, 51:333-336.
26. Perez-Campana C, Gomez-Vallejo V, Puigivila M, Martin A, Calvo-Fernandez T, Moya SE, Ziolo RF, Reese T, Llop J. Biodistribution of different sized nanoparticles assessed by positron emission tomography: a general strategy for direct activation of metal oxide particles. *ACS Nano* 2013, 7:3498-3505.
27. Taylor A, Herrmann A, Moss D, See V, Davies K, Williams SR, Murray P. Assessing the efficacy of nano- and micro-sized magnetic particles as contrast agents for MRI cell tracking. *PLoS One* 2014, 9:e100259.
28. Nemmar A, Al-Maskari S, Ali BH, Al-Amri IS. Cardiovascular and lung inflammatory effects induced by systemically administered diesel exhaust particles in rats. *Am J Physiol Lung Cell Mol Physiol* 2007, 292:L664-670.
29. Takenaka S, Karg E, Kreyling WG, Lentner B, Moller W, Behnke-Semmler M, Jennen L, Walch A, Michalke B, Schramel P, et al. Distribution pattern of inhaled ultrafine gold particles in the rat lung. *Inhal Toxicol* 2006, 18:733-740.
30. Heymann JA, Hayles M, Gestmann I, Giannuzzi LA, Lich B, Subramaniam S. Site-specific 3D imaging of cells and tissues with a dual beam microscope. *J Struct Biol* 2006, 155:63-73.
31. Haase A, Arlinghaus HF, Tentschert J, Jungnickel H, Graf P, Mantion A, Draude F, Galla S, Plendl J, Goetz ME, et al. Application of laser postionization secondary neutral mass spectrometry/time-of-flight secondary ion mass spectrometry in nanotoxicology: visualization of nanosilver in human macrophages and cellular responses. *ACS Nano* 2011, 5:3059-3068.
32. Lee PL, Chen BC, Gollavelli G, Shen SY, Yin YS, Lei SL, Jhang CL, Lee WR, Ling YC. Development and validation of TOF-SIMS and CLSM imaging method for cytotoxicity study of ZnO nanoparticles in HaCaT cells. *J Hazard Mater* 2014, 277:3-12.
33. Perna G, Lastella M, Lasalvia M, Mezzenga E, Capozzi V. Raman spectroscopy and atomic force microscopy study of cellular damage in human keratinocytes treated with HgCl2. *J Mol Struct* 2007, 834–836:182-187.
34. Pyrgiotakis G, Kundakcioglu OE, Pardalos PM, Moudgil BM. Raman spectroscopy and support vector machines for quick toxicological evaluation of titania nanoparticles. *J Raman Spectrosc* 2011, 42:1222-1231.
35. Zoladek A, Pascut FC, Patel P, Notingher I. Non-invasive time-course imaging of apoptotic cells by confocal Raman micro-spectroscopy. *J Raman Spectrosc* 2011, 42:251-258.
36. Uzunbajakava N, Lenferink A, Kraan Y, Volokhina E, Vrensen G, Greve J, Otto C. Nonresonant confocal Raman imaging of DNA and protein distribution in apoptotic cells. *Biophys J* 2003, 84:3968-3981.
37. Krafft C, Knetschke T, Funk RH, Salzer R. Studies on stress-induced changes at the subcellular level by Raman microspectroscopic mapping. *Anal Chem* 2006, 78:4424-4429.
38. Owen CA, Selvakumaran J, Notingher I, Jell G, Hench LL, Stevens MM. In vitro toxicology evaluation of pharmaceuticals using Raman micro-spectroscopy. *J Cell Biochem* 2006, 99:178-186.
39. le Roux K, Prinsloo LC, Hussein AA, Lall N. A micro-Raman spectroscopic investigation of leukemic U-937 cells treated with Crotalaria agatiflora Schweinf and the isolated compound madurensine. *Spectrochim Acta A Mol Biomol Spectrosc* 2012, 95:547-554.
40. Sinclair MB, Haaland DM, Timlin JA, Jones HD. Hyperspectral confocal microscope. *Appl Opt* 2006, 45:6283-6291.
41. Matthaus C, Chernenko T, Newmark JA, Warner CM, Diem M. Label-free detection of mitochondrial distribution in cells by nonresonant Raman microspectroscopy. *Biophys J* 2007, 93:668-673.
42. Klein K, Gigler AM, Aschenbrenner T, Monetti R, Bunk W, Jamitzky F, Morfill G, Stark RW, Schlegel J. Label-free live-cell imaging with confocal Raman microscopy. *Biophys J* 2012, 102:360-368.
43. Matthaus C, Kale A, Chernenko T, Torchilin V, Diem M. New ways of imaging uptake and intracellular fate of liposomal drug carrier systems inside individual cells, based on Raman microscopy. *Mol Pharm* 2008, 5:287-293.
44. Romero G, Estrela-Lopis I, Zhou J, Rojas E, Franco A, Espinel CS, Fernandez AG, Gao C, Donath E, Moya SE. Surface engineered Poly(lactide-co-glycolide) nanoparticles for intracellular delivery: uptake and cytotoxicity--a confocal raman microscopic study. *Biomacromolecules* 2010, 11:2993-2999.

45. Romero G, Ochoteco O, Sanz DJ, Estrela-Lopis I, Donath E, Moya SE. Poly(lactide-co-glycolide) nanoparticles, layer by layer engineered for the sustainable delivery of antiTNF-alpha. *Macromol Biosci* 2013, 13:903-912.
46. Romero G, Estrela-Lopis I, Castro-Hartmann P, Rojas E, Llarena I, Sanz D, Donath E, Moya SE. Stepwise surface tailoring of carbon nanotubes with polyelectrolyte brushes and lipid layers to control their intracellular distribution and "in vitro" toxicity. *Soft Matter* 2011, 7:6883-6890.
47. Estrela-Lopis I, Romero G, Rojas E, Moya SE, Donath E. Nanoparticle uptake and their co-localization with cell compartments – a confocal Raman microscopy study at single cell level. *Journal of Physics: Conference Series* 2011, 304:012017.
48. Worle-Knirsch JM, Pulskamp K, Krug HF. Oops they did it again! Carbon nanotubes hoax scientists in viability assays. *Nano Lett* 2006, 6:1261-1268.
49. Luque-Garcia JL, Cabezas-Sanchez P, Anunciacao DS, Camara C. Analytical and bioanalytical approaches to unravel the selenium-mercury antagonism: a review. *Anal Chim Acta* 2013, 801:1-13.
50. Kroll A, Dierker C, Rommel C, Hahn D, Wohlleben W, Schulze-Isfort C, Gobbert C, Voetz M, Hardinghaus F, Schnekenburger J. Cytotoxicity screening of 23 engineered nanomaterials using a test matrix of ten cell lines and three different assays. *Part Fibre Toxicol* 2011, 8:9.
51. Park EJ, Park K. Oxidative stress and pro-inflammatory responses induced by silica nanoparticles in vivo and in vitro. *Toxicol Lett* 2009, 184:18-25.
52. Yeon JH, Park JK. Cytotoxicity test based on electrochemical impedance measurement of HepG2 cultured in microfabricated cell chip. *Anal Biochem* 2005, 341:308-315.
53. Ceriotti L, Ponti J, Colpo P, Sabbioni E, Rossi F. Assessment of cytotoxicity by impedance spectroscopy. *Biosens Bioelectron* 2007, 22:3057-3063.
54. Hondroulis E, Liu C, Li CZ. Whole cell based electrical impedance sensing approach for a rapid nanotoxicity assay. *Nanotechnology* 2010, 21:315103.
55. Cimpan M, Mordal T, Allouni Z, Pliquett U, Cimpan E. An impedance-based high-throughput method for evaluating the cytotoxicity of nanoparticles. In: *Journal of Physics: Conference Series*: IOP Publishing; 2013.
56. Walker NJ, Bucher JR. A 21st century paradigm for evaluating the health hazards of nanoscale materials? *Toxicol Sci* 2009, 110:251-254.
57. Feliu N, Fadeel B. Nanotoxicology: no small matter. *Nanoscale* 2010, 2:2514-2520.
58. Guadagnini R, Moreau K, Hussain S, Marano F, Boland S. Toxicity evaluation of engineered nanoparticles for medical applications using pulmonary epithelial cells. *Nanotoxicology* 2015, 9:25-32.
59. Guadagnini R, Halamoda Kenzaoui B, Walker L, Pojana G, Magdolenova Z, Bilanicova D, Saunders M, Juillerat-Jeanneret L, Marcomini A, Huk A, et al. Toxicity screenings of nanomaterials: challenges due to interference with assay processes and components of classic in vitro tests. *Nanotoxicology* 2015, 9 Suppl 1:13-24.
60. Urcan E, Haertel U, Styllou M, Hickel R, Scherthan H, Reichl FX. Real-time xCELLigence impedance analysis of the cytotoxicity of dental composite components on human gingival fibroblasts. *Dent Mater*, 26:51-58.
61. Wegener J, Keese CR, Giaever I. Electric Cell–Substrate Impedance Sensing (ECIS) as a Noninvasive Means to Monitor the Kinetics of Cell Spreading to Artificial Surfaces. *Exp Cell Res* 2000, 259:158-166.
62. Thomas N. High-content screening: a decade of evolution. *J Biomol Screen* 2010, 15:1-9.
63. Hoffman AF, Garippa RJ. A pharmaceutical company user's perspective on the potential of high content screening in drug discovery. *Methods Mol Biol* 2007, 356:19-31.
64. Trask OJ, Jr., Baker A, Williams RG, Nickischer D, Kandasamy R, Laethem C, Johnston PA, Johnston PA. Assay development and case history of a 32K-biased library high-content MK2-EGFP translocation screen to identify p38 mitogen-activated protein kinase inhibitors on the ArrayScan 3.1 imaging platform. *Methods Enzymol* 2006, 414:419-439.
65. Xu JJ, Henstock PV, Dunn MC, Smith AR, Chabot JR, de Graaf D. Cellular imaging predictions of clinical drug-induced liver injury. *Toxicol Sci* 2008, 105:97-105.
66. Anguissola S, Garry D, Salvati A, O'Brien PJ, Dawson KA. High content analysis provides mechanistic insights on the pathways of toxicity induced by amine-modified polystyrene nanoparticles. *PLoS One* 2014, 9:e108025.
67. Jan E, Byrne SJ, Cuddihy M, Davies AM, Volkov Y, Gun'ko YK, Kotov NA. High-content screening as a universal tool for fingerprinting of cytotoxicity of nanoparticles. *ACS Nano* 2008, 2:928-938.
68. Harris G, Palosaari T, Magdolenova Z, Mennecozzi M, Gineste JM, Saavedra L, Milcamps A, Huk A, Collins AR, Dusinska M, et al. Iron oxide nanoparticle toxicity testing using high-throughput analysis and high-content imaging. *Nanotoxicology* 2015, 9:87-94.

69. Lin S, Zhao Y, Xia T, Meng H, Ji Z, Liu R, George S, Xiong S, Wang X, Zhang H, et al. High content screening in zebrafish speeds up hazard ranking of transition metal oxide nanoparticles. *ACS Nano* 2011, 5:7284-7295.
70. Damoiseaux R, George S, Li M, Pokhrel S, Ji Z, France B, Xia T, Suarez E, Rallo R, Madler L, et al. No time to lose--high throughput screening to assess nanomaterial safety. *Nanoscale* 2011, 3:1345-1360.
71. Edwards BS, Young SM, Saunders MJ, Bologa C, Oprea TI, Ye RD, Prossnitz ER, Graves SW, Sklar LA. High-throughput flow cytometry for drug discovery. *Expert Opinion on Drug Discovery* 2007, 2:685-696.
72. Peluso J, Tabaka-Moreira H, Taquet N, Dumont S, Muller CD, Reimund J-M. Can flow cytometry play a part in cell based high-content screening? *Cytometry Part A* 2007, 71A:901-904.
73. Goñi-de-Cerio F, Mariani V, Cohen D, Madi L, Thevenot J, Oliviera H, Uboldi C, Giudetti G. Biocompatibility study of two diblock copolymeric NPs for biomedical applications by in vitro toxicity testing. *J NP Res.* 2013, 11:1-17.
74. Errico C, Goñi-de-Cerio F, Alderighi M, Ferri M, Suarez-Merino B, Soroka Y, Frušić-Zlotkin M, Chiellini F. Retinyl palmitate–loaded poly(lactide-co-glycolide) nanoparticles for the topical treatment of skin diseases. *J Bioact Compat Polym* 2012, 27:604-620.
75. Zucker RM, Daniel KM. Detection of TiO2 nanoparticles in cells by flow cytometry. *Methods Mol Biol* 2012, 906:497-509.
76. Zucker RM, Massaro EJ, Sanders KM, Degn LL, Boyes WK. Detection of TiO2 nanoparticles in cells by flow cytometry. *Cytometry A* 2010, 77:677-685.
77. Schoelermann J, Burtey A, Allouni ZE, Gerdes H-H, Cimpan MR. Contact-dependent transfer of TiO2 nanoparticles between mammalian cells. *Nanotoxicology* 2015:1-12.
78. Zucker RM, Daniel KM, Massaro EJ, Karafas SJ, Degn LL, Boyes WK. Detection of silver nanoparticles in cells by flow cytometry using light scatter and far-red fluorescence. *Cytometry A* 2013, 83:962-972.
79. Paget V, Moche H, Kortulewski T, Grall R, Irbah L, Nesslany F, Chevillard S. Human cell line-dependent WC-Co nanoparticle cytotoxicity and genotoxicity: a key role of ROS production. *Toxicol Sci* 2015, 143:385-397.
80. Grall R, Girard H, Saad L, Petit T, Gesset C, Combis-Schlumberger M, Paget V, Delic J, Arnault JC, Chevillard S. Impairing the radioresistance of cancer cells by hydrogenated nanodiamonds. *Biomaterials* 2015, 61:290-298.
81. Vranic S, Boggetto N, Contremoulins V, Mornet S, Reinhardt N, Marano F, Baeza-Squiban A, Boland S. Deciphering the mechanisms of cellular uptake of engineered nanoparticles by accurate evaluation of internalization using imaging flow cytometry. *Part Fibre Toxicol* 2013, 10:2.
82. Giaever I, Keese CR. A morphological biosensor for mammalian cells. *Nature* 1993, 366:591-592.
83. Coffman FD, Cohen S. Impedance measurements in the biomedical sciences. *Stud Health Technol Inform* 2013, 185:185-205.
84. Lingwood BE. Bioelectrical impedance analysis for assessment of fluid status and body composition in neonates--the good, the bad and the unknown. *Eur J Clin Nutr* 2013, 67 Suppl 1:S28-33.
85. Kyle UG, Bosaeus I, De Lorenzo AD, Deurenberg P, Elia M, Manuel Gomez J, Lilienthal Heitmann B, Kent-Smith L, Melchior JC, Pirlich M, et al. Bioelectrical impedance analysis-part II: utilization in clinical practice. *Clin Nutr* 2004, 23:1430-1453.
86. Pliquett U. Bioimpedance: A Review for Food Processing. *Food Engineering Reviews* 2010, 2:74-94.
87. Lukaski HC. Evolution of bioimpedance: a circuitous journey from estimation of physiological function to assessment of body composition and a return to clinical research. *Eur J Clin Nutr* 2013, 67 Suppl 1:S2-9.
88. Xiao C, Lachance B, Sunahara G, Luong JH. Assessment of cytotoxicity using electric cell-substrate impedance sensing: concentration and time response function approach. *Anal Chem* 2002, 74:5748-5753.
89. Irelan JT, Wu MJ, Morgan J, Ke N, Xi B, Wang X, Xu X, Abassi YA. Rapid and quantitative assessment of cell quality, identity, and functionality for cell-based assays using real-time cellular analysis. *J Biomol Screen* 2011, 16:313-322.
90. Pan T, Huang B, Zhang W, Gabos S, Huang DY, Devendran V. Cytotoxicity assessment based on the AUC50 using multi-concentration time-dependent cellular response curves. *Anal Chim Acta* 2013, 764:44-52.
91. Pan T, Khare S, Ackah F, Huang B, Zhang W, Gabos S, Jin C, Stampfl M. In vitro cytotoxicity assessment based on KC(50) with real-time cell analyzer (RTCA) assay. *Comput Biol Chem* 2013, 47:113-120.

92. Kavlock R, Chandler K, Houck K, Hunter S, Judson R, Kleinstreuer N, Knudsen T, Martin M, Padilla S, Reif D, et al. Update on EPA's ToxCast program: providing high throughput decision support tools for chemical risk management. *Chem Res Toxicol* 2012, 25:1287-1302.
93. Xing JZ, Zhu L, Jackson JA, Gabos S, Sun XJ, Wang XB, Xu X. Dynamic monitoring of cytotoxicity on microelectronic sensors. *Chem Res Toxicol* 2005, 18:154-161.
94. Ke N, Wang X, Xu X, Abassi YA. The xCELLigence system for real-time and label-free monitoring of cell viability. *Methods Mol Biol* 2011, 740:33-43.
95. Otero-Gonzalez L, Sierra-Alvarez R, Boitano S, Field JA. Application and validation of an impedance-based real time cell analyzer to measure the toxicity of nanoparticles impacting human bronchial epithelial cells. *Environ Sci Technol* 2012, 46:10271-10278.
96. Paget V, Sergent JA, Grall R, Altmeyer-Morel S, Girard HA, Petit T, Gesset C, Mermoux M, Bergonzo P, Arnault JC, et al. Carboxylated nanodiamonds are neither cytotoxic nor genotoxic on liver, kidney, intestine and lung human cell lines. *Nanotoxicology* 2014, 8 Suppl 1:46-56.
97. Paget V, Dekali S, Kortulewski T, Grall R, Gamez C, Blazy K, Aguerre-Chariol O, Chevillard S, Braun A, Rat P, et al. Specific uptake and genotoxicity induced by polystyrene nanobeads with distinct surface chemistry on human lung epithelial cells and macrophages. *PLoS One* 2015, 10:e0123297.
98. Scrace S, O'Neill E, Hammond EM, Pires IM. Use of the xCELLigence system for real-time analysis of changes in cellular motility and adhesion in physiological conditions. *Methods Mol Biol* 2013, 1046:295-306.
99. Cheung KC, Di Berardino M, Schade-Kampmann G, Hebeisen M, Pierzchalski A, Bocsi J, Mittag A, Tarnok A. Microfluidic impedance-based flow cytometry. *Cytometry A* 2010, 77:648-666.
100. Moe B, Gabos S, Li XF. Real-time cell-microelectronic sensing of nanoparticle-induced cytotoxic effects. *Anal Chim Acta* 2013, 789:83-90.
101. Heileman K, Daoud J, Tabrizian M. Dielectric spectroscopy as a viable biosensing tool for cell and tissue characterization and analysis. *Biosens Bioelectron* 2013, 49:348-359.
102. Ponti J, Ceriotti L, Munaro B, Farina M, Munari A, Whelan M, Colpo P, Sabbioni E, Rossi F. Comparison of impedance-based sensors for cell adhesion monitoring and in vitro methods for detecting cytotoxicity induced by chemicals. *Altern Lab Anim* 2006, 34:515-525.
103. Kustermann S, Boess F, Buness A, Schmitz M, Watzele M, Weiser T, Singer T, Suter L, Roth A. A label-free, impedance-based real time assay to identify drug-induced toxicities and differentiate cytostatic from cytotoxic effects. *Toxicol In Vitro* 2013, 27:1589-1595.
104. Moodley K, Angel CE, Glass M, Graham ES. Real-time profiling of NK cell killing of human astrocytes using xCELLigence technology. *J Neurosci Methods* 2011, 200:173-180.
105. Wang T, Hu N, Cao J, Wu J, Su K, Wang P. A cardiomyocyte-based biosensor for antiarrhythmic drug evaluation by simultaneously monitoring cell growth and beating. *Biosens Bioelectron* 2013, 49:9-13.
106. Li JM, Zhao MX, Su H, Wang YY, Tan CP, Ji LN, Mao ZW. Multifunctional quantum-dot-based siRNA delivery for HPV18 E6 gene silence and intracellular imaging. *Biomaterials* 2011, 32:7978-7987.
107. Li JM, Wang YY, Zhao MX, Tan CP, Li YQ, Le XY, Ji LN, Mao ZW. Multifunctional QD-based co-delivery of siRNA and doxorubicin to HeLa cells for reversal of multidrug resistance and real-time tracking. *Biomaterials* 2012, 33:2780-2790.
108. Sun M, Fu H, Cheng H, Cao Q, Zhao Y, Mou X, Zhang X, Liu X, Ke Y. A dynamic real-time method for monitoring epithelial barrier function in vitro. *Anal Biochem* 2012, 425:96-103.
109. Diemert S, Dolga AM, Tobaben S, Grohm J, Pfeifer S, Oexler E, Culmsee C. Impedance measurement for real time detection of neuronal cell death. *J Neurosci Methods* 2012, 203:69-77.
110. Val S, Hussain S, Boland S, Hamel R, Baeza-Squiban A, Marano F. Carbon black and titanium dioxide nanoparticles induce pro-inflammatory responses in bronchial epithelial cells: need for multiparametric evaluation due to adsorption artifacts. *Inhal Toxicol* 2009, 21 Suppl 1:115-122.
111. Turci F, Ghibaudi E, Colonna M, Boscolo B, Fenoglio I, Fubini B. An integrated approach to the study of the interaction between proteins and nanoparticles. *Langmuir* 2010, 26:8336-8346.
112. Leng SX, McElhaney JE, Walston JD, Xie D, Fedarko NS, Kuchel GA. ELISA and multiplex technologies for cytokine measurement in inflammation and aging research. *J Gerontol A Biol Sci Med Sci* 2008, 63:879-884.
113. Purohit S, Sharma A, She JX. Luminex and other multiplex high throughput technologies for the identification of, and host response to, environmental triggers of type 1 diabetes. *Biomed Res Int* 2015, 2015:326918.
114. Ghosh R, Singh LC, Shohet JM, Gunaratne PH. A gold nanoparticle platform for the delivery of functional microRNAs into cancer cells. *Biomaterials* 2013, 34:807-816.

115. Mieszawska AJ, Mulder WJ, Fayad ZA, Cormode DP. Multifunctional gold nanoparticles for diagnosis and therapy of disease. *Mol Pharm* 2013, 10:831-847.
116. Connor EE, Mwamuka J, Gole A, Murphy CJ, Wyatt MD. Gold nanoparticles are taken up by human cells but do not cause acute cytotoxicity. *Small* 2005, 1:325-327.
117. Leite PE, Pereira MR, do Nascimento Santos CA, Campos AP, Esteves TM, Granjeiro JM. Gold nanoparticles do not induce myotube cytotoxicity but increase the susceptibility to cell death. *Toxicol In Vitro* 2015, 29:819-827.
118. Dusinska M, Boland S, Saunders M, Juillerat-Jeanneret L, Tran L, Pojana G, Marcomini A, Volkovova K, Tulinska J, Knudsen LE, et al. Towards an alternative testing strategy for nanomaterials used in nanomedicine: lessons from NanoTEST. *Nanotoxicology* 2015, 9 Suppl 1:118-132.
119. Azqueta A, Gutzkow KB, Priestley CC, Meier S, Walker JS, Brunborg G, Collins AR. A comparative performance test of standard, medium- and high-throughput comet assays. *Toxicol In Vitro* 2013, 27:768-773.
120. Gutzkow KB, Langleite TM, Meier S, Graupner A, Collins AR, Brunborg G. High-throughput comet assay using 96 minigels. *Mutagenesis* 2013, 28:333-340.
121. Huk A, Izak-Nau E, Reidy B, Boyles M, Duschl A, Lynch I, Dusinska M. Is the toxic potential of nanosilver dependent on its size? *Part Fibre Toxicol* 2014, 11:65.
122. Huk A, Collins AR, El Yamani N, Porredon C, Azqueta A, de Lapuente J, Dusinska M. Critical factors to be considered when testing nanomaterials for genotoxicity with the comet assay. *Mutagenesis* 2015, 30:85-88.
123. Magdolenova Z, Lorenzo Y, Collins A, Dusinska M. Can standard genotoxicity tests be applied to nanoparticles? *J Toxicol Environ Health A* 2012, 75:800-806.
124. Karlsson HL, Di Bucchianico S, Collins AR, Dusinska M. Can the comet assay be used reliably to detect nanoparticle-induced genotoxicity? *Environ Mol Mutagen* 2015, 56:82-96.
125. Azqueta A, Meier S, Priestley C, Gutzkow KB, Brunborg G, Sallette J, Soussaline F, Collins A. The influence of scoring method on variability in results obtained with the comet assay. *Mutagenesis* 2011, 26:393-399.
126. Wood DK, Weingeist DM, Bhatia SN, Engelward BP. Single cell trapping and DNA damage analysis using microwell arrays. *Proc Natl Acad Sci U S A* 2010, 107:10008-10013.
127. Watson C, Ge J, Cohen J, Pyrgiotakis G, Engelward BP, Demokritou P. High-throughput screening platform for engineered nanoparticle-mediated genotoxicity using CometChip technology. *ACS Nano* 2014, 8:2118-2133.
128. Cowie H, Magdolenova Z, Saunders M, Drlickova M, Correia Carreira S, Halamoda Kenzaoi B, Gombau L, Guadagnini R, Lorenzo Y, Walker L, et al. Suitability of human and mammalian cells of different origin for the assessment of genotoxicity of metal and polymeric engineered nanoparticles. *Nanotoxicology* 2015, 9 Suppl 1:57-65.
129. Decordier I, Papine A, Plas G, Roesems S, Vande Loock K, Moreno-Palomo J, Cemeli E, Anderson D, Fucic A, Marcos R, et al. Automated image analysis of cytokinesis-blocked micronuclei: an adapted protocol and a validated scoring procedure for biomonitoring. *Mutagenesis* 2009, 24:85-93.
130. Fenech M, Kirsch-Volders M, Rossnerova A, Sram R, Romm H, Bolognesi C, Ramakumar A, Soussaline F, Schunck C, Elhajouji A, et al. HUMN project initiative and review of validation, quality control and prospects for further development of automated micronucleus assays using image cytometry systems. *Int J Hyg Environ Health* 2013, 216:541-552.
131. Roemer E, Zenzen V, Conroy LL, Luedemann K, Dempsey R, Schunck C, Sticken ET. Automation of the in vitro micronucleus and chromosome aberration assay for the assessment of the genotoxicity of the particulate and gas-vapor phase of cigarette smoke. *Toxicol Mech Methods* 2015:1-14.
132. Nusse M, Kramer J. Flow cytometric analysis of micronuclei found in cells after irradiation. *Cytometry* 1984, 5:20-25.
133. Bryce SM, Bemis JC, Avlasevich SL, Dertinger SD. In vitro micronucleus assay scored by flow cytometry provides a comprehensive evaluation of cytogenetic damage and cytotoxicity. *Mutat Res* 2007, 630:78-91.
134. Bryce SM, Avlasevich SL, Bemis JC, Phonethepswath S, Dertinger SD. Miniaturized flow cytometric in vitro micronucleus assay represents an efficient tool for comprehensively characterizing genotoxicity dose-response relationships. *Mutat Res* 2010, 703:191-199.
135. Bryce SM, Avlasevich SL, Bemis JC, Tate M, Walmsley RM, Saad F, Van Dijck K, De Boeck M, Van Goethem F, Lukamowicz-Rajska M, et al. Flow cytometric 96-well microplate-based in vitro micronucleus assay with human TK6 cells: protocol optimization and transferability assessment. *Environ Mol Mutagen* 2013, 54:180-194.

136. Avlasevich S, Bryce S, De Boeck M, Elhajouji A, Van Goethem F, Lynch A, Nicolette J, Shi J, Dertinger S. Flow cytometric analysis of micronuclei in mammalian cell cultures: past, present and future. *Mutagenesis* 2011, 26:147-152.
137. Diaz D, Scott A, Carmichael P, Shi W, Costales C. Evaluation of an automated in vitro micronucleus assay in CHO-K1 cells. *Mutat Res* 2007, 630:1-13.
138. Scott A, Malcomber S, Maskell S, Moore C, Windebank S, Diaz D, Carmichael P. An assessment of the performance of an automated scoring system (Cellomics) for the in vitro micronucleus assay in CHO-K1 cells. *Toxicology* 2007, 231:111-112.
139. Mondal MS, Gabriels J, McGinnis C, Magnifico M, Marsilje TH, Urban L, Collis A, Bojanic D, Biller SA, Frieauff W, et al. High-content micronucleus assay in genotoxicity profiling: initial-stage development and some applications in the investigative/lead-finding studies in drug discovery. *Toxicol Sci* 2010, 118:71-85.
140. Westerink WM, Schirris TJ, Horbach GJ, Schoonen WG. Development and validation of a high-content screening in vitro micronucleus assay in CHO-k1 and HepG2 cells. *Mutat Res* 2011, 724:7-21.
141. Voelcker et al. Development of an automated high-throughput screening procedure for nanomaterials genotoxicity assessment *Safe Work Australia* 2013.
142. Bonner WM, Redon CE, Dickey JS, Nakamura AJ, Sedelnikova OA, Solier S, Pommier Y. GammaH2AX and cancer. *Nat Rev Cancer* 2008, 8:957-967.
143. Mah LJ, El-Osta A, Karagiannis TC. gammaH2AX: a sensitive molecular marker of DNA damage and repair. *Leukemia* 2010, 24:679-686.
144. Valdiglesias V, Costa C, Kilic G, Costa S, Pasaro E, Laffon B, Teixeira JP. Neuronal cytotoxicity and genotoxicity induced by zinc oxide nanoparticles. *Environ Int* 2013, 55:92-100.
145. Audebert M, Dolo L, Perdu E, Cravedi JP, Zalko D. Use of the gammaH2AX assay for assessing the genotoxicity of bisphenol A and bisphenol F in human cell lines. *Arch Toxicol* 2011, 85:1463-1473.
146. O'Driscoll M, Jeggo PA. The role of double-strand break repair - insights from human genetics. *Nat Rev Genet* 2006, 7:45-54.
147. McKinnon PJ, Caldecott KW. DNA strand break repair and human genetic disease. *Annu Rev Genomics Hum Genet* 2007, 8:37-55.
148. Helleday T, Petermann E, Lundin C, Hodgson B, Sharma RA. DNA repair pathways as targets for cancer therapy. *Nat Rev Cancer* 2008, 8:193-204.
149. Clingen PH, Wu JY, Miller J, Mistry N, Chin F, Wynne P, Prise KM, Hartley JA. Histone H2AX phosphorylation as a molecular pharmacological marker for DNA interstrand crosslink cancer chemotherapy. *Biochem Pharmacol* 2008, 76:19-27.
150. Redon CE, Nakamura AJ, Zhang YW, Ji JJ, Bonner WM, Kinders RJ, Parchment RE, Doroshow JH, Pommier Y. Histone gammaH2AX and poly(ADP-ribose) as clinical pharmacodynamic biomarkers. *Clin Cancer Res* 2010, 16:4532-4542.
151. Zhu L, Chang DW, Dai L, Hong Y. DNA damage induced by multiwalled carbon nanotubes in mouse embryonic stem cells. *Nano Lett* 2007, 7:3592-3597.
152. Cveticanin J, Joksic G, Leskovac A, Petrovic S, Sobot AV, Neskovic O. Using carbon nanotubes to induce micronuclei and double strand breaks of the DNA in human cells. *Nanotechnology* 2010, 21:015102.
153. Chattopadhyay N, Cai Z, Kwon YL, Lechtman E, Pignol JP, Reilly RM. Molecularly targeted gold nanoparticles enhance the radiation response of breast cancer cells and tumor xenografts to X-radiation. *Breast Cancer Res Treat* 2013, 137:81-91.
154. Msiska Z, Pacurari M, Mishra A, Leonard SS, Castranova V, Vallyathan V. DNA double-strand breaks by asbestos, silica, and titanium dioxide: possible biomarker of carcinogenic potential? *Am J Respir Cell Mol Biol* 2010, 43:210-219.
155. Trouiller B, Reliene R, Westbrook A, Solaimani P, Schiestl RH. Titanium dioxide nanoparticles induce DNA damage and genetic instability in vivo in mice. *Cancer Res* 2009, 69:8784-8789.
156. Toyooka T, Amano T, Ibuki Y. Titanium dioxide particles phosphorylate histone H2AX independent of ROS production. *Mutat Res* 2012, 742:84-91.
157. Bhogal N, Jalali F, Bristow RG. Microscopic imaging of DNA repair foci in irradiated normal tissues. *Int J Radiat Biol* 2009, 85:732-746.
158. Ivashkevich AN, Martin OA, Smith AJ, Redon CE, Bonner WM, Martin RF, Lobachevsky PN. gammaH2AX foci as a measure of DNA damage: a computational approach to automatic analysis. *Mutat Res* 2011, 711:49-60.
159. Cai Z, Vallis KA, Reilly RM. Computational analysis of the number, area and density of gamma-H2AX foci in breast cancer cells exposed to (111)In-DTPA-hEGF or gamma-rays using Image-J software. *Int J Radiat Biol* 2009, 85:262-271.

160. Hou YN, Lavaf A, Huang D, Peters S, Huq R, Friedrich V, Rosenstein BS, Kao J. Development of an automated gamma-H2AX immunocytochemistry assay. *Radiat Res* 2009, 171:360-367.
161. Roch-Lefevre S, Mandina T, Voisin P, Gaetan G, Mesa JE, Valente M, Bonnesoeur P, Garcia O, Voisin P, Roy L. Quantification of gamma-H2AX foci in human lymphocytes: a method for biological dosimetry after ionizing radiation exposure. *Radiat Res* 2010, 174:185-194.
162. Jucha A, Wegierek-Ciuk A, Koza Z, Lisowska H, Wojcik A, Wojewodzka M, Lankoff A. FociCounter: a freely available PC programme for quantitative and qualitative analysis of gamma-H2AX foci. *Mutat Res* 2010, 696:16-20.
163. Yip KW, Cuddy M, Pinilla C, Giulanotti M, Heynen-Genel S, Matsuzawa S, Reed JC. A high-content screening (HCS) assay for the identification of chemical inducers of PML oncogenic domains (PODs). *J Biomol Screen* 2011, 16:251-258.
164. Grafstrom RC, Nymark P, Hongisto V, Spjuth O, Ceder R, Willighagen E, Hardy B, Kaski S, Kohonen P. Toward the Replacement of Animal Experiments through the Bioinformatics-driven Analysis of 'Omics' Data from Human Cell Cultures. *Altern Lab Anim* 2015, 43:325-332.
165. Kohonen P, Ceder R, Smit I, Hongisto V, Myatt G, Hardy B, Spjuth O, Grafstrom R. Cancer biology, toxicology and alternative methods development go hand-in-hand. *Basic Clin Pharmacol Toxicol* 2014, 115:50-58.
166. Peck D, Crawford ED, Ross KN, Stegmaier K, Golub TR, Lamb J. A method for high-throughput gene expression signature analysis. *Genome Biol* 2006, 7:R61.
167. Andersen ME, McMullen PD, Krewski D. Developing tools for defining and establishing pathways of toxicity. *Arch Toxicol* 2015, 89:809-812.
168. Duan Q, Flynn C, Niepel M, Hafner M, Muhlich JL, Fernandez NF, Rouillard AD, Tan CM, Chen EY, Golub TR, et al. LINCS Canvas Browser: interactive web app to query, browse and interrogate LINCS L1000 gene expression signatures. *Nucleic Acids Res* 2014, 42:W449-460.
169. Foldbjerg R, Irving ES, Hayashi Y, Sutherland DS, Thorsen K, Autrup H, Beer C. Global gene expression profiling of human lung epithelial cells after exposure to nanosilver. *Toxicol Sci* 2012, 130:145-157.
170. Kong L, Tuomela S, Hahne L, Ahlfors H, Yli-Harja O, Fadeel B, Lahesmaa R, Autio R. NanoMiner - integrative human transcriptomics data resource for nanoparticle research. *PLoS One* 2013, 8:e68414.
171. Feliu N, Kohonen P, Ji J, Zhang Y, Karlsson HL, Palmberg L, Nystrom A, Fadeel B. Next-generation sequencing reveals low-dose effects of cationic dendrimers in primary human bronchial epithelial cells. *ACS Nano* 2015, 9:146-163.
172. Afshari CA, Hamadeh HK, Bushel PR. The evolution of bioinformatics in toxicology: advancing toxicogenomics. *Toxicol Sci* 2011, 120 Suppl 1:S225-237.
173. Smalley JL, Gant TW, Zhang SD. Application of connectivity mapping in predictive toxicology based on gene-expression similarity. *Toxicology* 2010, 268:143-146.
174. Gusenleitner D, Auerbach SS, Melia T, Gomez HF, Sherr DH, Monti S. Genomic models of short-term exposure accurately predict long-term chemical carcinogenicity and identify putative mechanisms of action. *PLoS One* 2014, 9:e102579.
175. Lamb J. The Connectivity Map: a new tool for biomedical research. *Nat Rev Cancer* 2007, 7:54-60.
176. Choi JY, Ramachandran G, Kandlikar M. The impact of toxicity testing costs on nanomaterial regulation. *Environ Sci Technol* 2009, 43:3030-3034.
177. Szymanski P, Markowicz M, Mikiciuk-Olasik E. Adaptation of high-throughput screening in drug discovery-toxicological screening tests. *Int J Mol Sci* 2012, 13:427-452.
178. Rossnerova A, Spatova M, Schunck C, Sram RJ. Automated scoring of lymphocyte micronuclei by the MetaSystems Metafer image cytometry system and its application in studies of human mutagen sensitivity and biodosimetry of genotoxin exposure. *Mutagenesis* 2011, 26:169-175.
179. Buchser W, Collins M, Garyantes T, Guha R, Haney S, Lemmon V, Li Z, Trask OJ. Assay Development Guidelines for Image-Based High Content Screening, High Content Analysis and High Content Imaging. In: Sittampalam GS, Coussens NP, Nelson H, Arkin M, Auld D, Austin C, Bejcek B, Glicksman M, Inglese J, Iversen PW, et al., eds. *Assay Guidance Manual*. Bethesda (MD): Eli Lilly & Company and the National Center for Advancing Translational Sciences; 2004.
180. Stone V, Nowack B, Baun A, van den Brink N, Kammer F, Dusinska M, Handy R, Hankin S, Hassellov M, Joner E, et al. Nanomaterials for environmental studies: classification, reference material issues, and strategies for physico-chemical characterisation. *Sci Total Environ* 2010, 408:1745-1754.
181. Kroll A, Pillukat MH, Hahn D, Schnekenburger J. Interference of engineered nanoparticles with in vitro toxicity assays. *Arch Toxicol* 2012, 86:1123-1136.

182. Ruenraroengsak P, Novak P, Berhanu D, Thorley AJ, Valsami-Jones E, Gorelik J, Korchev YE, Tetley TD. Respiratory epithelial cytotoxicity and membrane damage (holes) caused by amine-modified nanoparticles. *Nanotoxicology* 2012, 6:94-108.
183. Lunov O, Syrovets T, Loos C, Nienhaus GU, Mailander V, Landfester K, Rouis M, Simmet T. Amino-functionalized polystyrene nanoparticles activate the NLRP3 inflammasome in human macrophages. *ACS Nano* 2011, 5:9648-9657.
184. Farrera C, Fadeel B. It takes two to tango: Understanding the interactions between engineered nanomaterials and the immune system. *Eur J Pharm Biopharm* 2015.
185. Yu SJ, Kang MW, Chang HC, Chen KM, Yu YC. Bright fluorescent nanodiamonds: no photobleaching and low cytotoxicity. *J Am Chem Soc* 2005, 127:17604-17605.
186. Schrand AM, Huang H, Carlson C, Schlager JJ, Omacr Sawa E, Hussain SM, Dai L. Are diamond nanoparticles cytotoxic? *J Phys Chem B* 2007, 111:2-7.
187. Wang XZ, Yang Y, Li R, McGuinnes C, Adamson J, Megson IL, Donaldson K. Principal component and causal analysis of structural and acute in vitro toxicity data for nanoparticles. *Nanotoxicology* 2014, 8:465-476.
188. VILA L., L. RUBIO, B. ANNANGI, A. GARCÍA-RODRÍGUEZ, R. MARCOS, A. HERNÁNDEZ. Frozen dispersions of nanomaterials as a useful operational procedure in nanotoxicology. Nanotoxicology, 11: 31-40 (2017).
189. CHERAN L. E., CHEUNG S., WANG X., THOMPSON M. 2008, "Probing the bioelectrochemistry of living cells", *Electrochemica Acta,* 53 pp.6690-6697.
190. PRODAN, E., PRODAN, C. & MILLER, J. H. 2008. The Dielectric Response of Spherical Live Cells in Suspension: An Analytic Solution. *Biophysical Journal,* 95**,** 4174-4182.
191. Collins AR, Annangi B, Rubio L, Marcos R, Dorn M, Merker C, Estrela-Lopis I, Cimpan MR, Ibrahim M, Cimpan E, Ostermann M, Sauter A, El Yamani N, Shaposhnikov S, Chevillard S, Paget V, Grall R, Delic J, Goñi- de-Cerio F, Suarez-Merino B, Fessard V, Hogeveen KN, Fjellsbø LM, Runden-Pran E, Brzicova T, Topinka J, Silva MJ, Leite PE, Ribeiro AR, Granjeiro JM, Grafström R, Prina-Mello A and Dusinska M High throughput toxicity screening and intracellular detection of nanomaterials. WIREs Nanomed Nanobiotechnol 2016. doi: 10.1002/wnan.1413. [Epubahead of print] Review. PubMed PMID: 27273980.
192. Fenech, M. (2007). Cytokinesis-block micronucleus cytome assay. Nature Protocols, 2(5), 1084-1104.
193. Rubio L, El Yamani N, Kazimirova A, Dusinska M, Marcos R. Multi-walled carbon nanotubes (NM401) induce ROS-mediated HPRT mutations in Chinese hamster lung fibroblasts. Environ Res. 2016 Jan 8;146:185-190. doi: 10.1016/j.envres.2016.01.004. [Epub ahead of print] PMID: 26774957
194. Gábelová A, El Yamani N, Iglesias Alonso T, Buliaková B, Srančíková A, Bábelová A, Runden-Pran E, Fjellsbø LM, Elje E, Yazdani M, Silva MJ, Dušinská M. Fibrous shape underlies the mutagenic and carcinogenic potential of nanosilver while surface chemistry affects the biosafety of iron oxide nanoparticles, Mutagenesis 2016, Special issue on Nanogenotoxicity, The Author 2016. Published by Oxford University Press on behalf of the UK Environmental Mutagen Society. 1-10, doi:10.1093/mutage/gew045 Sep 22. pii: gew045. Jan;32(1):193-202. doi: 10.1093/mutage/gew045. Epub 2016 Sep 22. PubMed PMID: 27658822.
195. El Yamani N, Collins AR, Rundén-Pran E, Fjellsbø LM, Shaposhnikov S, Zielonddiny S, and Dusinska M. Genotoxicity testing of four reference metal nanomaterials, titanium dioxide, zinc oxide, cerium oxide and silver: Towards a robust and reliable hazard assessment, Mutagenesis 2016, Special issue on Nanogenotoxicity. 2016 Nov 12. pii: gew060. [Epub ahead of print] PubMed PMID: 27838631. Mutagenesis , 2017, 32(1), 117–126 doi:10.1093/mutage/gew06
196. Doak SH, Dusinska M. NanoGenotoxicology: present and the future Mutagenesis. 2017 Jan;32(1):1-4. doi: 10.1093/mutage/gew066. PubMed PMID: 28011747.
197. Magdolenova Z, Collins AR, Kumar A, Dhawan A, Stone V, Dusinska M. Mechanisms of Genotoxicity. Review of Recent in vitro and in vivo Studies with Engineered Nanoparticles. Nanotoxicology. 2014, 8, 233–278.
198. PONTI Jessica; KINSNER-OVASKAINEN Agnieszka; NORLEN H.; ALTMEYER Sandrine; ANDREOLI Cristina; BOGNI Alessia; CHEVILLARD Sylvie; DE ANGELIS Isabella; CHUNG Seung-Tae; EOM Igchun; FUJITA Katsuhide; GILLILAND Douglas; GROLLINO Maria Giuseppa; GULUMIAN Mary; HIRSCH Cordula; ICHIRAKU Kayo; IGARASHI Takuya; JEONG Jayoung; JO Eunhye; KIM Dang-Young; KAISER Jean-Pierre; LAGACHE Doris; LA SPINA RITA; LEE Jong Kwon; LEE Jieun; LOVERA Annalisa; MÄDER-ALTHAUS Xenia; NESSLANY Fabrice; OJEA JIMENEZ ISAAC; PACCHIEROTTI Francesca; PIANELLA FRANCESCA; PAGET Vincent; KIM Tae Rim; ROSZAK Joanna; ROSENKRANZ PHILIPP; SIMAR Sophie; STĘPNIK Maciej; VETTEN Melissa; SONG Nam Woong; YANG Jun-Young; ROSSI Francois. Interlaboratory comparison study

of the Colony Forming Efficiency assay for assessing cytotoxicity of nanomaterials, 2014, doi 10.2788/406937. http://publications.jrc.ec.europa.eu/repository/handle/JRC92910

199. Doak SH, Griffiths SM, Manshian B, Singh N, Williams PM, Brown AP, Jenkins GJ. Confounding experimental considerations in nanogenotoxicology. Mutagenesis. 2009 Jul;24(4):285-93. doi: 10.1093/mutage/gep010. Epub 2009 Apr 7. Review. PubMed PMID: 19351890.

200. Gonzalez L, Sanderson BJ, Kirsch-Volders M. Adaptations of the in vitro MN assay for the genotoxicity assessment of nanomaterials. Mutagenesis. 2011. Jan;26(1):185-91. doi: 10.1093/mutage/geq088. Review. PubMed PMID: 21164201.

201. linkhttp://www.nanogenotox.eu/files/PDF/web%20nanogenotox%20dispersion%20protocol.pdf

6 List of abbreviations

AES- Atomic Emission Spectroscopy
CLSM - Confocal Laser Scanning Microscopy, IBM (μPIXE and/or μRBS) – Ion Beam Microscopy
EPI, EMPA-Electron microprobe analysis
H2AX- phosphorylated histone H2AX, γH2AX - Foci of phospho-H2AX
HCA-High Content Analysis
HTS – High Throughput Screening
ICP-MS - Inductively Coupled Plasma Mass Spectrometry
IVMN - *in vitro* micronucleus
MRI - magnetic resonance imaging
PET - positron emission tomography
SPECT- single-photon computed emission tomography
TEM Transmission electron Microscopy
ToF-SIMS - time-of-flight secondary ion mass spectrometry

Annex 1

Published paper: Collins AR, Annangi B, Rubio L, Marcos R, Dorn M, Merker C, Estrela-Lopis I, Cimpan MR, Ibrahim M, Cimpan E, Ostermann M, Sauter A, El Yamani N, Shaposhnikov S, Chevillard S, Paget V, Grall R, Delic J, Goñi- de-Cerio F, Suarez-Merino B, Fessard V, Hogeveen KN, Fjellsbø LM, Runden-Pran E, Brzicova T, Topinka J, Silva MJ, Leite PE, Ribeiro AR, Granjeiro JM, Grafström R, Prina-Mello A and Dusinska M High throughput toxicity screening and intracellular detection of nanomaterials. *WIREs Nanomed Nanobiotechnol* 2016. doi: 10.1002/wnan.1413. [Epubahead of print] Review. PubMed PMID: 27273980.

Annex 2

Table 1 Advantages and limitations of high throughput screening methods to study toxicity of nanomaterials

Technique	Advantages	Limitations
Label-free fast qualitative and quantitative assessment of uptake and cellular screening of NMs		
Flow cytometry	Fast, cost-effective and validated assay. Multiplexing capabilities. Interference compensation and gating accounted for by side scatter versus forward scatter. Uptake can be followed. Discriminates cells with and without NPs, to study heterogeneity. Recommended for fast cell assay in cases where NMs do not interfere.	Requires fluorescent labels which may interfere with surface properties of NMs. Optical properties of NM can interfere with measurement of absorbance or fluorescence. NPs may also adsorb reagents, markers. NPs situated on cell membranes may bind or mask surface receptors. So far only developed for use with 96 wells. Needs proper controls to identify interference due to NMs.
HTS flow cytometry	Side scatter signal can detect NMs. Imaging flow cytometry relates physico-chemical characteristics of NMs to their uptake	
HTS flow cytometry for studying specific cellular uptake	Evaluates specific cellular uptake	If uptake is measured using side scatter, increased cellular density may also be due to apoptosis, so additional methods must be used for validation.
Confocal laser scanning spectroscopy	Cost effective and validated method, with multiplexing capabilities, Z-stacks option and combined imaging options. Recommended for particle localization/uptake.	Assay is low throughput unless automated.
AES	Quantifies specific chemical elements of NMs in cultured cells and tissues with ppb accuracy.	Expensive. Technical knowledge needed.

ICP-MS	High accuracy and low limit of detection (ppb). Can selectively screen for battery of elements.	Only applicable to inorganic NMs. Not possible to distinguish between NMs that are internalised in cells, extracellularly associated and/or just located between cells or within extracellular fluid.
Single particle ICP-MS	Records pulses related to single NM and distinguishes between dissolved and particulate forms of NMs	Same as for ICP-MS.
IBM techniques (μPIXE and/or μRBS)	Powerful tools for spatially resolved elemental imaging. Possible to determine concentration of cellular elements, with sensitivity in ppm range. Distinguishes between internalised NMs and NMs attached on outside of plasma membrane. Can quantify total cellular NP concentration in cells and tissues.	In most cases, difficult to distinguish between dissolved and particulate forms of NMs.
EMPA	Quantifies and visualises single elements in biological specimens.	Low signal/noise ratio and poor penetration of biological specimens compared to proton beam.
MRI, PET and SPECT	Clinical imaging applications, and detection of NPs in whole organism.	Only applicable with specifically designed and validated detection probes. Low resolution (about 1 mm).
TEM, ToF-SIMS	Simultaneous visualisation of NMs and their biological environment at sub-cellular level.	TEM and ToF-SIMS methods are relatively costly and time-consuming, and require heavy equipment.
CRM	Non-invasive fast screening 3D method to visualize and quantify NMs at subcellular level as well as to study adverse effects of NMs such as apoptosis/necrosis, ROS, Cyt C redox status, DNA fragmentation based on spectroscopic marker of individual cells *in vitro* and *in vivo.*	CRM is not able to detect dissolved NMs.

	Economical and relatively fast technique highly recommended for HTS analysis.	
High throughput screening and High Content Analysis for NM-induced cytotoxicity		
Flow cytometry	Fast, cost effective and validated assay with multiplexing capabilities, Interference compensation and gating accounted for by side scatter versus forward scatter. Recommended for fast cell viability testing.	
HTS flow cytometry for studying cell death	Can investigate several parameters in one sample.	Further investigation needed to ensure there is no interference with NMs.
HTS flow cytometry for ROS	Detects several early intracellular indicators at much low NM concentrations. Flexible, allowing for study of several NPs in one single experiment.	Further investigation needed to ensure there is no interference with NMs.
Multiplex analysis of secreted products	Allows quantification of up to 500 analytes in same sample at same time. Reduction of reagents and sample volume, and number of experimented animals; Possible to perform repeated measures of multiplex panels in same experimental assay. Detection of analytes over broad range of concentrations.	Assay costs are moderately high.
Impedance-based monitoring of NM induced cytotoxicity		
Impedance-based spectroscopy / Impedance-based HTS	Enhanced sensitivity compared to traditional assays and label free (no interference with impedance-based readings).	Relatively high cost for plates with electrodes and for microfluidic impedance-based chips.

xCELLigence ®, CellKey and ECIS systems	Not labour-intensive, label-free, non-invasive, biophysical assay, detecting dynamic cell responses. Measure real-time electrical impedance, up to 384-well plate format.	Observes cellular responses to effectors without giving any indication of underlying mechanisms. Adherent cells only. Relatively high cost for plates with electrodes. Effects of ions and particulate matter difficult to differentiate for soluble NMs.
IFC, Ampha Z30	Label-free. Measures single cells in suspension, giving information about size and number of cells, membrane capacitance and cytoplasmic conductivity, with capacity to differentiate between viable, apoptotic and necrotic cells.	Endpoint assay; does not identify underlying mechanisms. Recently introduced; more time needed for optimisation and validation.
HTS/HCA for imaging and quantitative screening of NMs		
HCA and High content Screening coupled with CLSM or EPI	Fast, reliable, real time, 384 wells. Quantitative and qualitative data. Allows multiparametric analysis, Easy to use.	Assay costs are moderately high compared to standard kit even allowing for multiparametric screening.
High-throughput omics	96-1536 wells. Label-free. Multiplexing of 50-1500 parallel gene expression measurements. High sensitivity with linear response: measurements possible without amplification of the target. Permits single-cell sensitivity and extremely high specificity. Results can be compared to/validated against existing repositories of gene expression profiles.	Assay costs are moderately expensive, but lower than traditional microarray or RNA-seq analyses. Not a substitute for phenotype assays.
Genotoxicity / mutagenicity		

HTS Comet Assay	Well-known and simple assay allowing testing of several NMs simultaneously. Automatic scoring systems have been developed.	Semi-automatic scoring is time-consuming. Fully automatic scoring is expensive and still might need validation.
'CometChip'	Uses micro-array on an agarose-coated plate.	Long-term sample storage needs to be improved.
HCS approach to IVMN	Efficient method with high sensitivity and specificity.	Requires multiple assays as developed within FP7 (QualityNANO). Not fully automated. Tested on polystyrene and iron oxide NMs.
γH2AX assay – foci	Several orders of magnitude more sensitive than method measuring overall protein level. Allows distinction between pan-nuclear staining and focus formation.	Automated scoring still needs improvements. Validation needed against other methods.

Annex 3 - Excel file, Table 2

Table 2. An overview of all HTS/HCA experiments and characterization performed according to the NANoREG Guidance document

Endpoint/method		NM100	NM101	NM103	NM104	NM110	NM111	NM200	NM203	NM212	NM220	NM300k	NM300kdisp	NM302	NM302disp	NM400	NM401	NM411	iO2@IIT 50 red-	iO2@IIT 50 red-	iO2@IIT 50 green+	iO2@IIT 50 green	iO2@IIT 115 red-	iO2@IIT 115 red-
Characterisation	**Partner**																								
Z-sizer Nano ZSP	UiB	UiB(39)	UiB(39)	UiB(39)		UiB(39)		UiB(39)	UiB(39)	UiB(39)	UiB(39)	UiB(39)	UiB(39)	UiB(39)	UiB(39)				UiB(39)	UiB(39)	UiB(39)	UiB(39)	UiB(39)	UiB(39)
DLS (Dynamic Light Scattering)	INSA	INSA	INSA					INSA		INSA		INSA	INSA				INSA								
DLS (Dynamic Light Scattering)	CBT	CBT	CBT	CBT	CBT	CBT		CBT	CBT	CBT	CBT	CBT	CBT	CBT	CBT		CBT								
DLS (Dynamic Light Scattering)	CEA		CEA			CEA		CEA		CEA	CEA			CEA	CEA										
DLS (Dynamic Light Scattering)	TCD			TCD				TCD	TCD																
DLS (Dynamic Light Scattering)	ANSES			ANSES	ANSES	ANSES		ANSES	ANSES			ANSES													
DLS (Dynamic Light Scattering)	ULEI			ULEI	ULEI					ULEI	ULEI														
Nanoparticle Tracking Analysis (NTA)	ULEI			ULEI	ULEI					ULEI	ULEI														
Nanoparticle Tracking Analysis (NTA) NanoSight	NILU	NILU	NILU	NILU	NILU	NILU		NILU	NILU	NILU	NILU	NILU	NILU	NILU	NILU		NILU								
Cytotoxicity (colorimetric methods)																									
Cytotoxicity by Alamar blue (NILU)	NILU	A549	A549	A549	A549	A549		A549	A549	A549	A549	A549	A549	A549	A549		A549								
Cytotoxicity using CFE (NILU)	NILU	A549	A549						A549	A549	A549	A549	A549	A549	A549		A549								
Cytotoxicity using CFE INSA	INSA	A549	A549					A549		A549		A549	A549				A549								
Cytotoxicity by MTS, 24h (IEM)	IEM	A549	A549	A549		A549		A549	A549	A549	A549	A549	A549	A549	A549										
Other cytotoxic methods	methods																								
Cytotoxicity by Colony forming efficiency (CFE)chornic (NILU)	NILU	A549	A549	A549	A549	A549		A549	A549	A549	A549	A549	A549	A549	A549		A549	A549							
Cytotoxicity by cell lab beckman counter (UAB)	UAB	A549	A549			A549		A549	A549	A549		A549					A549								
Cell death (apoptosis/necrosis), Immunotoxicity, oxidative stress																									
RT_Real Time PCR (UiB, 39)	UiB	A549, GF	A549, GF	A549, GF							A549, GF	A549, GF							A549, GF	A549, GF					
Genotoxicity / mutagenicity																									
HTS Comet Assay with FPG, 3h, 24h (NILU)	NILU	A549	A549	A549	A549	A549		A549	A549	A549	A549	A549	A549	A549	A549		A549	A549							
HTS Comet Assay, 24h (UAB)	UAB	A549	A549			A549		A549	A549	A549	A549	A549					A549								
HTS Comet Assay with FPG, 3h, 24h (CBT)	CBT	TK6	TK6	TK6	TK6	TK6		TK6	TK6	TK6	TK6	TK6	TK6	TK6	TK6		TK6								
HTS Comet Assay with FPG 6h, 24h (NILU/INSA)	NILU/INSA	V79								V79				V79											
HTS Comet Assay w/wo FPG, 24h (IEM)	IEM					A549		A549	A549	A549	A549	A549		A549											
mammalian gene mutation test (HPRT) NILU/INSA	NILU/INSA	V79	V79							V79				V79			V79								
mammalian gene mutation test (MLA) NILU	NILU	MLA	MLA	MLA	MLA	MLA		MLA	MLA		MLA	MLA		MLA			MLA								
HTS/HCA for imaging and quantitative screening of NMs																									
HCA (cell count, nuclear size, nuclear intensity, active Caspase-3, gH2AX, phospho-p53, phospho ATM, Ki-67), ANSES	ANSES			A549, Caco-2	A549, Caco-2	A549, Caco-2		A549, Caco-2	A549, Caco-2			A549, Caco-2													
HCSA (cell number, changes in lysosomal mass/pH, changes in mitochondrial membrane potential), 24h TCD	TCD			A549				A549	A549																
Uptake and localisation																									
IBM techniques (µPIXE and/or µRBS), 24h (ULEI)	ULEI									A549															
CRM, 24h (ULEI)	ULEI			HEPA-RG	HEPA-RG					A549	A549														

Annex 4 - Table 5

Table 5. Data analysis and draft publication plan for TASK_5.6

	Leading / responsible	TOPICS	Contributors	APPROACH/notes
1	UiB/CEA/NILU	Cytotoxicity, all NMs	INSA, IEM, TCD, INMETRO	All cytotoxicity methods (Alamar blue, PE, etc.), methods comparison and validation with several NMs, several cell lines
2	UAB	Genotoxicity – micronucleus assay	INSA, IEM, all WP5	Several NMs, several cell lines comparison; HTP vs conventional method, need inclusion of MN results from all WP5 (KI, FIOH etc)
3	NILU/CBT	Genotoxicity – comet assay – comparison	INSA, All WP5	Method comparison with several NMs within one cell line – consistency of results – validation exercise; need to include all comet data
4	NILU/CBT	Genotoxicity – comet assay 2	INSA, IEM, all comet	Compare results across several NMs and several cell lines – potency for genotoxicity, cell lines sensitivity
5	UAB	SiO2 NMs (200, 203)	NILU, INSA, IEM, TCD, ANSES,	SiO2 NM – different methods for cyto- and genotoxicity in several cell lines,
6	ANSES/ULEI	ZnO NMs (110, 111)	INSA, IEM,	Include all methods for all endpoints (cyto and genotoxicity, if possible in several cell lines) including HCA, IBM and CRM, additional experiments needed
7	ULEI/ANSES	HCA x CRM x RT-PC, TiO_2	TCD	Methods comparison, all. Uptake study for different cell lines; uptake versus adverse response relationship
8	CEA/UiB	NMs ranking impedance/ cytotox	IEM, NILU	NMs ranking according to cytotoxicity, different cell types
9	ANSES/ULEI	Ag NMs	INSA, IEM, NILU	Different methods for cyto and genotoxicity in several cell lines.
10	UiB/ULEI	Uptake of TiO_2 NMs (103 and 104)		Molecular dose characterization. Uptake and intracellular concentration. Quantification of NPs in A549, osteosarcoma, Caco, etc
11	INSA/NILU/UiB	Characterisation, NM by DLS, NTA, TEM	INSA, IEM, INMETRO, All	NMs dynamic behavior, size, characterized batch dispersion, in culture medium along time, methods comparison , impact on toxicity, etc. all in WP5

12	**NILU/CBT/All**	**Overal HTP paper – evaluation of all NMs**	**All**	**Overall evaluation and overview - including all methods; multi-comparison of results. This needs extended data analysis and statistics, this will be final outcome**
13	**NILU**	**Ag NM300, NM302**	**INSA, IEM**	**Comparison of these two nanosilvers and all methods in one cell type or go for mode of action related to different shapes**
14	**ULEI/INSA/UiB/NILU**	**Barium NM212 Cerium NM220**	**INSA, IEM**	**All data on CeO_2 and BaSO4**
15	**UiB**	**HTS problems**		**A general problem in high throughput testing of nanomaterials, data quality, throughput cytotoxicity screening of nanomaterials, artifacts**
16	**IEM, NILU**	**All TiO_2s (NNM100, 101, 103, 104)**	**IEM/All, TCD**	**Cytotoxicity Data on MTS, AB, neutral red, CFE, impedance, all 5.5 and 5.6 groups mostly in THP (A549, BEAS2B)**
17	**NILU**	**Genotoxicity/ mutagenicity**	**INSA, UaB and others**	**Comparison of TiO2 genotoxicty (A549) and mutagenicity (NNM100, 101, 103, 104, NM105) with uptake All who have data to contribute with**

Annex 5 - Standard operating procedures handbook (SOPs) – methods used for the NANoREG Task 5.6

SOP No	SOP name - Method used in Task 5.6	Author/Partner
1	SOP for Dispersion NANoREG D5.07 SOP 01 SOP for Dispersion	CEA
2	SOP for real time label free impedance based nanotoxicity assessment (Impedance xCELLigence®) NANoREG D5.07 SOP 02 Real-time label-free impedance-based nanotoxicity assessment	UiB*
3	SOP for High Throughput Cell Impedance Measurement NANoREG D5.07 SOP 03 SOP for High Throughput Cell Impedance Measurement	CEA
4	SOP for Label free nanotoxicity assessment by impedance - based flow cytometry Impedance Ampha Z30 NANoREG D5.07 SOP 04 Label-free nanotoxicity assessment by impedance-based flow cytometry	UiB
5	Cytotoxicity by cell lab beckman counter NANoREG D5.07 SOP 05 Viability protocol by using a Cell Counter	UAB
6	Cytotoxicity by Alamar blue NANoREG D5.07 SOP 06 HEL16T008 AlamarBlue Assay	NILU
7	Cytotoxicity using CFE NANoREG D5.07 SOP 07 HEL17T010 Colony forming efficiency assay	NILU
8	Cytotoxicity by MTS NANoREG D5.07 SOP 08 Cytotoxicity by MTS - reference to NanoValid protocol	IEM/NanoValid
9	TaqMan real time Reverse Transcription PCR (RT_Real Time PCR) NANoREG D5.07 SOP 09 TaqMan real-time Reverse Transcription PCR	UiB
10	HTS Comet Assay with and without FPG (12 gels) NANoREG D5.07 SOP 10 HEL11T005 HTS Comet Assay with and without FPG - 12 wells	NILU*
11	HTS Comet Assay with and without FPG (20 gels) NANoREG D5.07 SOP 11 HTS Comet Assay with and without FPG - 20 wells	IEM
12	Mammalina gene mutation HPRT NANoREG D5.07 SOP 12 HEL11T007 Mammalian in vitro HPRT Mutation test	NILU
13	Mammalian gene mutation MLA NANoREG D5.07 SOP 13 HEL16T009 Mouse Lymphoma Assay in vitro	NILU
14	Micronucleus assay NANoREG D5.07 SOP 14 Micronucleus Assay	IEM

15	HTS Micronucleus Assay by Flow Cytometry NANoREG D5.07 SOP 15 Micronucleus assay using Flow Cytometry	UAB
16	High Content Analysis** NANoREG D5.07 SOP 16 High Content Analysis-based nanotoxicity assessment	ANSES
17	IBM techniques (µPIXE and/or µRBS), NANoREG D5.07 SOP 17 Ion Beam Microscopy	ULEI
18	CRM NANoREG D5.07 SOP 18 Confocal Raman Mcrospectroscopy	ULEI
19	NANoREG D5.07 SOP 19 Whole blood assay for cytokine production	CRN